Stern vs Side installation of Monopiles from floating vessels

Thesis

E.B. Rosenboom

Objective comparison methods to make a distinction between side and stern installation of future Monopiles.

TUDelft

Huisman

Stern vs Side installation of Monopiles from floating vessels

Thesis

by

E.B. Rosenboom

to obtain the degree of Master of Science

at the Delft University of Technology,

to be defended publicly on Friday the 22nd of July, 2022 at 10:00.

Student number: 4270606
Project duration: November 8, 2021 – July 22, 2022
Thesis committee: Ir. A. C. M. van der Stap,   TU Delft, supervisor
                    Dr. ir. B. C. Ummels,   TU Delft
                    Ir. J. Dijkstra,   Huisman

TUDelft   Huisman

Abstract

As the world economy and population grow, energy consumption grows too at a never before seen pace. Reducing costs and increased environmental awareness resulted in renewable energy sources being the fastest-growing sources in the last decade. Due to its high potential, many offshore wind turbines will be installed in the coming years. These turbines will be installed in deeper waters, using mainly monopiles as support structures.

In the variety of monopile (MP) installation methods, a distinction exists between installation over the side of a vessel and a novel method where the procedure is repositioned to the vessel's stern. Experts in the field were convinced that stern installation would be necessary for growing MPs and extended installation timeslots. This thesis aims to create an objective distinction between the installation directions by looking at the following two installation steps.

First, the storage of MPs on the deck of an installation vessel is investigated. For side installation, the MPs are positioned transversely on the deck. This method uses little deck space per MP but includes an overhang which might badly influence the vessel's behaviour. The latter has been investigated using the Moment of Inertia (MoI) of the vessel as an indicator of this behaviour. It has been found that transverse storage affects the MoI significantly more than longitudinal storage. However, this longitudinal storage is limited to 4 MPs per transit due to stability, whereas the transverse method can take 6 MPs. The stresses in the MP itself have also been evaluated for these storage methods, as the support locations were different. It has been concluded that there is indeed a difference, but the stress level has been found not governing for this choice.

Second, the upending procedure is investigated, as this is a step in the procedure which is highly influenced by motions and external wave impact. A model is developed that uses tugger line connections from the vessel to the MP to define forces in equipment objectively. It has been found that loads in the tugger lines were significantly lower for stern installation compared to side installation, which leads to a workability comparison. This comparison is based on a specific tugger cable, limited to a $300mt$ tugger load. A range of sea states has been analysed and checked on this maximal tugger load. The workability difference for full-year performance is found to go from 64% for side installation to 96% for stern installation. It is realised that these numbers are high compared to the actual installation, but as the assumptions made for this model are equal for side and stern, these percentages are a good comparison between the two methods. The assumptions on which this model is based are checked on sensitivity, which results in reasonable trend lines and an interesting prospect into the future.

The model presented in this thesis could pose as a hypothetical concept for future installation, and therefore a determination of the natural frequency is added in this thesis. With this natural frequency, the feasibility of a concept can be quickly assessed even though no time-domain simulations have been executed. The model stays clear from natural periods of the control system and periods of the waves for a large range of upending angles. However, in a nearly vertical position, the control frequency is crossed and later, the regime of wave frequencies is encountered. Adjusting the model slightly in terms of geometry shows that these issues can be solved. However, future research is highly recommended into a time simulation of the model.

Finally, some practical applications of the installation over the side and stern are discussed. Concluding this thesis, the main research question can be answered positively by stating that stern installation can be used to improve the all-year MP installation performance of a floating installation vessel.

Preface

This thesis is performed to obtain my masters degree in Offshore & Dredging Engineering, a multidisciplinary cooperation between Civil Engineering, Mechanical Engineering and Marine Technology of the Delft University of Technology.

This project is written in cooperation with Huisman, a well-known producer of equipment for the offshore wind industry. Together with Huisman, a subject was found which combines a knowledge gap in the market with my personal interests. I'm very enthusiastic to have worked on this project and happy with the results as presented in this thesis. I especially want to thank Jeroen Dijkstra for his guidance throughout the project, helping me see a complex problem as a range of smaller, simpler problems.

From TU Delft I would like to thank Bart Ummels for his endless enthusiasm in coaching me. I have learned many things from Bart, considering this thesis but also about life in general. I look forward to meeting Bart again in a professional environment, as I'm sure we will.

Thirdly, I would like to thank Hugo, Eduard and Joris, my fellow graduation interns at Huisman. Going for a round of coffee, and discussing what we were doing and how issues were solved really helped a lot. Sharing your views on ways to present data and make clear figures definitely influenced this report.

Finally, I want to thank my family, girlfriend and friends, for a welcome distraction from time to time, making it possible to finish this whole project in slightly less than nine months without driving myself crazy. Asking out-of-the-box questions about my work really challenged me to keep the research accessible, whilst diving deep into the model.

E.B. Rosenboom
Delft, July 2022

Contents

List of Tables

List of Figures

Nomenclature

Latin Symbols

a	Acceleration
A	Area
B_{vessel}	Beam of Vessel
C_d	Drag Coefficient
C_m	Added Mass Coefficient
d	Water Depth
dx	Segment Length
D	Diameter
D_{vessel}	Depth of Vessel
E	Young's Modulus
f	Frequency
F	Force
g	Gravitational Acceleration
h	Height
H_s	Significant Wave Height
I_{xx}	Moment of Inertia over specific axis
k	Wave Number
K	Stiffness
KC	Keulecan-Carpenter Number
L	Length
m	Specific Weight
M_{xx}	Moment over specific axis
n_{mp}	Number of Monopiles
r	Vectorial arm
R	Radius
Re	Reynolds Number
S_ζ	Wave Spectral Density
t_{mp}	Thickness of MP segment
T_p	Peak Period
T_{vessel}	Draught of Vessel
T_z	Zero-crossing Period
u	Horizontal water velocity

$u_{current}$	Current velocity
u_p	Perpendicular water velocity
$u_{p,red}$	Perpendicular water velocity w/o current
U_w	Wind speed
$U_{w,p}$	Perpendicular wind speed
w	Vertical water velocity
W	Weight
X	X-coordinates
Y	Y-coordinates
Z	Z-coordinates
z_0	Surface Roughness

Greek Symbols

α	Power ratio
α_{roll}	Rotational Acceleration
β	Crane Angles
γ	Peakedness Factor
λ	Wave Length
ν	Kinematic Viscocity
ω	Angular Velocity
ϕ	Roll
ψ	Yaw
ψ_{vessel}	Heading
ψ_{wind}	Angle of wind origin
ρ	Density
θ	Pitch
θ_{mp}	Relative angle between MP and Vessel
ζ_a	Wave Height

Abbreviations

CoG	Centre of Gravity
CT	Constant Tension
DAF	Dynamic Amplification Factor
DP	Dynamic Positioning
EoM	Equation of Motion

GBF	Gravity Based Foundation	RF	Rotational Factor
GM	Metacentric Height	$SPAR$	Single Point Anchor Reservoir
HLV	Heavy Lift Vessel	$SPMT$	Self-propelled Modular Transporter
mh	Main Hoist	$SSCV$	Semi-Submersible Crane Vessel
MoI	Moment of Inertia	SWL	Safe Working Load
MP	Monopile	$T_{1..5}$	Tugger Line
mt	metric Tons (1000kg)	TLP	Tension Leg Platform
OWF	Offshore Wind Farm	TMC	Tub Mounted Crane
OWT	Offshore wind Turbine	wh	Whip Hoist
RAO	Response Amplitude Operator		

1

Introduction

1.1. Relevance

1.1.1. Energy Transition

Energy consumption is one of the core indicators of a nation's economic wealth, as it is the key input to almost all consumption and production processes. Due to a substantial growth of the world economy, combined with an increasing world population, energy consumption has been growing at a never before seen pace, as seen in Figure 1.1a. On the one hand, this increase is positive, as more and more people get access to new technologies. On the other hand, expanding this scale leads to high demand for our energy sources. Although the growth of energy consumption in fully developed countries has stabilised, more and more new countries are developing thriving economies with an increasing need for energy. Energy can be extracted from multiple sources, such as fossil fuels (petroleum, coal, natural gas, etc.), renewables (biomass, hydro, wind, solar, geothermal, etc.), and nuclear plants [5]. Fossil fuels are mature energy sources and occupy a large share of the total energy consumption. When burning fossil fuels, greenhouse gasses such as carbon dioxide are emitted into the air, which is a primary cause of global warming [38]. In Figure 1.2, it can be seen that never before in the earth's anthropological history the carbon dioxide concentration was as high as it is nowadays. Note that this figure only presents the Pleistocene and Holocene, but as humanity only began to develop itself in this period [42], this is representative of the world as stable as we know it. To stop this trend, a shift towards renewable energy has started. Due to increasing environmental awareness and a considerable cost reduction compared to fossil fuels, renewable energy has been the fastest-growing energy source in the last decade. Traditionally, renewable energy consists mainly in the form of electricity. Still, a lot of research is ongoing into creating hydrogen or other fuel types from renewable energy [3, 34, 39]. The need for this research is mainly since electricity has a share of only 19% in the final global consumption, while oil as a fuel is still responsible for 40% of the consumption (see Figure 1.1a). If renewable energy could be used in more ways, its share could significantly increase [27].

Within renewable energy, various sources are exploited in the current market. In Figure 1.1b the share of each source can be seen from 1985 until 2020. Other renewables consist of tidal, geothermal and wave energy. As can be seen, traditional hydropower has been increasing and has still the largest contribution, but wind and solar are rising quickly and are expected to keep growing in the coming years.

1

(a) Global primary energy consumption by source from 1880 to 2019. Date published by Vaclav Smil (2017). Energy Transitions: Global and National Perspectives. & BP Statistical Review of World Energy.[8]

(b) Renewable energy generation by source from 1985 to 2020. Data published by BP Statistical Review of World Energy & Ember [9]
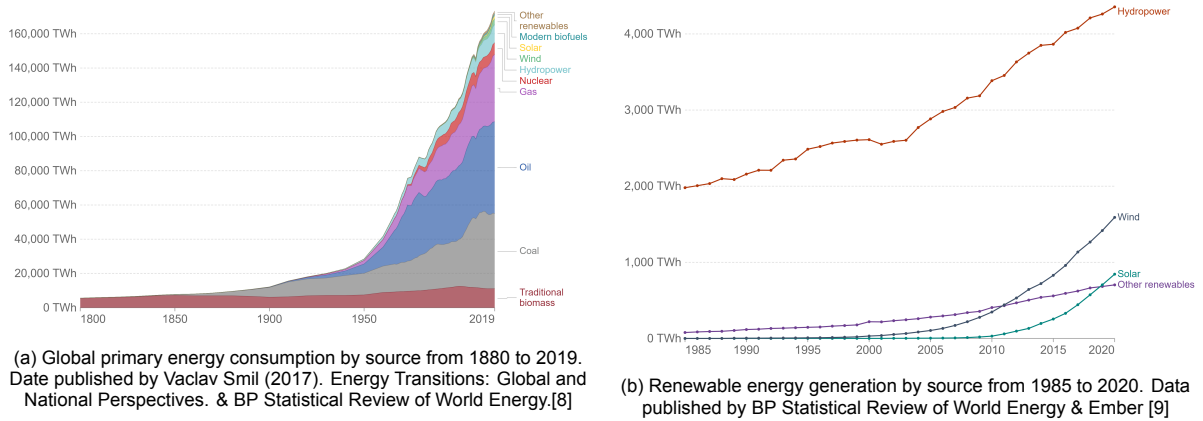
Figure 1.1: Statistics of global energy consumption and generation.
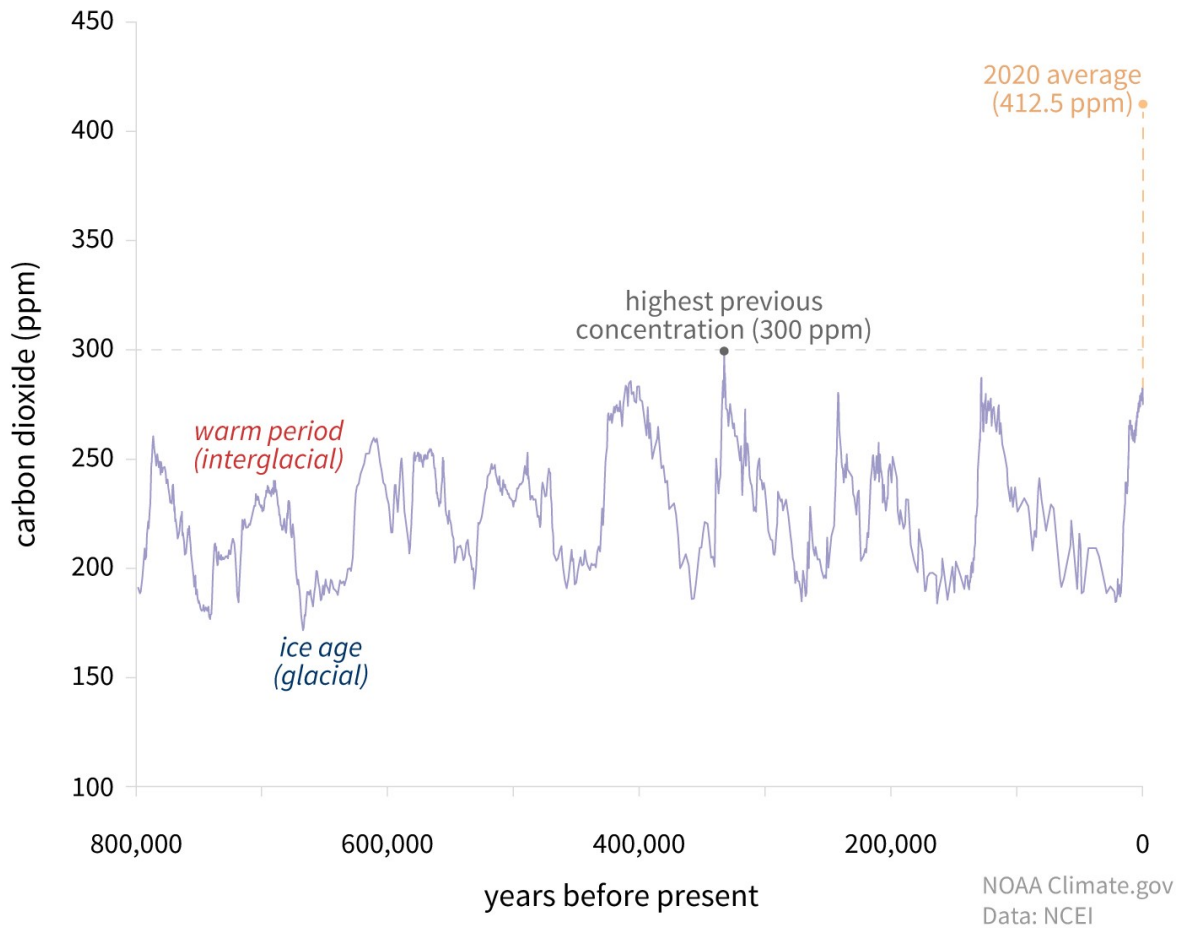
Figure 1.2: Global atmospheric carbon dioxide concentrations (CO2) in parts per million (ppm) for the past 800,000 years. CO2 was never higher than 300 ppm before 1950. On the geologic time scale, the increase (orange dashed line) looks virtually instantaneous. Graph by NOAA Climate.gov based on data from Lüthi, et al. NOAA NCEI Paleoclimatology Program

1.1.2. Offshore Wind

Wind has been a source of electricity since the late 19th century, when Charles F. Brush built the first 12kW wind turbine to power local electrical devices and batteries. When the public electricity grid was expanded from the city to the rural areas in the middle of the 20th century, wind turbines began to deliver power to the grid. The turbines grew larger to make a significant impact (up to 1250kW). After years of concept research, it appeared that the Danish concept, consisting of 3 upwind blades, constant speed and stall control, was the most robust type of turbine. Multiple big companies tried to create large turbines, but the reliability of these machines never reached the kind of reliability the relatively small danish concept reached. Gradually increasing the size of the turbine appeared to be the crux, and slowly three-bladed turbines began to dominate the market. The addition of variable speeds and pitch-controlled blades led to growth to power levels of 14MW already operational, and 16MW announced [14, 15, 53].

Traditionally, turbines were placed on land in rural areas close to cities to supply energy to the grid. In 1991 the first wind farm was established off the coast of the town of Vindeby, on the Danish island of Lolland [50]. After a successful couple of years, developers realised that offshore wind had a high potential due to higher and more stable wind speeds. It can be seen in Figure 1.3 that offshore wind slowly started, whereas onshore wind quickly increased. Because offshore wind is relatively expensive to install, these farms can only become economical when large turbines are used. As said before, turbines grow in size slowly and therefore, only from 2010 onward offshore wind turbines (OWT) were increasingly installed. More efficient electrical gear, advanced support structures and offshore substations make it possible to increase the distance to shore, gain more power from one farm and decrease electrical losses to a minimum. Additional drives to move from on- to offshore wind farms can be visual, noise or areal constraints.
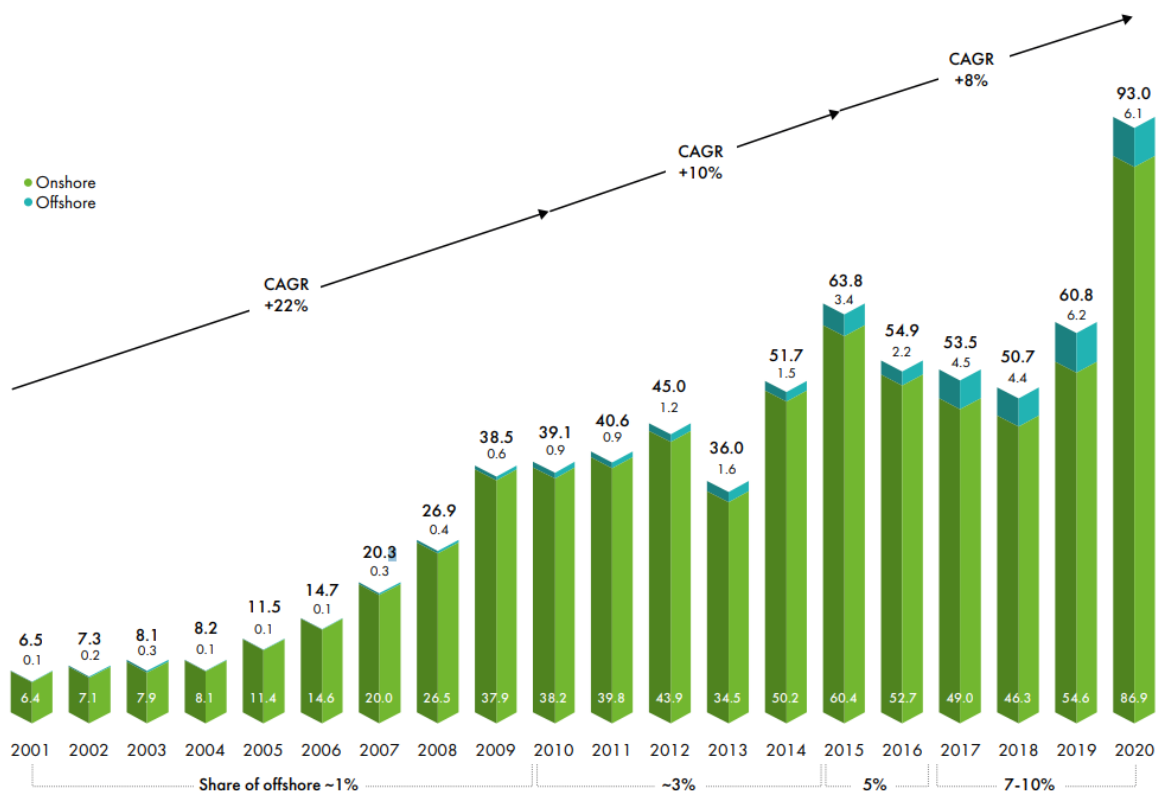
Figure 1.3: Historic Development of global new wind installations (in GW) from 2001 to 2020 with an indication for onshore and offshore turbines.[32]

1.1.3. Foundations for Offshore Wind

Bottom-fixed offshore wind turbines

Bottom-fixed foundations have been used since 1991 when the first-ever offshore wind farm (OWF) Vindeby was commissioned [50]. In Figure 1.4, an overview is given of the current foundations available. The gravity-based foundation was the first installed and consisted of a heavy concrete base, which rests on the seabed. The self-weight of this structure prevents it from overturning. This foundation mainly was used for waters in which ice can cause damage to the structure. For seabeds consisting of soft clay, the suction bucket foundation might be more suitable. This concept is relatively cheap to install while still reliable. However, this method is not often used and will not be further discussed in this report. Monopiles (MP) are the simplest form of foundation, as they consist only of one pipe hammered into the soil. MP's are used in water depths of 0-40m, but estimations have been made that this depth will increase significantly in the coming years [35]. Tripod foundations consist of three steel pipes arranged in a triangular shape. This concept is stable, lightweight and can be suitable for water depths of 10-35m. Finally, Jacket foundations are constructed from steel tubular members connected in a space frame structure. This structure is lightweight and thus cheap, but storage, logistics and installation can be expensive due to their size. However, jacket structures can be placed in deeper waters, and the frequency response of jackets is significantly different from monopiles. This last difference can be advantageous in waters with high seismic activity. [1, 30, 52]
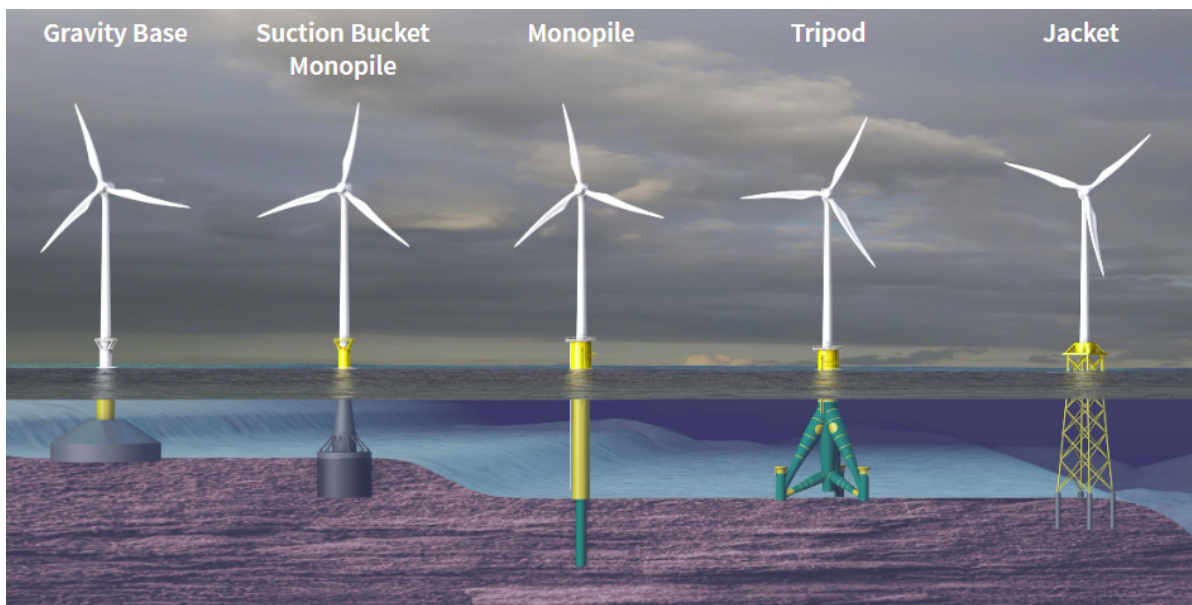
Figure 1.4: Graphical overview of fixed foundations for offshore wind turbines [18]

Floating offshore wind turbines

Comparably to oil and gas platforms, the offshore wind industry experiences a shift into deeper waters. At depths above 50m or sites with unfavourable soil characteristics, a fixed foundation might not always be the commercially best option, and therefore, floating foundations have been developed. From 2007 onward, pioneers in the floating wind market installed the first floating foundations. There are currently three main types of floaters, which either use ballast, buoyancy or tension to create stability. First, the Single Point Anchor Reservoir (SPAR) buoy consists of a long pile with ballast in the lower part of the pile. Second, the semi-submersible foundation uses buoyancy. Both methods use additional mooring systems to increase stability and keep their position. Thirdly, the tension leg platform (TLP) consists of multiple steel cables, which are pre-tensioned by the buoyancy of the platform. These concepts have all been used in the oil and gas industry. Besides these well-known concepts, which are presented in Figure 1.5, novel floating types are developed as well, which are discussed in [7, 45]. Despite the wide range of technologies available, bottom-fixed foundations with mainly MPs still dominate the offshore wind market and will therefore be the focus of this thesis.

Figure 1.5: Graphical overview of floating foundations for offshore wind turbines [19]

1.2. Installation vessel

The process of OWF installation is a large-scale operation, spanning multiple months and requiring a variety of specialised vessels at specific moments in time. Support vessels, consisting of crew transport vessels, heavy transport vessels, feeder barges and cable layers, will provide the installation vessel with equipment, material and personnel. For the actual installation of the OWT and its foundation, an installation vessel is necessary. A range of vessel types is known in the current market, varying in stabilisation method, crane capacity, sailing speed, and day rate [30, 40]. It should be noted that ongoing research is investigating novel installation methods, where installation vessels in the current market might not be necessary anymore. For example, floating turbines might be installed solely by anchor handling vessels, and newly developed equipment can change the requirements for floating installation vessels [44].

In the current market, the distinction between jack-up vessels and floating installation is made. Jack-up vessels create a stable working platform with little to no motions by lifting the complete vessel on retractable pillars. The vessel stands on the seabed, which can only be done at specific locations and for limited depths. The lack of motions makes these vessels excellent for wind turbine installation, where tolerances are low, and motions could be harmful to equipment and turbine. On the other hand are floating installation vessels, such as Heavy Lift Vessels (HLV) (usually mono-hulls) and Semi-Submersible Crane Vessels (SSCV). These vessels are equipped with Dynamic Positioning (DP) and create stability with ballast. As no jacking is required, these vessels can begin an installation procedure relatively quick and at almost every location. However, the motions on these vessels are significantly higher and can cause issues. Intelligent equipment such as a tug control system [20] with motion compensation is required to achieve equal installation performance as jack-ups. Floating installation vessels are considered to have future potential, and will therefore be used in this thesis. To make this thesis widely applicable, a single crane installation vessel is selected, since dual crane vessels are more scarce in the current market.

(a) Jack-Up Platform The Noble Hans Deul over the Blythe Platform[16]

(b) Jack-Up Barge Aeolus, Van Oord, installing a Monopile[37]

(c) Heavy Lifting Vessel Oleg Strashnov, Seaway 7, upending a Monopile[46]

(d) Semi-Submersible Crane Vessel Sleipnir, Heerema, installing XXL turbine of DOT and TU Delft [11]

Figure 1.6: Selection of installation vessels that can be used for the installation of an OWF

1.3. Monopile Installation Methods

The installation of the foundation of a wind turbine is becoming more complex in the coming years. Due to the scarcity of shallow waters, OWFs are moving into deeper waters, which makes the foundations larger and heavier. This thesis focuses on the MP foundation type, which, as seen in subsection 1.1.3, consists of a single tubular partly driven into the seabed. The full installation sequence of a monopile (MP) is presented in Appendix B, where a variety of methods is shown.

In the current market, the installation procedure is usually executed on the side of a vessel's hull. An example of this is seen in Figure 1.6c, where the MP is upended in a bucket. It is believed that, to optimise the installation in the future, stern installation might prove to be a strong alternative method. Within the installation sequence, three steps are found where the difference between side and stern is unknown. These three steps will be shortly discussed here, and thoroughly discussed later in this thesis.

1.3.1. Storage on an installation vessel's deck

The MPs can be transported to the field using shuttling or feeder barges, but eventually, the piles need to be stored on the installation vessel's deck. The installation direction (side or stern) will determine the direction of storage on the vessel. This direction influences vessel response to waves, as the Moment of Inertia (MoI) and metacentric height (GM) are affected by MPs on deck. An example of transverse MP storage on a deck can be seen in Figure 1.7. The influence of this is yet unknown and will be investigated further in this thesis.
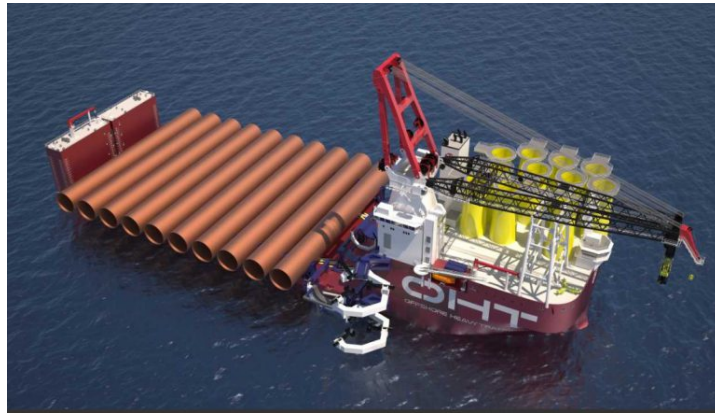
Figure 1.7: Semi-Submersible Heavy Transport Vessel OHT Alfa Lift shuttling MPs [12]

1.3.2. Transport of MPs on a vessel's deck

Besides influencing the vessel's behaviour, the MPs also experience loads while stored on deck. If the installation sequence calls for a shuttling installation vessel, the storage direction might significantly influence the loads on an MP. Discussions with experts in this field led to the realisation that a knowledge gap exists in this field. Transverse storage causes an overhang of the MPs, which leads to less favourable support distribution. Longitudinal storage, however, takes a lot of deck space, leading to a lower vessel capacity. Both global bending stresses, as well as local stresses at the supports, can govern this step.

1.3.3. Upending of the MP

One of the main steps in the installation of an MP is upending. During this step, the MP is rotated along its short axis such that it can be installed. As seen in Appendix B, a large variety of methods exists for this step. However, only two methods are considered optional for both side and stern installation. The current status of these, and some modifications which could make the concept work for future installations, are shown here.

Trolley Method

The MP is supported by a trolley support, which can rotate and acts as a hinge and by the crane, which lifts the top part until the MP is vertical. In the following sketches, the trolley has already been driven to the upending location and in some cases, has been assumed to be locked on location (with retractable locks of some sort).

When drawing the trolley method (Figure 1.8) it quickly becomes clear that the lifting height of the crane is problematic in this approach. Although a crane with a longer boom can be selected, it is believed that the currently drawn crane has a typical boom length compared to the current fleet of installation vessels.
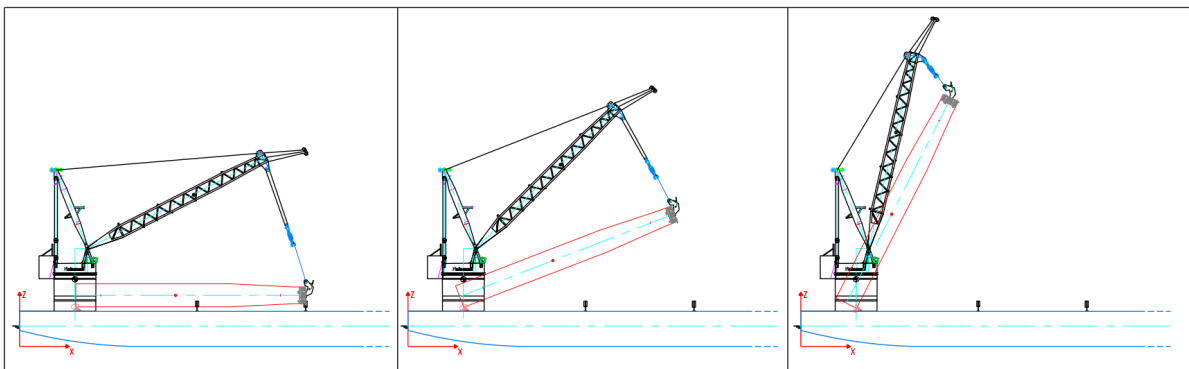
Figure 1.8: Simple Trolley method with a hinge at MP bottom flange

Modified Trolley Method

To complete the sequence without installing a longer crane boom, a stinger-like approach is drawn to check its achievability. A beam is connected to the stern recess, which can rotate such that the crane height is reduced. Note that this begins to look like an upending bucket, but the constraints in the hinge are only in the Y direction, which makes it complex to control the load.
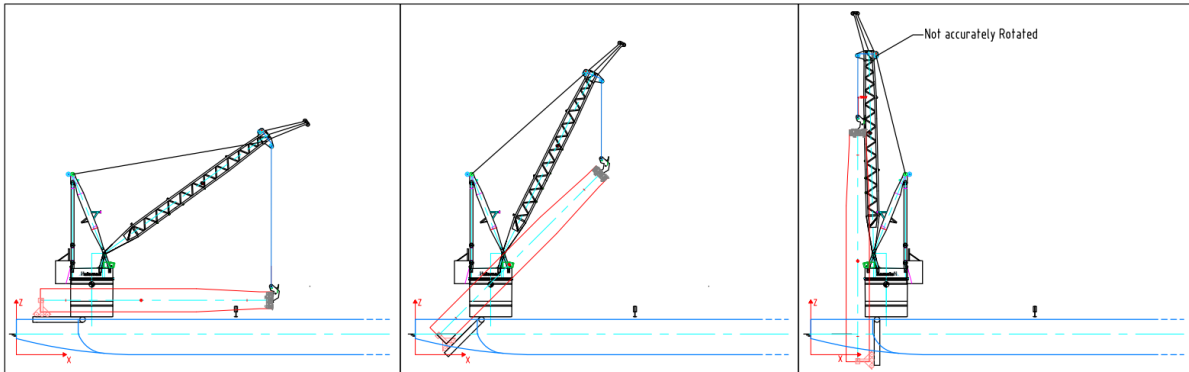
Figure 1.9: Trolley method with hinge at MP bottom flange and stinger-type vessel expansion

The before-mentioned lack of constraints in this upending method is addressed in the following sketch, where the stinger is extended to the bow, where it constraints the MP using a sling. In this method, the advantages of a free carriage (which can drive over the deck) are combined with that of a bucket (constraints at multiple points along the axis of the MP). This concept has not been seen in the market, but it gives a good indication of the options.
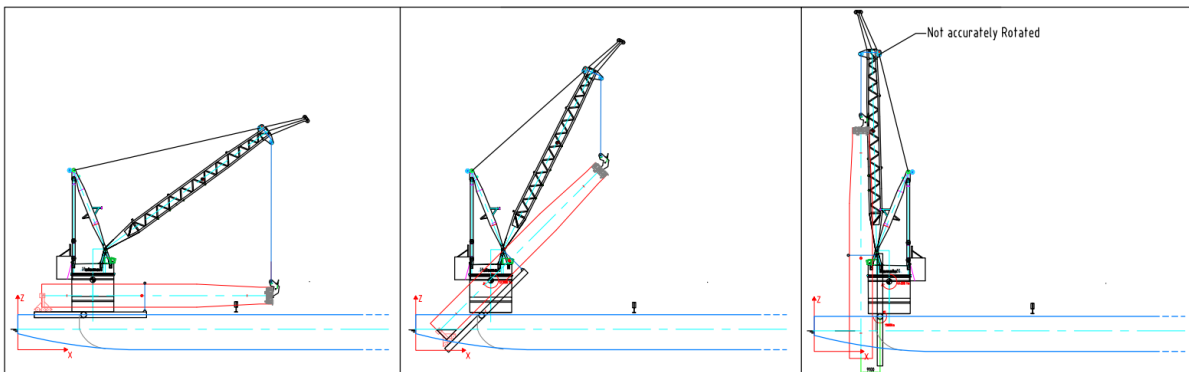
Figure 1.10: Trolley method with hinge at MP bottom flange and dual-direction stinger-type support

The most novel version of this method functions mainly as a transition into the chosen concept. This method consists of a trolley which is positioned in the middle of the MP. By driving to the back of the vessel, towards a stinger, the MP is basically launched into the water. This procedure is then controlled by a back tension winch and the main hoist. Control in other modes of motion poses an issue in this design, as the MP is quite poorly constrained. However, the idea of not lifting the MP as a whole but driving it towards the water proposes an interesting opportunity.
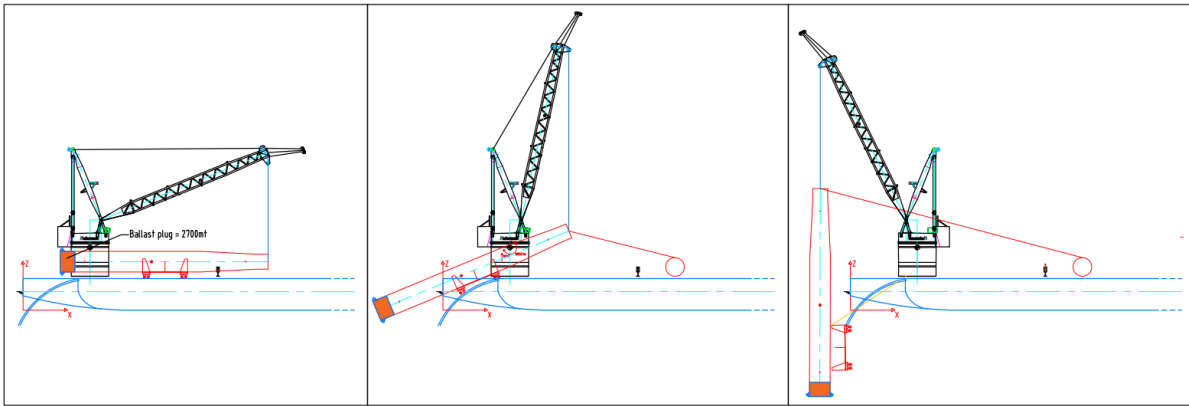
Figure 1.11: Novel method consisting of a trolley which drives off the vessel via stinger

Upend Bucket

The concept of the upending bucket is well-known, as multiple vessels currently install MPs using this piece of equipment. A currently used bucket is sketched on the stern of the vessel in Figure 1.12. All details of the upending bucket are removed to keep the focus on the working principle. In this principle, it can be seen that a part of the MP crosses the waterline, thus, this method is the semi-submerged version of an upending bucket. The required crane height for this method is relatively high, as the MP is rotated at roughly $23m$ from its bottom around a hinge that is $10m$ above the deck. Secondly, the Center of Gravity (CoG) is lifted from $9m$ above deck to $35m$ above deck, which costs significant energy.
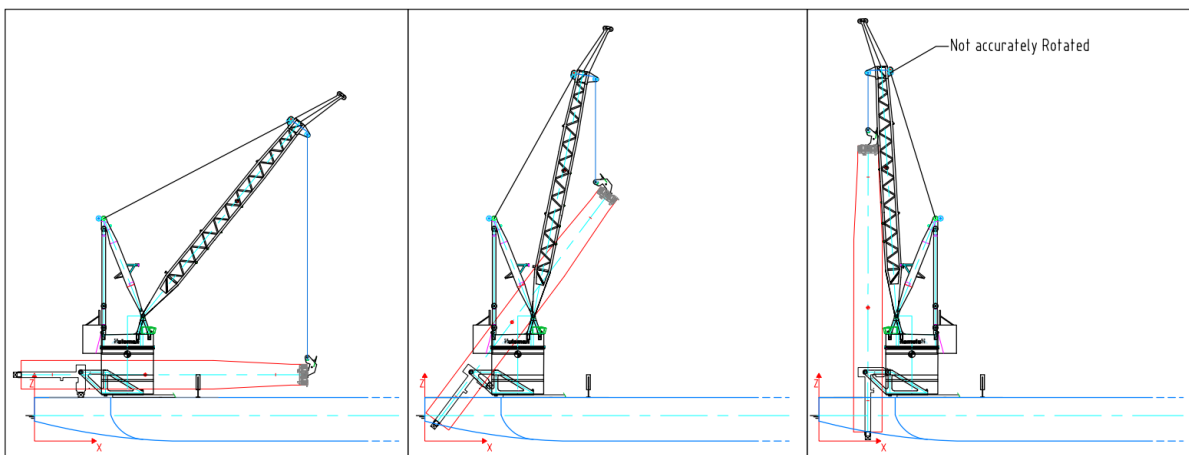
Figure 1.12: Currently used upending bucket, positioned on stern of the vessel for reference.

Modified Upend Bucket

A method to reduce required crane height and energy use is to create a longer bucket which can facilitate the MP rotating around its CoG. However, the bucket needed for this is a massive piece of steel with a significantly increased weight compared to the original design. Secondly, wave loading is affected by this longer bucket. The effect hereof can be positive and negative. On the one hand, the MP is submerged deeper, which causes more wave impact on the MP. On the other hand, the arm of the wave loading, creating a moment in the hinge, is reduced. This reduction is the result of less wave loading in deeper waters and higher wave loading higher on the MP.

The upending bucket is considered the most future-proof method, as the MP is relatively well constrained during the upending. As mentioned, this method is currently used for side installation and therefore provides the perfect opportunity to compare this method for side and stern installation.
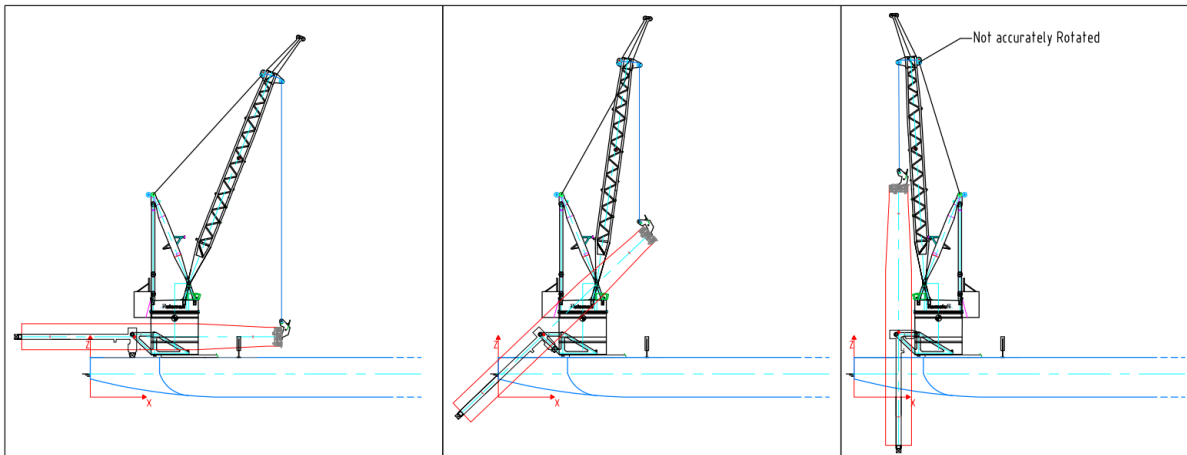
Figure 1.13: Currently used upending bucket, positioned on stern of the vessel for reference.

1.4. Literature Findings

A large variety of installation steps can be chosen by the contractor. Most of these decisions depend on the installation vessel designed specifically for such tasks. In the design process of a new installation vessel, the logistics of wind installation should be considered to optimise installation and be ready for the future. One of the most influential design choices is the direction of installation, stern or side. This choice influences storage options, upending choices, motions and accelerations of the vessel and thus workability. In this regard, some main findings are presented.

Stern Installation

Many contractors are currently installing MPs over the side of the vessel. Advantages of this method can be found in the vessel's storage logistics and shielding capabilities. However, as MPs are increasing significantly in the near future, it is believed that stern installation might improve the workability of an installation vessel. As the response of a vessel in the pitch direction is usually less sensitive to waves, and a recess in the hull can still provide shielding for the MP, this method might be an interesting alternative for harsher weather conditions.

Future Monopiles

As discussed in section 2.1, monopiles will significantly grow in size and weight due to the increasing sizes of wind turbines and water depths in the coming years. As a result, installing these MPs can become increasingly more complex, so research is needed. This report presents a range of MPs, with the "MP Small" as a reference pile and the "MP Giga" as an extreme case.

All-year installation

To say something about the installation windows of different methods, the environmental conditions are characterised for four distinct seasons. Currently, installation only takes place in spring and summer, but it might be needed to include autumn and maybe even winter in the installation schedule to achieve renewable energy ambitions.

Installation Performance

To compare different installation methods fairly, it is essential to qualify and quantify certain aspects of the installation. Such aspects are translated to Key Performance Indicators, which will be used to state the differences between side and stern installation objectively.

Floating Vessels

Traditionally, wind turbines are installed by jack-up vessels, which have developed from general crane barges to purpose-built wind installation vessels. Jack-up vessels, however, have downsides, which can be found in the time it takes to position itself and the size of the legs, which significantly limit the use of deck space. To overcome these limitations, floating vessels are used more often, as these can relocate quickly and can have a huge usable deck space. However, these floating vessels experience more motions, are more weather dependent and experience changing behaviour throughout the installation procedure due to the MPs. These issues are to be addressed in this thesis.

1.5. Problem Statement

In the wind installation industry, a shift is seen from jack-up vessels to floating installation vessels. Currently, a range of vessels is used or manufactured, which are all based on the side-installation principle. However, it is unknown whether this principle is future proof and experts at Huisman believe that longitudinal storage and stern installation might propose a strong concurrent method.

Currently, no objective comparison has been made between side and stern installation. There appear to be significant benefits for stern installation, but the current market focuses on side installation. The comparison should look into three steps of installation; the effect MPs have on an installation vessel, the loads on MPs during transfers and the upending procedure.

1.6. Research Questions

Taking the above-stated problems in mind, a research question is derived. This question is supported by a series of sub-questions, which will guide the project. The main research question is formulated as follows:

> *"Can stern installation of monopiles improve all-year installation performance for floating vessels?"*

To complete this research, multiple sub-questions have been formulated:

1. What are performance indicators for the installation of an MP?
2. Which step governs the installation sequence of an MP?
3. What is the difference in dynamics between stern and side on an equal vessel?
4. What is the difference in installation performance between side and stern on an equal vessel?
5. What are equipment requirements for over stern installation?

1.7. Aim and Scope

This thesis focuses on the difference between the side and stern installation of Monopiles. Three aspects are selected, which have not been investigated yet. First the change in the vessel's behaviour due to MPs stored on its deck. Second, the loads the MP has to endure while being transported on such a vessel. Last is the difference in loads on the equipment during the upending procedure.

This thesis aims to give an objective distinction between the side and stern installation while creating a framework in which concepts can be easily checked on their feasibility. Assumptions are checked on their sensitivity and practical implications of the research are evaluated.

1.8. Structure of Report

After an introduction stating the importance of future monopile installation and the potential growth hereof, this thesis presents a knowledge gap which requires investigation in chapter 1. Chapter 2 focuses on the inputs needed for analysis, such as environmental loads, monopile selection, vessel characterisation, and key indicators that can objectively determine how the results will be evaluated. In Chapter 3, the first of the two unknowns is addressed, namely the storage of MPs on the deck of an installation vessel and the effects of such storage. In Chapter 4, the second unknown is looked into; here, the upending procedure is investigated by developing a model which can position the upending anywhere on a vessel and, therefore, objectively evaluate the accelerations, loads and limits of such operation. This chapter is ended with a short analysis of the feasibility of the hypothetical concept, which is created by the model, and a sensitivity analysis of the model. In Chapter 5, practical aspects of this thesis are emphasised, which could be used to develop the model and concept further. In Chapter 6, the workability difference between upending over the side vs stern is calculated, which is found to be an objective method. Finally, conclusions and recommendations are presented in Chapter 7.

2

Basis of Design for MP installation

In this chapter, the inputs for an objective comparison method are presented. First, a variety of mono-piles is given, on which this thesis is based. Presenting both current MPs as well as future XXL MPs gives some insight into the scale of MPs. Second, environmental data is gathered for a specific site, with which the vessel's and MP's motions and loading can be calculated. Third, a reference vessel is presented on which the MPs will be stored, transported and installed in this thesis. Relevant vessel data such as RAOs are shown, as these will be used throughout this thesis. Fourth, a reference crane is given, which is used to check concepts and ideas on their feasibility. At last, an evaluation of the key performance indicators is executed, where the focus for the following chapters is determined.

2.1. Monopile characteristics

In this report, a range of MPs is taken into account, which can be seen below. The dimensions and weight of these MPs have been given by Huisman experts, who use these MPs for the development of equipment. Naming conventions are trivial and are only used to refer to this table. Storage loads are evaluated for the full range of MPs, whereas the upending method is primarily evaluated using the MP L. The length dimensions S1-3 are indicated on MP Small in Figure 2.1.

Information about the MPs is stored in arrays. One unknown and site-specific characteristic, being the diameter over thickness ratio (D/t), has been assumed to increase linearly from bottom to top. The ratios for each MP have been iteratively adjusted to match the given weight. It is realised that this thickness varies from reality, however, it is presumed to be accurate enough for the scope of this thesis. The arrays used in this thesis are:

$$x_{mp} = \text{X-coordinate of MP segments with } x_{mp} = 0 \text{ at CoG}$$
$$W_{mp} = \text{Weight of MP segment}$$
$$D_{mp} = \text{Diameter of MP segment}$$
$$t_{mp} = \text{Thickness of MP segment}$$

Table 2.1: Dimensions of a range of MPs

Name	Diameter		Length				D/t		Weight
	Bottom [m]	Top [m]	S1 [m]	S2 [m]	S3 [m]	Total [m]	Bottom [-]	Top [-]	[mT]
MP Small	9.5	6.5	40	21	6	67	145	105	1000
MP L	11	8	74	30	6	110	131	95	2600
MP XL	14	8	83	36	6	125	162	122	3500
MP XXL	15	8	83	46	6	135	185	119	4000
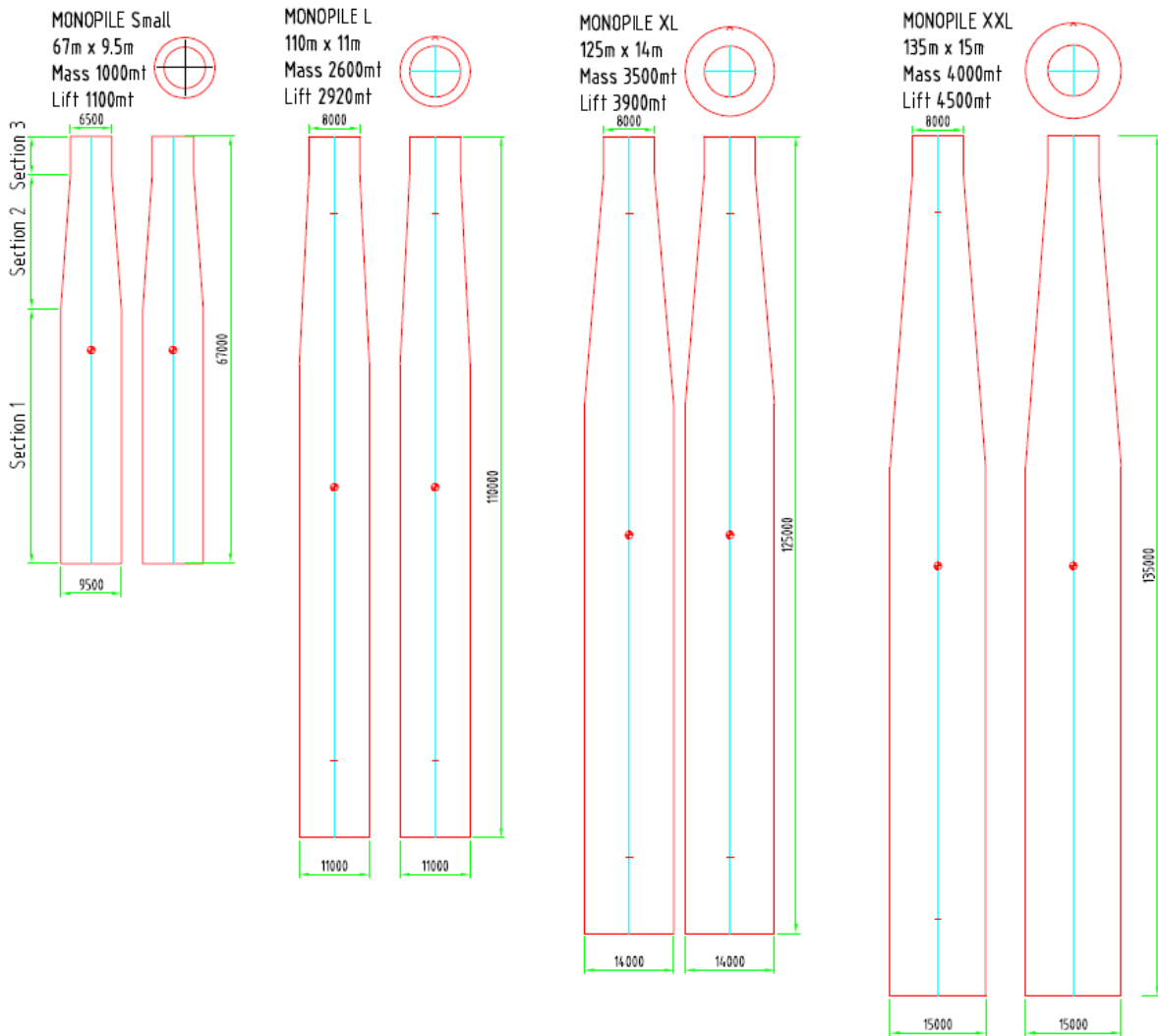
Figure 2.1: Dimensions of four selected monopiles to be used for further research. Section 1 2 and 3 as used in Table 2.1 are indicated on MP Small

2.2. Environmental Data

When installing an MP using a floating vessel, the major source of loads on the structure comes from environmental loading. Both the vessel and the MP experience loading from waves and wind. The difference in response of the vessel, and the particular direction of loading on the MP is what distinguishes side from stern installation. In this section, the environmental states of a specific site in the north sea are described, which will be translated into loads in the following sections.

2.2.1. Wave Conditions

Global Wave Statistics [23] provides seasonal information on waves, such as wave heights and periods. Scatter tables per 3 months are given, which indicate the probability of a particular significant wave height (H_s) and zero-crossing period (T_z) combination within that season. The seasons as described here are winter (December-February), Spring (March-May), Summer (June-August) and Autumn (September-November). For example, in Figure 2.3 this table can be found for spring (March-May)[23]. It should be noted that this information was published in 1986. However, for this thesis, the accuracy of this information is proficient. The aim is to provide insight into a workability comparison throughout the year, not to do day-to-day planning for an actual installation. All the information is combined in bar plots which can be found in Figure 2.2, where each colour represents a season.
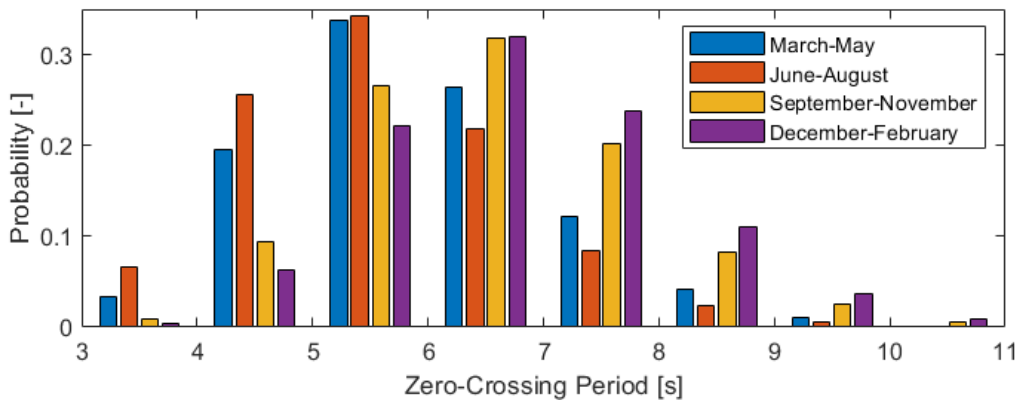
(a) The zero-crossing period probability distribution for 4 seasons as seen in the North Sea, given by GWS[23]
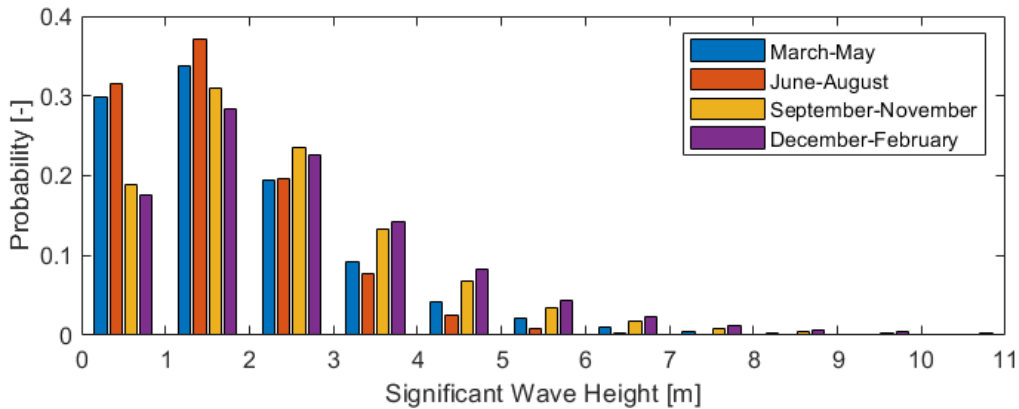
(b) Significant wave height probability distribution for 4 seasons as seen in the North Sea, given by GWS[23]

Figure 2.2: Seasonal Wave conditions of North Sea

Hs, bin		Hs,Mean	34	196	338	264	122	41	10	0	0	0	1005
> 14		14.5											0
13	14	13.5											0
12	13	12.5											0
11	12	11.5											0
10	11	10.5											0
9	10	9.5											0
8	9	8.5					1	1	1				3
7	8	7.5			1	2	1	1					5
6	7	6.5			2	3	3	1	1				10
5	6	5.5		1	4	7	5	3	1				21
4	5	4.5		2	10	12	11	5	1				41
3	4	3.5		6	25	32	20	8	2				93
2	3	2.5	1	20	62	65	33	11	3				195
1	2	1.5	5	60	128	97	37	9	2				338
0	1	0.5	28	107	106	45	11	2					299
Tz, Mean			3.5	4.5	5.5	6.5	7.5	8.5	9.5	10.5	11.5	12.5	
Tz, Bin			4	5	6	7	8	9	10	11	12	> 12	
			0	4	5	6	7	8	9	10	11		

Figure 2.3: Scatter Plot of wave height and peak period probability from March to May.

JONSWAP

A wave spectrum exists for every significant wave height and zero-crossing time. This wave spectrum results from wind-generated waves, white-capping and quadruplet wave-wave interaction. All these effects cause a non-linear combination of waves to occur at a specific moment in time and location. To reproduce an accurate time series of waves for simulations, standard wave spectra are described by researchers of the late 1900s. These models are still considered valid and therefore used in this report. The oldest spectrum, found by Bretschneider [6], is commonly used for open sea areas. ISSC and ITTC have accepted this formulation in the form of the Modified Two-Parameter Pierson-Moskowitz Wave spectrum, which describes fully developed seas. However, in fetch limited (coastal) wind-generated seas, it appeared that the peak was not correctly described. To solve this, an extensive measurement program was carried out in 1968 and 1969, called the Joint North Sea Wave Project (JONSWAP)[22]. This spectrum is considered accurate for the north sea, which will be investigated in this report. The spectrum gives a relation between the Wave Spectral Density (S_ζ) and the angular velocity (ω) for a specific peak period (T_p) and significant wave height (H_s).

The following set of equations gives the JONSWAP spectrum:

$$S_\zeta(\omega) = \frac{320 \cdot H_s^2}{T_p^4} \cdot \omega^{-5} \cdot exp\left\{\frac{-1950\omega^{-4}}{T_p^4}\right\} \cdot \gamma^A \qquad (2.1)$$

with:

$$H_s = \text{Significant Wave Height}$$
$$T_p = \text{Peak Period}$$
$$\omega = \text{Angular velocity}$$
$$\gamma = 3.3 \text{ (peakedness factor)}$$
$$A = exp\left\{-\left(\frac{\frac{\omega}{\omega_p}-1}{\sigma\sqrt{2}}\right)^2\right\}$$
$$\omega_p = \frac{2\pi}{T_p}$$
$$\sigma = \begin{cases} 0.07 & \text{if } \omega < \omega_p \\ 0.09 & \text{if } \omega > \omega_p \end{cases}$$

For a range of peak periods (T_p), the JONSWAP spectrum is plotted in Figure 2.4. Here the difference with Pierson-Moskowitz is clearly seen for $T_p = 9s$. To get insight into the actual wave behaviour of such a spectrum, a random time series realisation for $H_s = 2m$ and $T_p = 9s$ is presented in Figure 2.5. Here it can be seen that the actual wave height overshoots the H_s at least ten times during these 200 seconds. This is something to consider in a later stage of the research.
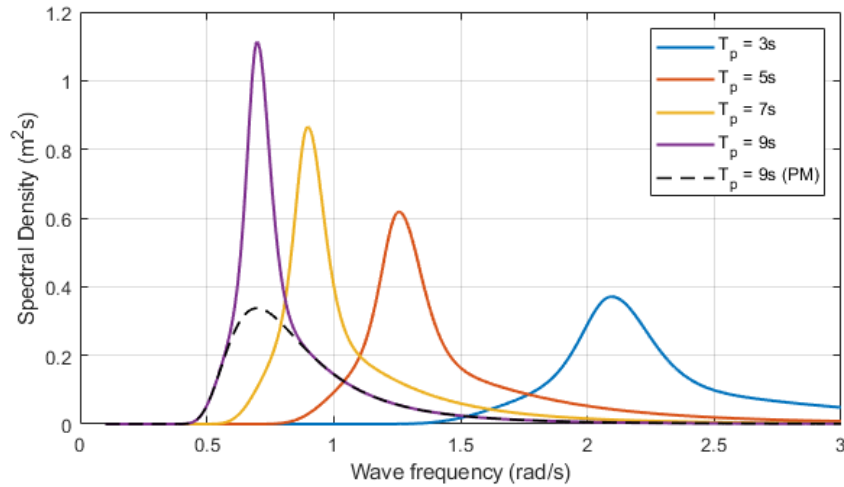
Figure 2.4: JONSWAP wave spectra for significant wave height ($H_s = 2m$) and variable Peak Periods (T_p). For $T_p = 9s$ the Pierson-Moskowitz spectrum is added to indicate the peak enhancing characteristic of JONSWAP
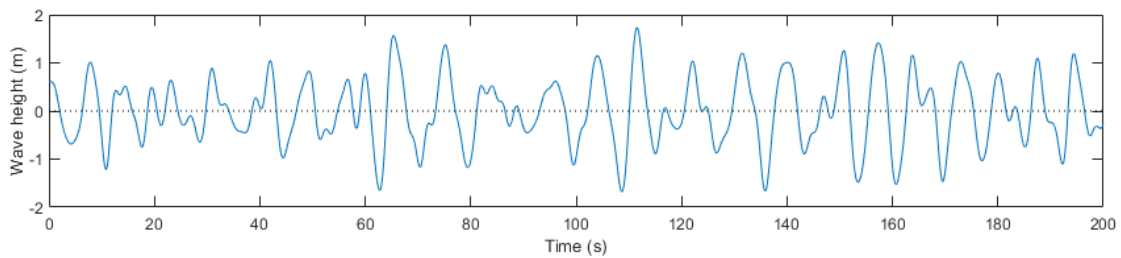
Figure 2.5: Time series realisation of a JONSWAP spectrum for significant wave height ($H_s = 2m$) and variable Peak Periods ($T_p = 9s$)

2.2.2. Wind Conditions

For handling and transferring, a crane is often used. The suspended load, being the MP, can begin to swing due to vessel motions leading to crane motions. However, the second source of swinging requires some attention too. A wind turbine is usually installed in a location with high wind speeds, and a suspended MP is quite a wind catcher. A Marine Warranty Surveyor can choose to not allow a lift due to high wind loads. However, when the lift is permitted, the wind still affects the MP, and this load must be considered in this comparison.

To get insight into the wind speeds, Figure 2.6b shows the average wind per month generated from the IRENA Global Atlas [2]. The Global Wind Atlas [4] has been used to find a location in the North Sea that could govern this analysis. The site can be seen in Figure 2.6a. As can be seen, the wind speed varies quite strong within a year. For this thesis, the worst case of each season is selected for the workability analysis. For winter, January is governing with an average wind speed of $12.29m/s$ at the height of $60m$. As the wind varies over time, locally, the wind can significantly exceed the average wind speed. A Weibull Probability Distribution can characterise North Sea winds with a shape factor of 2.3, and a scale factor dependant on the location [51]. In Figure 2.7 a Weibull distribution is presented, which is chosen such that the average wind speed is $12.29m/s$. Additionally, an 85th percentile line is added, which indicates a probability of 85% for wind speeds reaching $19.2m/s$. This probability is considered to include all possible weather windows suitable for MP installation; therefore, this wind speed is used as a load case for this season.
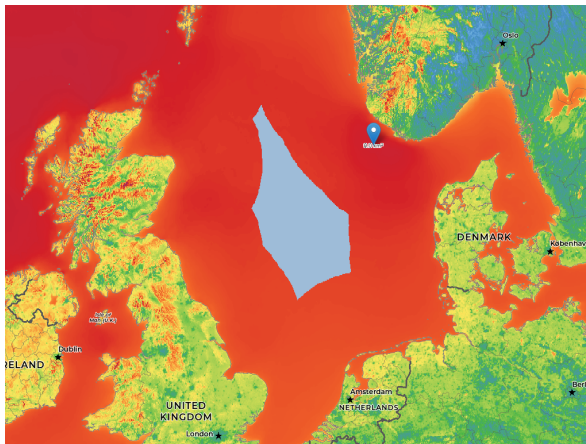
(a) Snapshot from the global wind atlas indicating Mean Wind Speed at a height of 10m. A point is placed at roughly the highest mean wind speed [4]
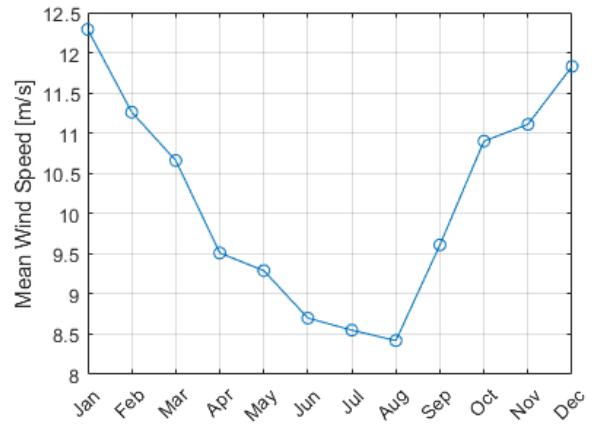
(b) Mean wind speed at a height of 60m per month for the coordinate as indicated in Figure 2.6a, 57.80°,5.71° taken from IRENA Global Atlas [2]

Figure 2.6: Wind conditions analysis

Besides variations of wind speed in time, the wind speed varies locally over height due to the friction of the Earth's surface. Additional analysis has been done on the wind speeds at different heights. The reference wind speed is measured at $60m$, generally used as blending height. Below this blending height, the atmospheric boundary layer is reducing the wind speeds due to the before-mentioned frictional effects. For heights lower than $60m$, the logarithmic wind profile can be used. Above $60m$, the Power law is used [53]. Both are evaluated using the equation below. The wind speed at a height from $0m$ to $100m$ is presented visually in Figure 2.7

$$U_w(h) = \begin{cases} U_w(h_{ref}) \dfrac{ln\left(\frac{h}{z_0}\right)}{ln\left(\frac{h_{ref}}{z_0}\right)} & 0 < h \leq 60 \\[3ex] U_w(h_{ref}) \left(\dfrac{h}{h_{ref}}\right)^{\alpha} & h > 60 \end{cases} \tag{2.2}$$

with:

$$U_w = \text{Wind Speed } (m/s)$$
$$h = \text{Height } (m)$$
$$h_{ref} = 60m$$
$$z_0 = 0.0002m \text{ (surface roughness at sea [53])}$$
$$\alpha = 0.11 \text{ (power ratio at sea [53])}$$
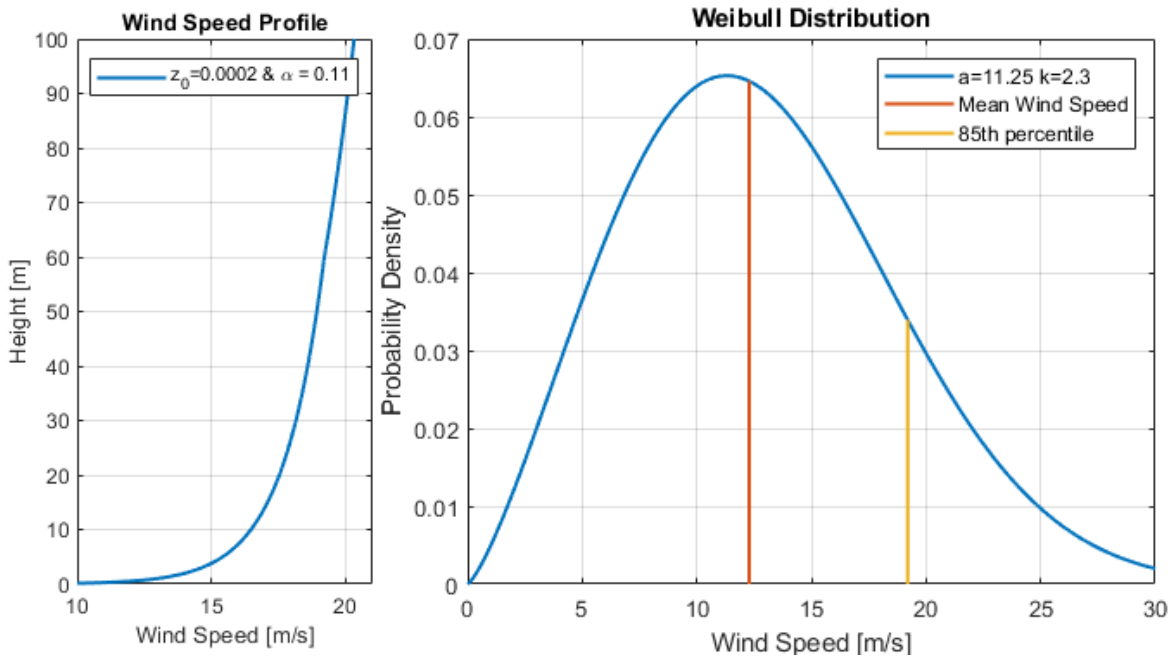
Figure 2.7: Wind speed information, consisting of a vertical wind profile and Weibull distribution for a shape factor as seen in the North Sea and a scale factor chosen such that the mean wind speed is 12.29m/s as seen in Figure 2.6b.

2.3. Environmental Loading

Now that the environmental data is known, the next step in this research is finding the loads that these waves and wind exert on the MP. In this section, the calculations for this are presented.

2.3.1. Wave Loading

As discussed, future-proof upending procedures will most likely be semi-submerged to keep the boom lengths to a minimum. The wave impact on the submerged part leads to a significant loading, which has to be taken into account for this analysis. In this section, the method used for this wave analysis is shown. In Figure 2.8 a sketch is presented to clarify the following equations. The Morison equation, as given by [31] takes both drag and inertia effects into account. This equation is given as follows:

$$F(t) = \frac{\pi}{4}\rho C_M D^2 \cdot \dot{u}(t) + \frac{1}{2}\rho C_D D \cdot u(t)|u(t)| \qquad (2.3)$$

To calculate the speed and acceleration of the water, a few steps must be taken. First, an accurate wavelength is calculated using dispersion relation with an initial guess of deep water waves. Then, this step is iterated to find the actual wavelength.
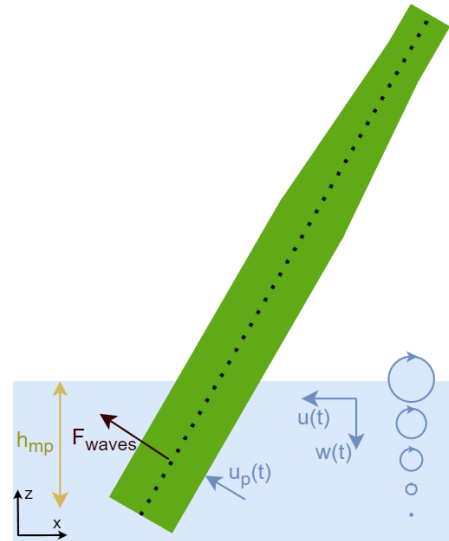
Figure 2.8: Sketch of wave velocities and drag load induced by this on the MP.

$$\lambda_0 = \frac{gT_p^2}{2\pi} \qquad (2.4)$$

$$\lambda = \frac{gT_p^2}{2\pi}\tanh\left(\frac{2\pi d}{\lambda}\right) \qquad (2.5)$$

with:

$$\lambda = \text{Wave Length } (m)$$
$$T_p = \text{Peak Period of waves } (s)$$
$$d = \text{Water depth } (m)$$

Secondly, the MP is divided into pieces, and the depth of these parts is stored in a vector. For the part of the MP where the centerline is above the water level but the edge of the MP is still below water level, the force on this below-water piece is calculated using a reduced diameter and an effective depth of half the depth of the edge.

$$h_{mp} = x_{mp}sin\left(\theta_{mp}\right) + h_0 \tag{2.6}$$

with:

$$h_{mp} = \text{Z coordinate of each element with length } dx \text{ of MP } (m)$$
$$x_{mp} = \text{X coordinate of MP with 0 being the CoG location } (m)$$
$$\theta_{mp} = \text{Angle of MP with Y axis of vessel } (rad)$$
$$h_{CoG} = \text{Height of CoG of MP while horizontal on deck } (m)$$

Subsequently, the speed and acceleration at every depth are calculated in both the horizontal (u) as well as the vertical (w) direction.

$$u(t) = \frac{\omega H_s}{2} \frac{\cosh\left(k(h_{mp} + d)\right)}{\sinh\left(kd\right)} \cos(\omega t) \tag{2.7}$$

$$w(t) = \frac{\omega H_s}{2} \frac{\sinh\left(k(h_{mp} + d)\right)}{\sinh\left(kd\right)} \sin(\omega t) \tag{2.8}$$

$$\dot{u}(t) = \frac{-\omega^2 H_s}{2} \frac{\cosh\left(k(h_{mp} + d)\right)}{\sinh\left(kd\right)} \sin(\omega t) \tag{2.9}$$

$$\dot{w}(t) = \frac{-\omega^2 H_s}{2} \frac{\sinh\left(k(h_{mp} + d)\right)}{\sinh\left(kd\right)} \cos(\omega t) \tag{2.10}$$

with:

$$\omega = 2\pi/T_p = \text{Angular velocity } (rad/s)$$
$$k = 2\pi/\lambda = \text{Wave number } (rad/m)$$
$$H_s = \text{Significant Wave Height } (m)$$

From this, a perpendicular speed and acceleration are determined, where the current speed is also taken into account.

$$u_p = (u(t) + u_{current})sin(\theta_{mp}) + w(t)cos(\theta_{mp}) \tag{2.11}$$
$$\dot{u}_p = \dot{u}(t)sin(\theta_{mp}) + \dot{w}(t)cos(\theta_{mp}) \tag{2.12}$$

With this, the behaviour of the water around the MP can be qualified using the Reynolds and Keulecan-Carpenter number. Note that the KC number is calculated with a reduced velocity, neglecting the current velocity.

$$Re = \frac{u_p D_{mp}}{\nu_{water}} \tag{2.13}$$

$$KC = \frac{u_{p.red} T_p}{D_{mp}} \tag{2.14}$$

with:

$$D_{mp} = \text{Diameter of MP at every x-coordinate } (m)$$
$$v_{water} = 10^{-6} \ m^2/s \text{ Kinematic Viscosity of water}$$
$$u_{p.red} = \text{Reduced perpendicular velocity without current}$$

With the calculated Re and KC, the Added Mass Coefficient C_M and Drag Coefficient C_D can be found. Typical numbers for these values can be found in the table below.

Table 2.2: Morison Coefficients as given by Journée [31]

	$Re < 10^5$		$Re > 10^5$	
KC	C_D	C_M	C_D	C_M
< 10	1.2	2.0	0.6	2.0
≥ 10	1.2	1.5	0.6	1.5

Finally, with all the gathered information Equation 2.3 can be evaluated for each of the MP segments below water.

$$F_{waves}(t) = \frac{\pi}{4} \ \rho_{water} \ C_M \ D_{mp}^2 \ \dot{u}_p(t) \ dx + \frac{1}{2} \ \rho_{water} \ C_D \ D_{mp} \ u_p(t) \ |u_p(t)| \ dx \qquad (2.15)$$

with:

$$\rho_{water} = 1025 kg/m^3$$
$$dx = \text{Segment length } (m)$$

2.3.2. Wind Loading

Similarly to wave loading, the wind induces a load in the MP. This wind load is calculated for a changing angle of upending (θ_{mp}) and various wind directions (ψ_{wind}). The height of the MP segments is calculated similarly to sub-section 2.3.1 and is thus not reported. The wind speed at a specific height is calculated in subsection 2.2.2; this information is used in this analysis. Note that for this analysis, the wind is considered to have a constant speed with no defined oscillation.

As before, the wind speed in the perpendicular direction of the MP is evaluated for each segment.

$$U_{w.p} = (U_w)\left(1 - cos(\theta_{mp})\frac{2(\pi - \psi_{wind})}{\pi}\right) \qquad (2.16)$$
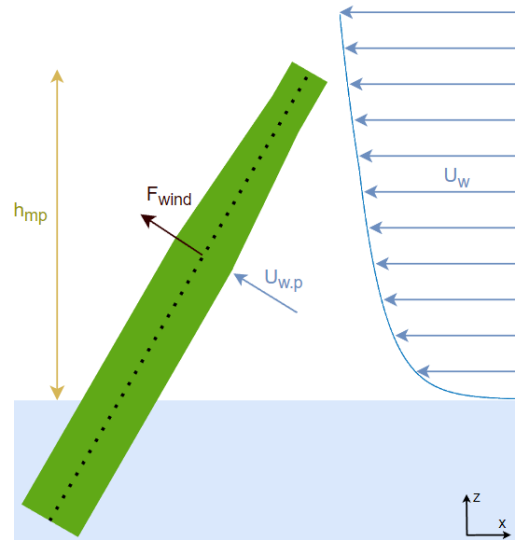
Figure 2.9: Sketch of wind velocities and drag load induced by this on the MP.

with:

$$U_w = \text{Horizontal wind speed at a certain height } (m/s)$$
$$\theta_{mp} = \text{Angle of MP with Y axis of vessel } (rad)$$
$$\psi_{wind} = \text{Angle of wind origin as defined by Figure 2.11 } (rad)$$

After that, the Reynolds number is calculated to find the drag coefficient of the air passing the MP. Note that the kinematic viscosity of air is now used. With this Reynolds number Table 2.2 is consulted to find an accompanying drag coefficient (C_D).

$$Re = \frac{U_{w.p} D_{mp}}{v_{air}} \tag{2.17}$$

with:
$$U_{w.p} = \text{Perpendicular Wind speed at a certain height from subsection 2.2.2}$$
$$v_{air} = 1.5 \cdot 10^{-5} m^2/s \text{ (Kinematic Viscosity of Air)}$$

Finally, the wind load is calculated using the Morison equation's drag part.

$$F_{wind} = \frac{1}{2} \rho_{air} C_D D_{mp} U_{w.p} |U_{w.p}| dx \tag{2.18}$$

with:

$$\rho_{air} = 1.225 kg/m^3$$
$$dx = \text{Segment length } (m)$$

2.4. Vessel characteristics

To make a fair comparison between side and stern installation, a single vessel is selected on which both methods will be modelled. The reference vessel has a stern recess included in its design, which can be used as shielding for wave impact during installation. This stern recess is evaluated in chapter 6. Figure 2.10 has been included for reference. The dimensions of this vessel are comparable to many of the new-built wind installation vessels, and experts at Huisman indicate that the vessel's behaviour is typical for these kinds of vessels. Therefore, this vessel is considered a good reference.

Table 2.3: Vessel Characteristics of the reference installation vessel

Parameter	Symbol	Value	Unit
Dimensions			
Length at Waterline	$L_{vessel,wl}$	219	m
Length of Deck	L_{deck}	174	m
Beam	B_{vessel}	56	m
Draught	T_{vessel}	9.8	m
Depth	D_{vessel}	16.8	m
Weight			
Displacement	W_{vessel}	93845000	kg
Center of Gravity in X	X_{cog}	101.7	m
Center of Gravity in Y	Y_{cog}	0	m
Center of Gravity in Z	Z_{cog}	14.5	m
Moment of Inertia			
Moment of Inertia in X axis	I_{11}	$6.4 \cdot 10^{10}$	kgm^2
Moment of Inertia in Y axis	I_{22}	$3.0 \cdot 10^{11}$	kgm^2
Moment of Inertia in Z axis	I_{33}	$2.7 \cdot 10^{11}$	kgm^2
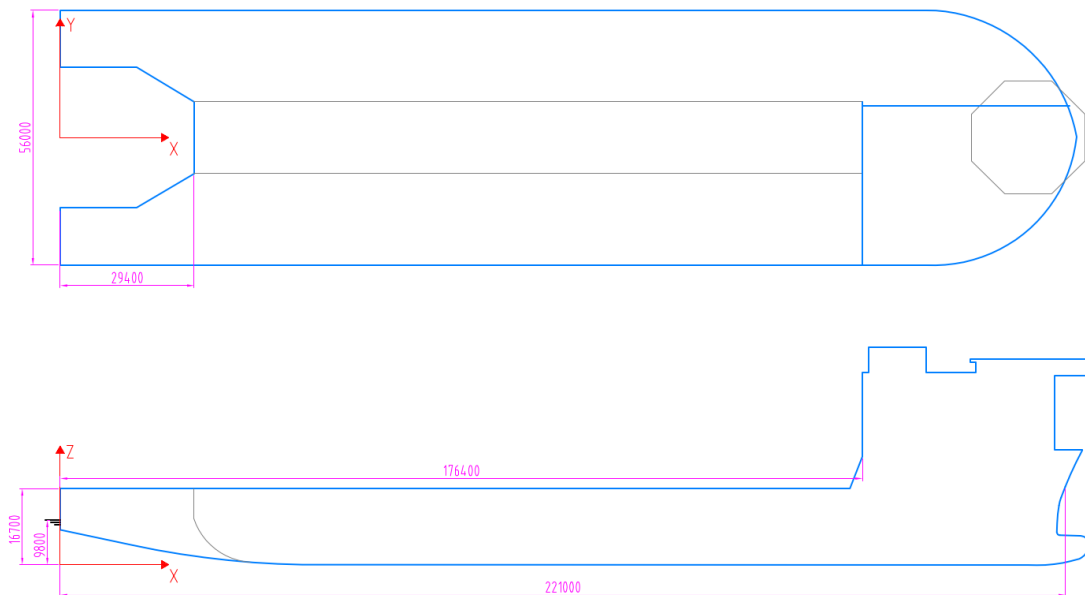
Figure 2.10: Drawing of the hull of reference vessel for this report.

2.4.1. Response Amplitude Operator

When a spectrum of waves is set to excite the vessel, it is essential to know how it will respond to specific frequencies and amplitudes. A Response Amplitude Operator is a table that connects the wave excitement with the vessel responses and can be used to generate a vessel's motions, velocities and accelerations. A separate RAO can be found for every orientation of the vessel with respect to the waves.

A significant difference between stern and side installation is the vessel heading. When installing over the stern, the installation vessel is usually positioned head seas, corresponding with waves coming between $150 \deg$ and $180 \deg$, following the direction conventions as presented in Figure 2.11. When installing over the side, the vessel is usually positioned in bow or beam seas (between $135 \deg$ and $165 \deg$, such that shielding of the waves occurs on the installation side. Figure 2.12 combined with Table 2.4 explains the used definitions.
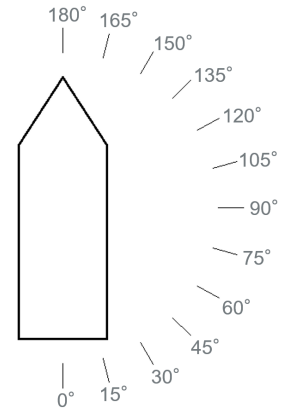
Figure 2.11: Convention of wave directions used for RAO calculations

A few things can be noted when looking at the RAOs of the reference vessel for different directions. First, the straightforward facts are that surge is highest for a head sea and sway for a beam sea. In roll, the natural frequency of the vessel in this direction can be seen, as the amplitude at a period of $23s$ is much higher than 1 for all seas which are not purely head. In pitch, it is remarkable that a 120° sea has a high peak at lower wave periods compared to the more head seas. In the heave graph, it is seen that the 90° sea approaches some eigenfrequency around a wave period of $10s$, whereas the more head seas appear to have a high resistance to this wave period. Lastly, it should be noted that a slight increase in response occurs in the yaw direction for wave periods of around $23s$ for all non-head seas.

The RAOs as presented here are taken from an empty load condition of the vessel. This means that this response will not precisely be the vessel's response when (fully) loaded. Therefore, further research into the effect of loads and the sensitivity thereof is required to calculate how the vessel will respond in full detail. However, due to the lack of this information, the current RAOs will be used to get the first insight into the motions and accelerations.
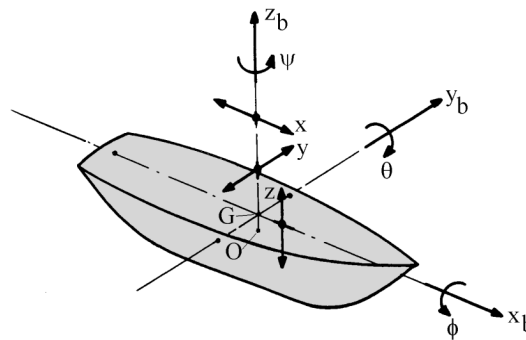
Figure 2.12: Definition of vessel motions in six degrees of freedom according to [31]

Table 2.4: Explanation of vessel motion definitions

Symbol	Definition
x_b	Surge
y_b	Sway
x_b	Heave
ϕ	Roll
θ	Pitch
ψ	Yaw
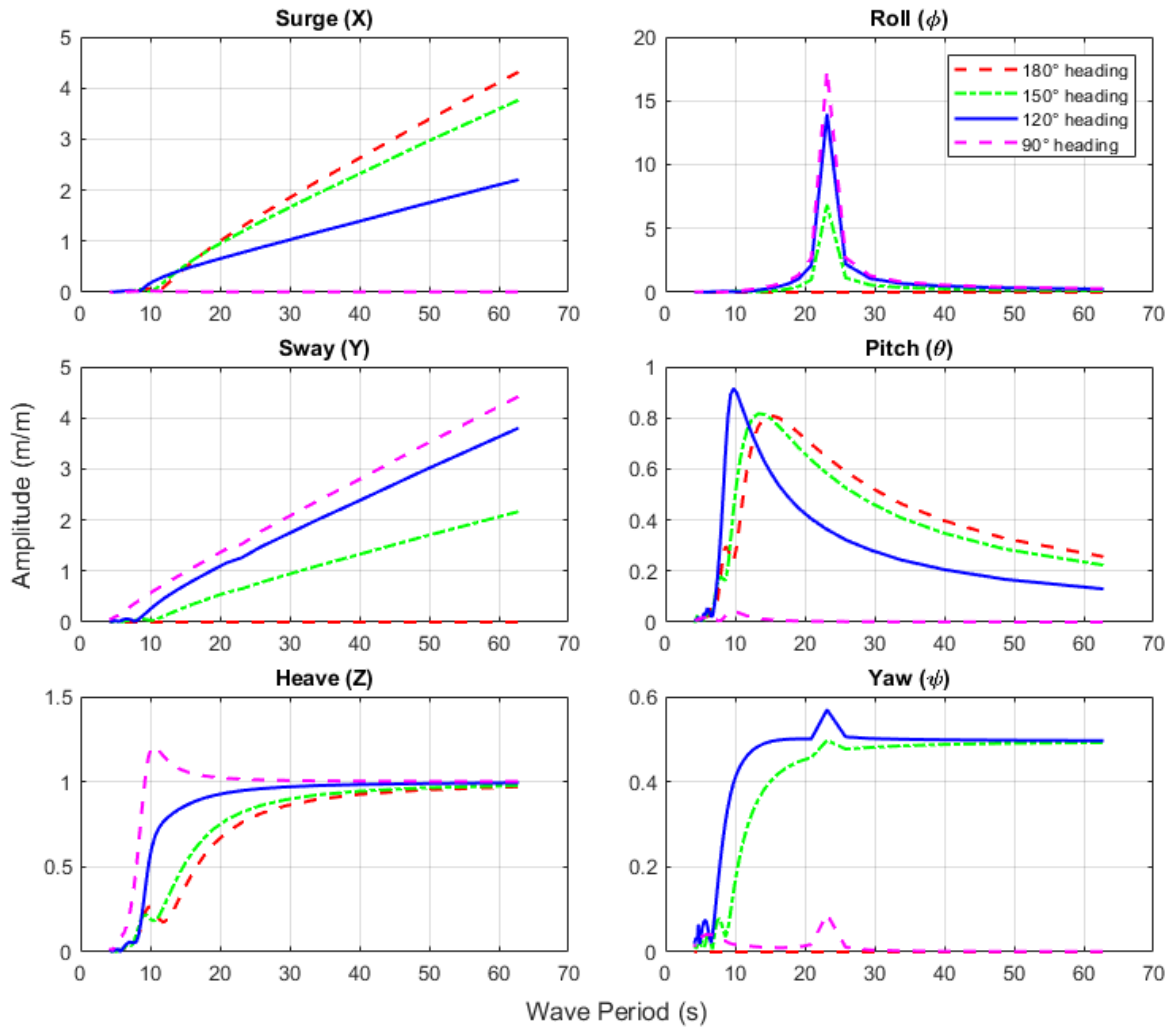
Figure 2.13: RAOs of the principal axes of the reference vessel for a range of wave directions.

2.4.2. Shielding

The main difference between a floating installation and a jack-up installation vessel is the motions imposed by the waves. Jack-up vessels are rising high above the waves, where they provide a stable working and lifting platform. HLVs experience wave loading on the hull and, therefore, will move in all six degrees of freedom. However, an advantage of the floating installation is that the vessel interacts with the waves in such a way that wave loading on the MP can be significantly reduced compared to a jack-up. When a vessel is positioned in a favourable direction compared to the waves, the energy of these waves is diminished in the wake of the vessel. Numerical research has been performed to find which directions and wavelengths are favourable [33]. Although such responses are vessel-specific, some helpful insight is generated. After a discussion with an expert in system dynamics, the effect of shielding has been deduced into two main findings, which will be considered in this thesis.

- Shielding is necessary for the installation of MPs. The vessel's heading for side installation should be around $\psi_v = 150°$ and for side around $\psi_v = 165°$. As seen in Figure 2.15, a deviation from this heading would still provide some shielding.

- All waves with $T_p < 6s$ will be blocked by the vessel when in the orientation as stated before. This is implemented in the model by capping the wave loading on the MP on $T_p = 6s$ and using this value for all $T_p < 6s$ waves.

To visualise the effect shielding has, the wave loading on the MP is presented in Figure 2.14. This figure shows the sum of forces and the moment at the hinge for a range of upending angles. During the upending, the angle between MP and waves changes. This influences the drag force on the MP and the arm with which this force acts on the hinge. It can be seen that if periods below $T_p = 6s$ are blocked by the vessel, a significant load reduction in the MP is achieved.

In Figure 2.15, the results of a thorough shielding analysis executed by Huisman are graphically presented. The arrows indicate the required heading, the marked area shows where a reduction of waves is present, and the coloured dots indicate how effective the location is shielded. Here it can be seen that the recess on the stern of the vessel improves the shielding quality for stern installation.

(a) Sum of forces perpendicular to the MP induced by waves of varying Peak Periods and Significant wave height $H_s = 2.25m$ and current of $u_{current} = 0.75m/s$

(b) Moment in Hinge ($47m$ from bottom of MP) induced by waves of varying Peak Periods and Significant wave height $H_s = 2.25m$ and current of $u_{current} = 0.75m/s$
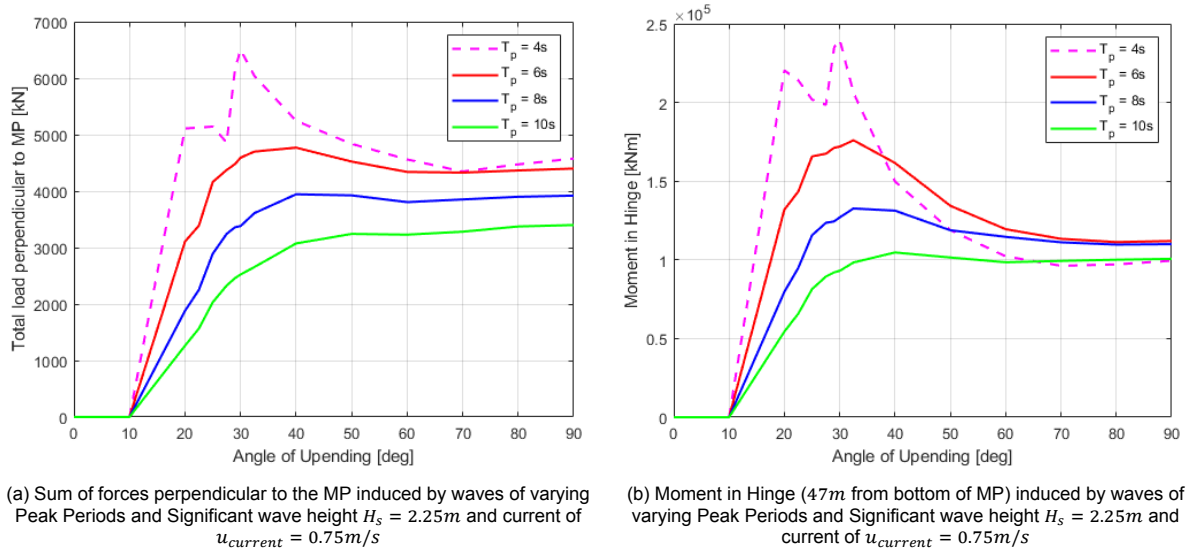
Figure 2.14: Wave loading on an MP for a range of Peak periods
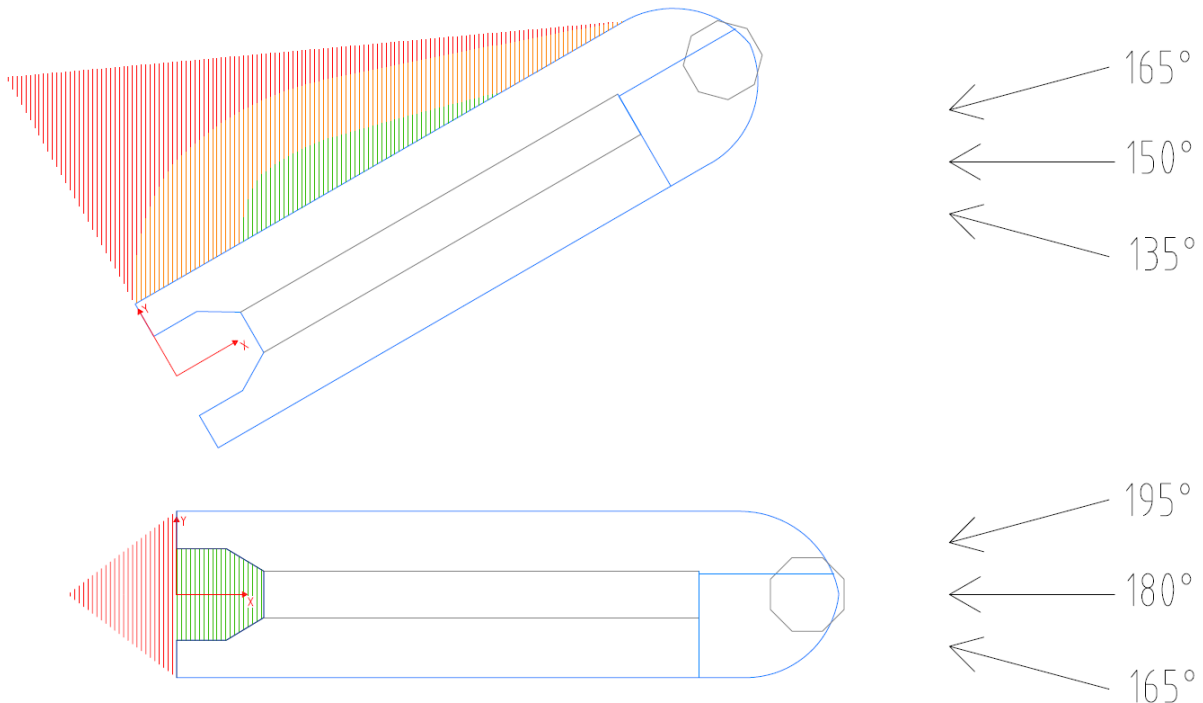
Figure 2.15: Sketch of shielding areas for side and stern installation, using $\psi_v = 150 \pm 15°$ for side installation and $\psi_v = 180 \pm 15°$ for stern installation.

2.5. Crane characteristics

To check concepts, a reference crane is generated. A 5000 mT Tub Mounted Crane (TMC) with a dual main hoist is selected [26]. General characteristics are presented below. In the model design, the crane has been placed on the vessel's port side at a distance of $33m$ from the stern of the vessel. Using the capacity of the crane, the deck logistics of the vessel are checked for all concepts.

Table 2.5: Crane Characteristics of the reference crane

Parameter	Symbol	Value	Unit
Main Hoist			
Working Load @21m	SWL_{mh}	5000	mT
Working Load @55m	$SWL_{mh.55m}$	3000	mT
Working Load @98m	$SWL_{mh.98m}$	1000	mT
Hook Height above deck	h_{mh}	129.5	m
Minimal Radius	$R_{mh.min}$	21	m
Maximal Radius	$R_{mh.max}$	98	m
Whip Hoist			
Working Load	SWL_{wh}	250	mT
Hook Height above deck	h_{wh}	153	m
Minimal Radius	$R_{wh.min}$	25	m
Maximal Radius	$R_{wh.max}$	117.5	m
General Dimensions			
Boom Length	L_{boom}	114	m
Tub Diameter	D_{tub}	20	m
Pivot Height	H_{pivot}	47	m
Maximal Luffing speed	ω_{boom}	0.0014	rad/s
Maximal Slewing speed	ω_{tub}	0.031	rad/s

2.6. Key Performance Indicators

Workability

This statistical property indicates the percentage of time during which a specific procedure could be executed. Since no actual time series are considered in this thesis, some caution on the exact numbers is needed, as workability in the actual installation will be lower. However, this offset will be equal for side and stern installation and therefore, a comparison is possible.

Stresses in MP

For the first step in the installation procedure, the storage, a suitable performance indicator would be the maximal stress in the MP, as this is a quantity which incorporates the forces, moments, shape and size of the material.

Moment of Inertia of a vessel

One way to quantify the vessel's behaviour is through its Moment of Inertia in the three rotational axes. This quantity is both suitable for adjustment through hand calculations (instead of advanced software) and for generating insight into the behaviour of the vessel. It is realised that this is not the only influencing factor on the behaviour. However, this thesis accepts the inaccuracy since a comparison is made.

Motions of the vessel

As mentioned before, the major difference between the current installation with jack-ups and the future installation with floating vessels is the vessel's behaviour. A floating vessel experiences motions induced by the waves, which influence the installation performance. The vessel's rotation and translation, in a certain period, cause accelerations in every part of the vessel. Around the centerline, these will be minor, but at points far from the CoG these can be significant. An aspect of these motions,

which is not always incorporated into research, is the human factor. At certain sea states, the vessel can move with high amplitudes and high velocity, making it impossible to safely work on the deck of the vessel. In this research, the vessel's motions are used as input to generate accelerations of MP and equipment. The human limit is not taken into account.

Installation Time

As installing an offshore wind farm is a repetitive process, the focus is on keeping the cycle times as low as possible. A delay of 1 hour in installation time, repeated a hundred times, can cost more than a few weeks of delay at the end of a project. This delay is costly and gravely undesired. Therefore installation time would be a commonly used KPI in this analysis. However, it is decided that for this thesis, a probabilistic approach is taken, and therefore the time of an installation is not explicitly calculated. The overall number and duration of activities are confirmed to be similar for side and stern installation, and the performance of upending is expressed in workability rather than duration. Installation time is therefore put out of scope for this research. However, it is recommended for future research, as the next step in validating this model would be time simulations.

Accelerations of MP

Accelerations on a load which is not fully constrained are an excellent indication of the forces needed to keep this load in control. It is therefore believed that these accelerations are a suitable indicator for the difference between the side and stern installation, as long as the direction of acceleration is correctly compared.

Velocity/Stroke

When the complete installation procedure of an MP is considered, the stroke and velocity of the gripper during the lowering and pile-driving phase would be a natural addition to the accelerations indicator. However, these phases are not considered, so these indicators will not be used in this thesis.

Safety

When the offshore installation is addressed, usually safety is included in the discussion. This is because offshore operations are by definition dangerous, and minor accidents can cause significant downtime, damage or casualties. Within the comparison made in this thesis, safety distinctions are present. However, the scope of the research question is limited to an operational distinction between side and stern and therefore, safety is only addressed in this section. Some risks are reduced by altering the installation procedure from side to stern. For instance, the main hoist is connected above the deck instead of at a distance from the deck, which can be seen as an improvement. On the other hand, when the possibility of executing an installation is extended into rougher sea states, harsher weather can be encountered, which could lead to unexpected risks. As stated, safety is not considered in this thesis but should definitely be included in further research.

3

Offshore transportation on deck

During the installation sequence of MPs for an OWF, it is desired that an installation vessel can store multiple MPs on its deck. Therefore, the direction in which the MP is installed determines the deck layout of a vessel. In this chapter, some general aspects of MP storage and loading will be presented, after which a more thorough investigation into the effects of storage on the vessel and MP is executed.

3.1. Loading, transporting and storing monopiles

As said, vessel logistics are highly dependent on the direction of installation. Some aspects are pre-determined when the choice is made between side and stern installation, and some aspects are project-specific. A visualisation of both methods is seen in Figure 3.1 and 3.2. It should be noted that in these sketches, no upending tools are incorporated. In reality, one of these MPs would be positioned in an upending tool during transport. Secondly, the numbers used in the sketches are an indication of how the optimal deck layout would be for an increasing number of MPs. This is not the order in which the MPs are to be stored or removed. For both side and stern installation, some logistical remarks are made.

Side installation:

- When MPs are stored in the transverse direction on the vessel, a skidding system can be used to ease the load-in. A crane transfer to supports close by the crane can be followed by an on-deck skidding system which stores the MP further from the crane.

- The deck of the vessel is relatively well used during side installation. The MPs are sticking out of the vessel's hull, which requires less deck space per MP.

- During the installation procedure, the skidding system can be used again to position MPs in an upending tool.

- When a skidding system is not present, a lift from the storage position to the tool is required. This could significantly reduce the storage capacity of a vessel, as the crane's capacity on a high radius vastly decreases.

Stern installation:

- When stern installation is chosen, the deck use is significantly lower. As the vessel's centerline is required for the upending procedure, only the port and starboard sides can be used for storage. On these sides, only one MP fits directly on the deck.

- When it is desired to transfer more MPs, stacking these might be an option [48]. This requires lifting the MPs from storage to the upending tool, as skidding tools cannot reach this high. Storage loads for stacked MPs are considered equal to those of MPs stored directly on the deck. Therefore, stacking is only considered in the Moment of Inertia and stability. Figure 3.4 shows a stack of three MPs on the vessel.

- The load-in for stern installation is slightly more advanced, as the MPs need to be lifted over the stacking frame. However, the order of loading is somewhat flexible, as the crane should be able to reach all positions.

- During installation, the MPs need to be lifted from the (stacked) stored position into the upending tool. This operation is weather-dependent, and future research is recommended to optimise this procedure.
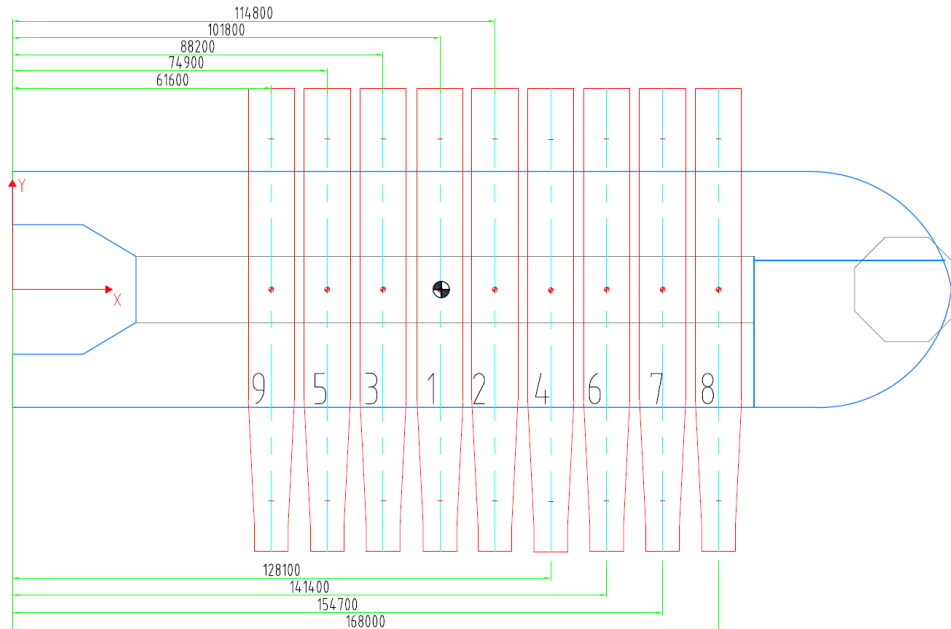
Figure 3.1: Transverse Storage of MP on a vessel with CoG location as reference for vessel impact calculations
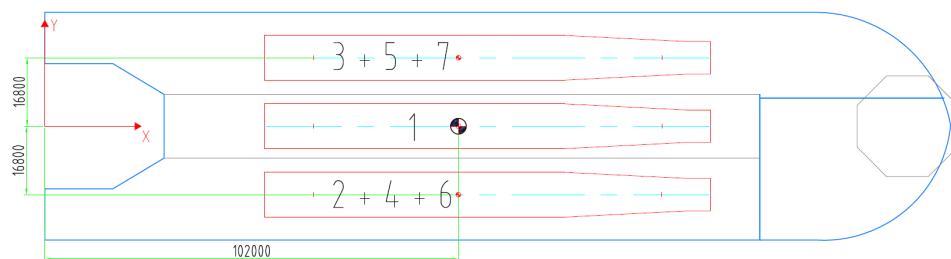
Figure 3.2: Longitudinal Storage of MP on a vessel with CoG location as reference for vessel impact calculations

3.2. Effect of storage on Moment of Inertia

Storage influences the vessel's response, due to a change in weight, moment of inertia and stability. In this section, these effects are evaluated for the storage of an "L" pile ($L = 110m$, $D = 11m$, $W = 2600mT$), of which more details are given in section 2.1. The moment of inertia of a vessel influences the response to wave loading. An increase in MoI leads to an increase in the natural period. When looking at the vessel's RAO for roll, which will be influenced the most by an increase in MoI, the natural period is already quite high compared to the expected wave periods. An increase in this period will be beneficial for the vessel's motions in the North Sea. However, a big change of MoI during a campaign might be experienced negatively, as this means that the installation boundaries of the last MP will be different from the boundaries of the first. Remedies for this change in behaviour might be present, but these will make planning the campaign even more complex. Thus, a large difference is considered unwanted in this analysis.

The MoI of the vessel is increased using the Parallel-Axis Theorem, in which the distance from the vessel's CoG is incorporated in the added MoI. Information about the reference vessel contains the MoI of the vessel in an empty state with a draft of $10.5m$. This draft is contained in the MoI calculation using deballasting.

To take the effects of monopiles on the MoI into account, first, the MoI of the MP itself needs to be calculated. This is done in Equation 3.1 and 3.2. Subsequently, a summation is executed to know the total inertia of an MP. This MoI, at a certain distance from the vessel's CoG is then added to the original MoI.

$$I_x = \frac{1}{2} W_{mp} \left(\left(\frac{D_{mp}}{2} \right)^2 + \left(\frac{D_{mp}}{2} - t_{mp} \right)^2 \right) \tag{3.1}$$

$$I_y = \frac{1}{12} W_{mp} \left(3 \left(\left(\frac{D_{mp}}{2} \right)^2 + \left(\frac{D_{mp}}{2} - t_{mp} \right)^2 \right) + dx^2 \right) \tag{3.2}$$

$$I_{y,added} = W_{mp} x_{mp}^2 \tag{3.3}$$

$$I_{x,total} = \sum (I_x) \tag{3.4}$$

$$I_{y,total} = \sum \left(I_y + I_{y,added} \right) \tag{3.5}$$

With:

I = Vector of Moment of Inertia of MP segment over a specific axis
W_{mp} = Weight of MP segment
D_{mp} = Diameter of MP segment
t_{mp} = Thickness of MP segment
dx = Segment length
x_{mp} = x coordinate of segments, with $x = 0$ at CoG

This analysis evaluates the increase in MoI for all three rotational axes for various stored MPs. The positioning of the MPs can be seen in Figure 3.1 and Figure 3.2.

In Figure 3.3, the bars indicate the increase in MoI in the three rotational axes. A few things can be noted from this graph. First, for roll, the impact per MP in the transverse direction is significantly higher than that of an MP in the longitudinal direction. Also, the MoI increase of the transverse MPs is linear, whereas the increase with longitudinally placed MPs is not. This is because the MPs have to be stacked to fit more than 3 MPs on deck. A higher positioned MP causes a higher increase in roll MoI.

Second, in the pitch direction, at first longitudinal storage affects the vessel's MoI more, but when MPs are (transversely) stored more towards the bow and stern of the vessel, transverse storage impact becomes greater. In general, the effect in pitch direction is smaller due to the high Moment of Inertia of the vessel in this direction.

Third, in the yaw direction, the impact for both transverse and longitudinal is equal at first. But, as seen in the pitch direction, when storing MPs more to the bow and stern of the vessel, the MoI quickly increases.

Overall, the difference of 30% is considered quite significant; therefore, the vessel's behaviour difference is too. However, it should be noted that this latter statement has not been checked in this thesis due to a lack of data considering the vessel's behaviour in different loading conditions.
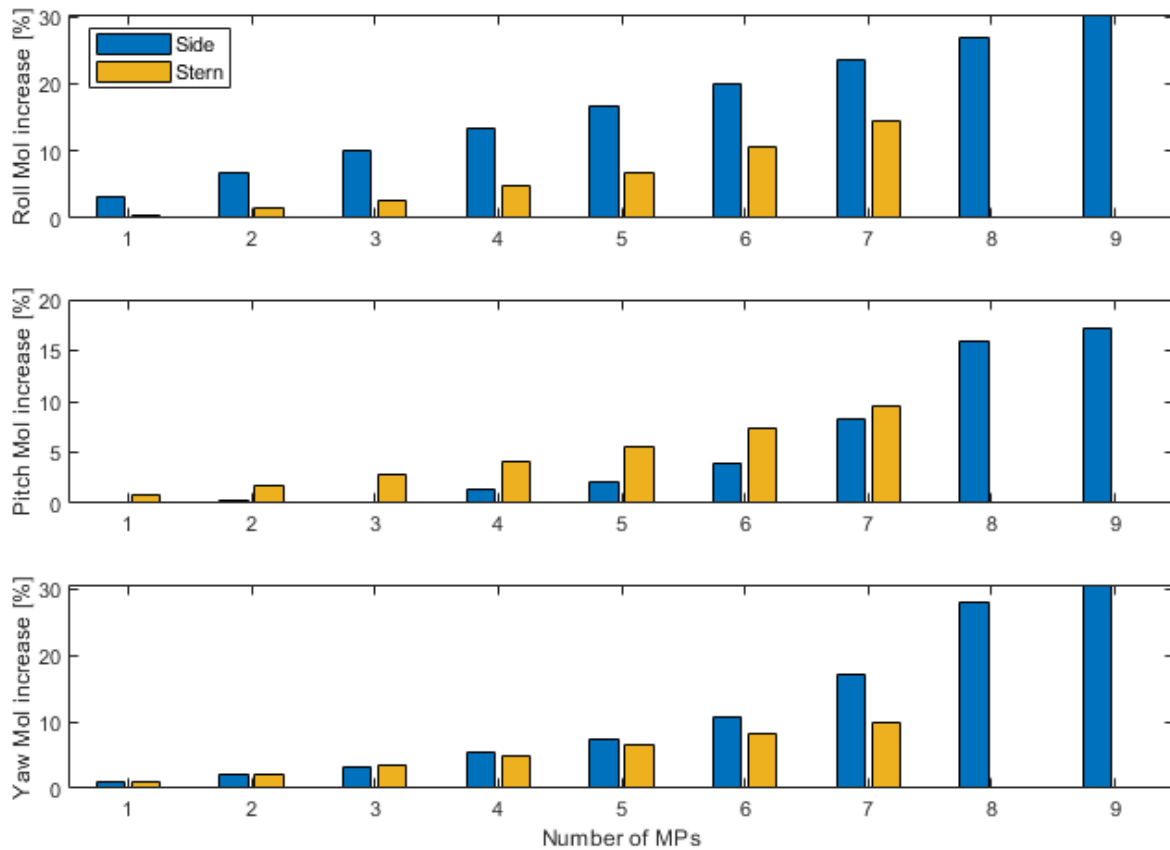
Figure 3.3: Increase in Moment of Inertia due to storage of MP on vessel while keeping vessel draught constant.

3.3. Effect of storage on stability

The stability of a vessel is directly related to its metacentric height (GM), which is the distance between the centre of gravity and the metacentre [31]. When the GM is high, the vessel has large initial stability against overturning. For installation vessels, experts at Huisman indicate that the minimal GM is usually limited to $2.5m$. When MPs are positioned on the vessel's deck, the height of the Cog increases, which leads to a decrease in GM. This effect is emphasised by the fact that it is desired to keep a certain draught, which is realised by deballasting the vessel when MPs are placed on deck. Therefore, an analysis of vessel stability is required. A few conditions have to be met during this analysis.

- To keep the draught of the vessel constant, the total mass should be kept constant.

- Ballasting tanks can be positioned everywhere on the vessel at a $4m$ distance from the keel.

- Original GM of the vessel equals $6.965m$

- Original KG of the vessel equals $18.55m$

- By combining the two statements above, the original M equals $25.515m$

As mentioned, a minimal GM of $2.5m$ is considered, noting that a GM smaller than $3m$ might already be undesirable. However, the vessel still needs to be able to lift an MP without becoming unstable. Therefore an additional analysis is executed to find the reduction in GM when an MP is lifted. The necessary lifting height is shown in Figure 3.4. The GM reduction which occurs during the lift of an MP from $z_{mp} = 24.4m$ to $z_{mp} = 50m$ is $GM_{red} = 0.71m$. Therefore the required minimal GM is increased to $3.21m$.

The updated CoG in the Z direction of the vessel, due to deballasting, can be found in Equation 3.7. The other directions are calculated equally. Then, the new CoG is combined with the CoG of the MPs. This combined CoG is then used to find the GM.
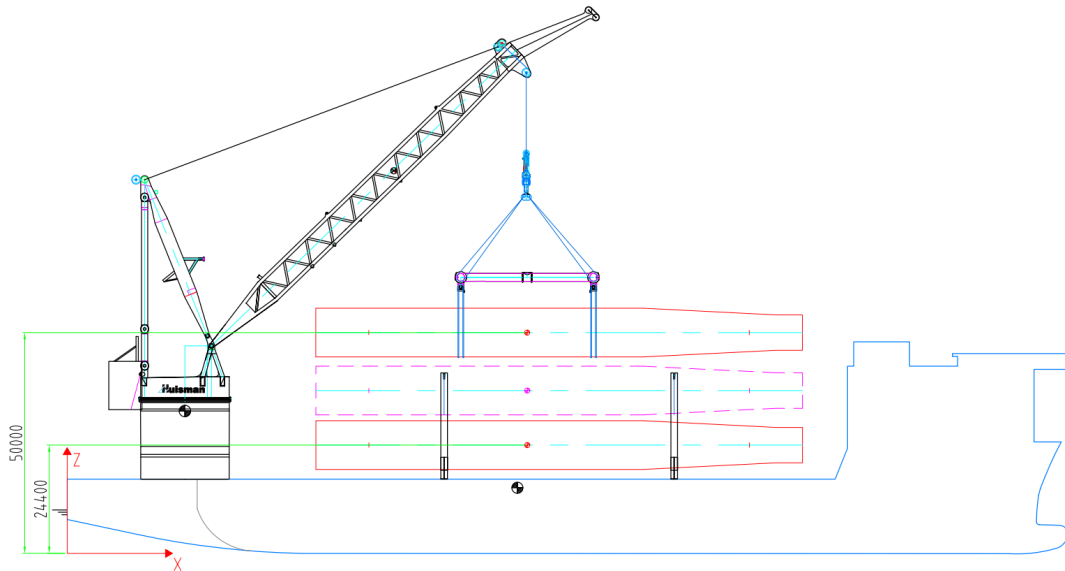
Figure 3.4: Indication of necessary lifting height for a stack of two MPs stored in the longitudinal direction on the reference vessel

$$W_{vessel} = W_{vessel,empty} - n_{mp}W_{mp} \tag{3.6}$$

$$Z_{CoG} = \frac{W_{vessel,empty}Z_{CoG,empty} - (W_{vessel,empty} - W_{vessel})Z_{ballast}}{W_{vessel}} \tag{3.7}$$

$$Z_{CoG,comb} = \frac{W_{vessel}Z_{CoG} + n_{mp}W_{mp}z_{mp}}{W_{vessel,empty}} \tag{3.8}$$

With:

$$W_{vessel} = \text{Weight of Vessel}$$
$$n_{mp} = \text{Number of MPs}$$
$$W_{mp} = \text{Weight of MP}$$
$$Z_{CoG} = \text{Z-coordinate of CoG of vessel}$$
$$Z_{ballast} = 4m \text{ (Z-coordinate of ballast from keel)}$$
$$Z_{mp} = \text{Z-coordinate of CoG of all MPs on vessel}$$

In Figure 3.5 the impact on the GM is presented for an increasing number of piles on the vessel. Also, in red (dashed), the minimal desired GM and the original minimal GM are shown. Some remarks on these results are:

- When the modified minimal GM is used, a vessel's storage is limited to 4 MPs longitudinally and 6 MPs transversely. This difference results from the required stacking of MPs for longitudinal storage. Storing more than 4 or 6 MPs on this vessel results in unacceptably low stability.

- When an installation method is used where no additional $0.71m$ GM is required, an extra MP can be stored on deck in either configuration. Such a method would be pretty beneficial as it leads to an increase of 25% or 16.7% depending on the storage direction.

- The necessity to store more than 4 MPs on a vessel is unknown. Sailing a fully loaded vessel to an installation field while only being able to install one or two MPs in a particular weather window might not be beneficial. However, this logistical consideration is out of scope for this thesis.
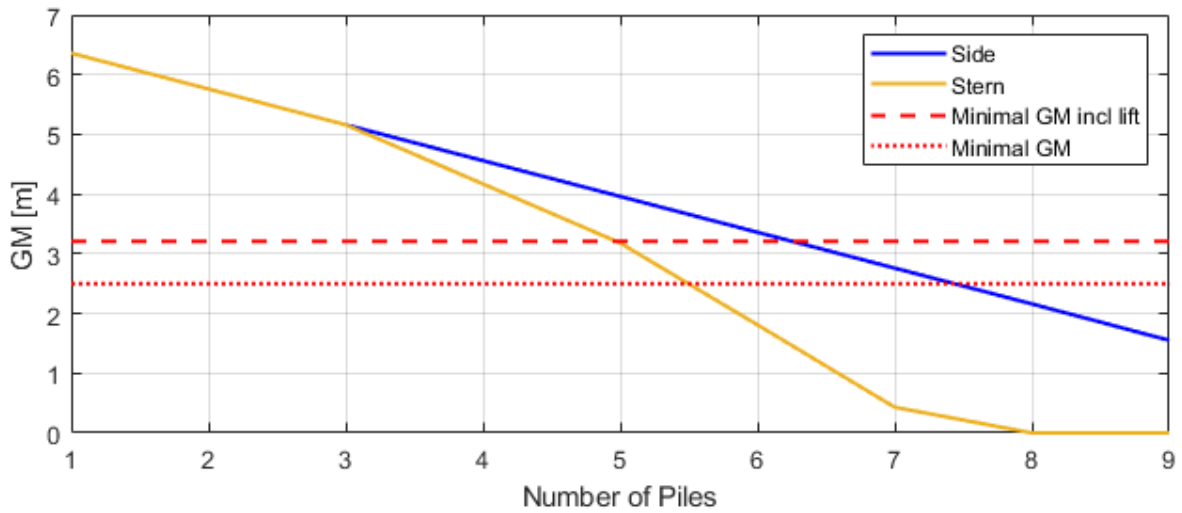
Figure 3.5: Impact of MPs on the vessel's GM for both longitudinal and transverse storage, where the minimal GM and modified minimal GM are indicated with a red lines.

3.4. Effect of storage on Monopile

The direction of storage of MPs on an installation vessel influences the loads in the MP. Longitudinally stored MPs can be supported at favourable positions, whereas the vessel's width bounds the support positions for transverse MPs. In this section, an analysis is executed to find the differences in stress in the MP.

3.4.1. Load Cases

First, a difference is made between three states: Operational, transit and survival, which are shortly summarised in the Table 3.1, the values that are used are a combination of data from Figure 2.2 and Basis of Design as used by Huisman [25]. These three will then be evaluated for MP Small and MP XXL to get insight into the sensitivity. Finally, the direction of the MP on the vessel will be compared using transverse or longitudinal storage.

MPs are placed at an unfavourable location on the vessel regarding the accelerations, creating a worst-case scenario for each MP. A sketch of the transverse situation is shown in Figure 3.6. By varying the support locations (l_1 and l_2), this sketch represents all types of MPs. The stacked MPs for longitudinal storage are considered to experience somewhat higher loads, but due to the level of uncertainty in their support, these are placed out of scope for this thesis.
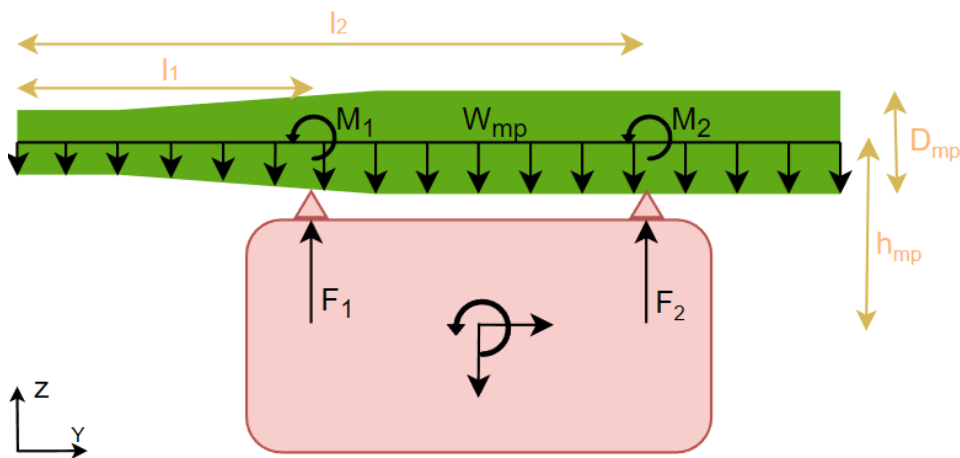
Figure 3.6: Sketch of loads on transversely stored MP

Table 3.1: Definition of environmental states used for load cases for storage.

	Hs $[m]$	Tp $[s]$	Heading [°]
Operational	2.25	$6 - 10$	150
Transit	6	$6 - 16$	any
Survival	9.5	$6 - 16$	180

Table 3.2: Load Cases for Storage of MPs

	State	Direction	MP
1.1.1	Operational	Transverse	Small
1.1.2	Operational	Transverse	XXL
1.2.1	Operational	Longitudinal	Small
1.2.2	Operational	Longitudinal	XXL
2.1.1	Transit	Transverse	Small
2.1.2	Transit	Transverse	XXL
2.2.1	Transit	Longitudinal	Small
2.2.2	Transit	Longitudinal	XXL
3.1.1	Survival	Transverse	Small
3.1.2	Survival	Transverse	XXL
3.2.1	Survival	Longitudinal	Small
3.2.2	Survival	Longitudinal	XXL

In this analysis, a few assumptions have been made.

- As discussed in section 2.1, the D/t ratio of the MP is assumed to be linearly distributed over the length. In reality, the MP thickness will be optimised for its operational lifetime and not for transport. Therefore, this "random" D/t is considered accurate enough for this analysis.

- The MP is divided into segments of 100mm for this analysis, this relatively small step size has been chosen due to the low order of mathematical errors for this step size.

- The CoG of the MP is positioned on the centre line of the vessel for transverse storage.

- l_1 and l_2 are x-coordinates of the two saddles on which the MP rests, as seen from the top. These locations were optimised for each load case while keeping the vessel's width in mind. It is realised that the positions of actual installation will not always be ideal due to vessel restrictions or logistical considerations. However, for this thesis, it will be useful to compare the most optimal positions for changing directions.

- The moment introduced in the MP due to the horizontal acceleration in the MPs CoG and the shear in the saddles is taken up by the two saddles. During actual installation, a project-specific approach is taken to solve the remaining moment. However, such considerations are out of scope for this thesis.

3.4.2. Load evaluation

Reaction forces F_1 and F_2 are calculated as follows, with which a shear and moment diagram is generated. Results can be found in Figure 3.7a and 3.7b.

$$F_{v.roll} = \alpha_{roll}x_{mp}W_{mp} \tag{3.9}$$

$$F_v = (9.81 + a_z)W_{mp} \tag{3.10}$$

$$M = \frac{D_{mp}}{2}\sum W_{mp}\left(a_x + \alpha_{roll}h_{mp}\right) \tag{3.11}$$

$$F_2 = \frac{\sum(F_{v.roll} + F_v)\cdot(x_{mp} + x_{cog}) + M - l_1\sum(F_{v.roll} + F_v)}{l_1 - l_2} \tag{3.12}$$

$$F_1 = -\sum(F_{v.roll} + F_v) - F_2 \tag{3.13}$$

with:

$$\alpha_{roll} = \text{Maximal Roll acceleration}$$
$$a_x = \text{Horizontal Acceleration of MP due to vessel motions}$$
$$a_z = \text{Vertical Acceleration of MP due to vessel motions}$$
$$x_{mp} = \text{X coordinate of MP with 0 being the CoG location}$$
$$W_{mp} = \text{Mass of each element of MP with } dx = 0.1m$$
$$D_{mp} = \text{Maximal Diameter of MP}$$
$$h_{mp} = 25.7m$$
$$x_{cog} = \text{Distance of CoG from top of MP}$$

Shear and Moment diagrams from this analysis for MP Small and XXL can be found in Figure 3.7. These two MPs are used to get insight into the most critical load case. One major difference between the two types of MPs can be seen in the diagrams. The supports of the small MP are placed such that the positive and negative bending moments are roughly equal, and thus, the absolute bending moment is reduced to a minimum. This is no longer possible for the XXL MP due to the vessel's width restrictions. The supports are now placed at $y = \pm 27m$ from the vessel's centerline. This results in a negative bending moment over the entire length, with higher absolute maxima.

3.4.3. Global Stresses

To compare these two MPs fairly, the maximal bending moment has been translated to bending stress in the MP, as this is related to both the bending moment and the section modulus of the MP. In Figure 3.8, it can be seen that the transit load cases are most critical for the global load in the MP. This might be counter-intuitive, but this occurs because the transit state considers all headings, whereas the survival state only considers head seas. For the MPs, more beam sea headings will be more harmful, so the transit state is governing. It can be seen that the difference between transverse and longitudinal storage is consistent for all operational states.

It should be noted here that MPs will not often see the survival state, as vessels will likely not sail during weather windows in which such heavy sea states can develop. However, as this thesis is looking for methods to stretch the workability of a vessel into the winter, chances increase that such weather might be encountered. Therefore, including these rough sea states in this analysis is believed to be valid.

One additional aspect of transverse storage on the deck is considered, which is wave impact on the MPs. The vessel's roll motions cause the MP's overhanging part to get close to the sea level, which could lead to waves hitting the MPs. The probability of this is analysed in Appendix C, and it turns out that the chances are very close to zero for operational and transit states. However, for the survival state, the chances are higher than 75% for XXL MPs. The loading from this impact is left out of scope for this thesis, as the operational state is considered. However, future research should look into these loads.

(a) MP Small: LC 2.1.1   (b) MP XXL: LC 2.1.2
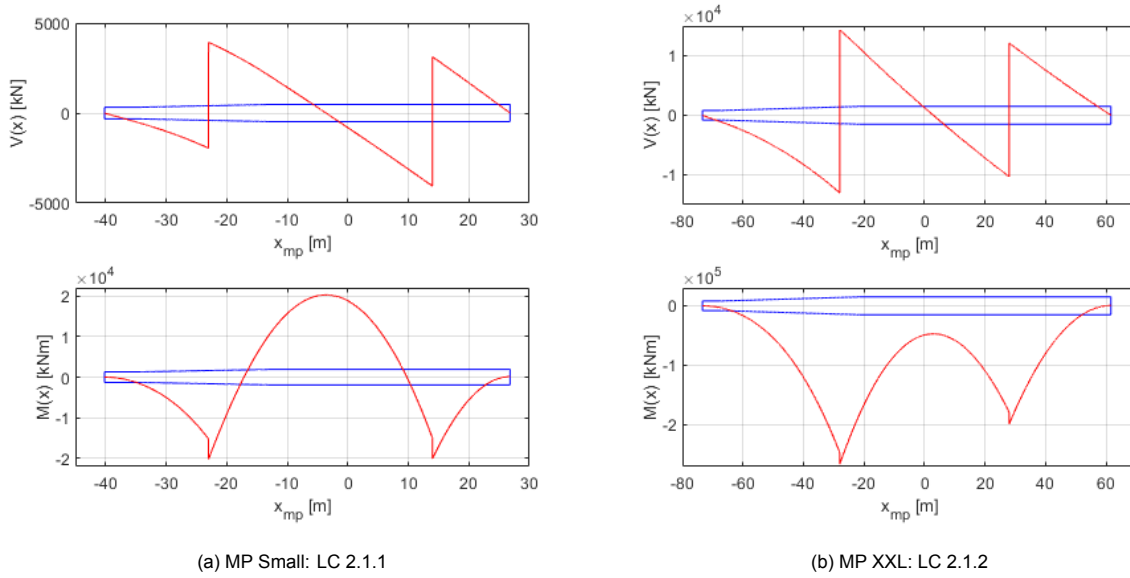
Figure 3.7: Shear and Moment diagram of two MPs, as a result of the described analysis
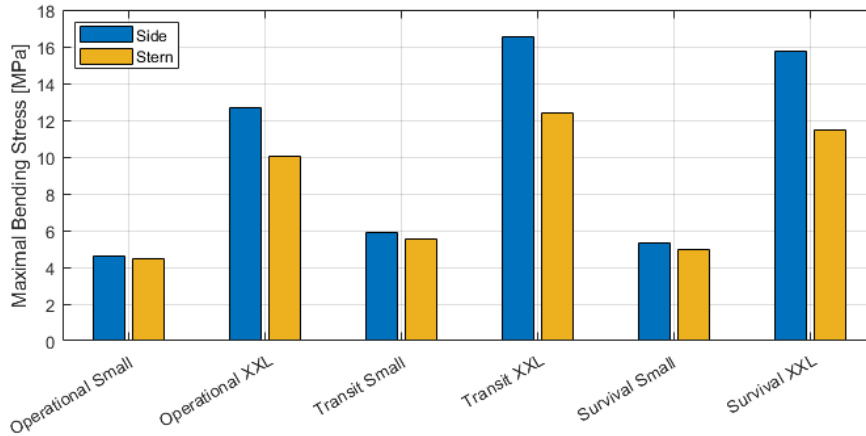
Figure 3.8: Maximal bending stress in MP due to storage loads for a variety of loadcases, which are described in Table 3.2

To complete the global stress analysis, it has been extended for the complete range of MPs, to get insight into the evolution of a potential issue in the storage loads. The additional load cases can be found in Table 3.3 and the results of the governing transit state are presented in Figure 3.9. Here, it should be noted that, in general, global stress is fairly low. Stresses of $16MPa$ are significantly lower than the (usual) yield stress of a MP, which is roughly $\sigma_Y = 250MPa$.

Table 3.3: Additional Load Cases for Storage of MPs

	State	Direction	MP
2.1.3	Transit	Transverse	L
2.1.4	Transit	Transverse	XL
2.2.3	Transit	Longitudinal	L
2.2.4	Transit	Longitudinal	XL
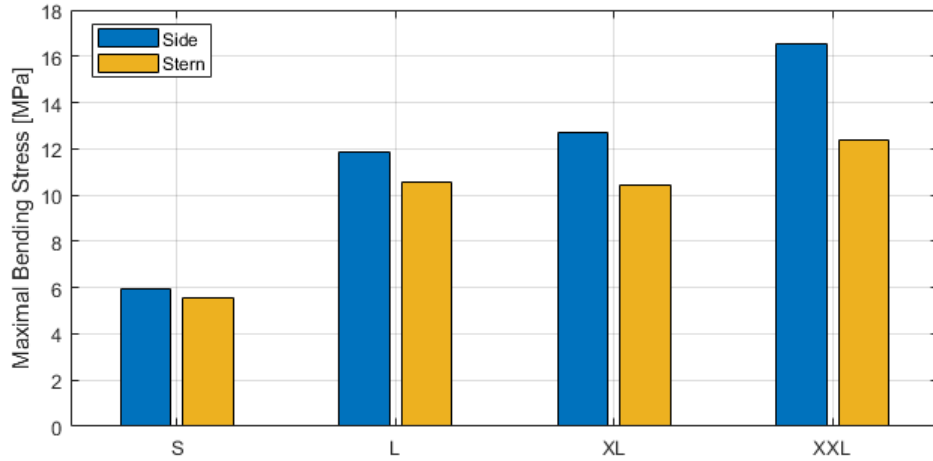
Figure 3.9: Extended analysis of maximal bending stress of governing transit state for multiple MPs stored in transverse or longitudinal direction.

3.4.4. Local Stresses

The reaction force of the supports is introduced into the MP via a saddle. This saddle might cause local stresses, which can be significantly higher than global stresses. This stress introduction is calculated according to ROARK's formulas for stress and strain, section 9.2.12 [41], of which the load diagram can be found in Figure 3.10. This section uses radial support with constant pressure as a saddle. Necessary equations for this analysis are presented here for a saddle with $\theta = 60°$ and width of $1m$. In Figure 3.11, it can be seen that the loads are still well below the yield stress, and thus, deformations will only occur in the elastic regime. Research is ongoing into the local load limits of an MP, especially when it is positioned in a gripper with rollers. These rollers cause an even smaller area to take up the loads [17].
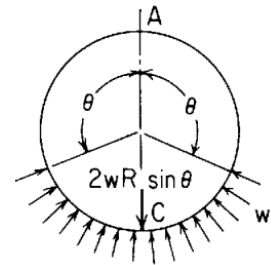
Figure 3.10: Roark 9.2.12 Diagram

$$I = \frac{\pi}{4}\left(R_{mp}^4 - (R_{mp} - t_{mp})^4\right) \tag{3.14}$$

$$A = \pi\left(R_{mp}^2 - (R_{mp} - t_{mp})^2\right) \tag{3.15}$$

$$\alpha = I/AR^2 \tag{3.16}$$

$$k_2 = 1 - \alpha \tag{3.17}$$

$$M_A = \frac{-wR^2}{\pi}\left[s + \pi c - \theta c - k_2(\pi - \theta - s)\right] \tag{3.18}$$

$$M_C = \frac{-wR^2}{\pi}\left[\pi - s + \theta c - k_2(\pi - \theta - s)\right] \tag{3.19}$$

with:

$$w = \frac{F_{support}}{2\sqrt{2}}$$

$$s = \sin\theta$$

$$c = \cos\theta$$
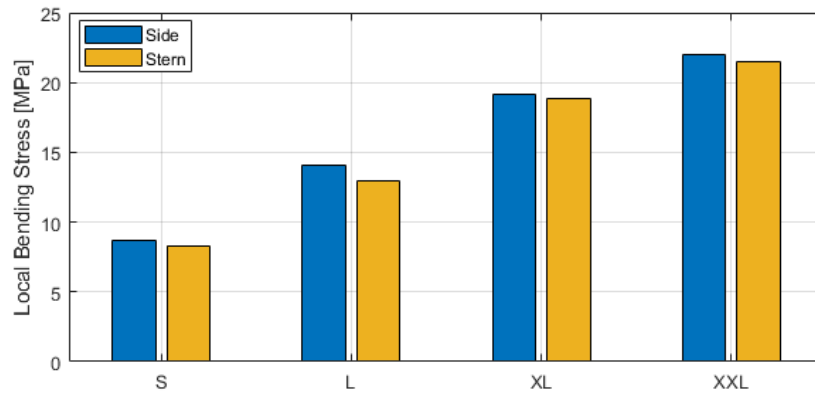
Figure 3.11: Maximal local stress in MP due to load introduction in saddle according to ROARK 9.2.12 [41]

3.5. Conclusions

This chapter has evaluated the effect that storing MPs on an installation vessel has on both the vessel's behaviour and the stresses on the MP.

First, the vessel's behaviour has been analysed using the Moment of Inertia as an indicator of performance, while the vessel's stability is posed as a boundary. It was seen that transverse storage of MPs on a vessel is affecting the behaviour significantly more. Although an increase in MoI will not cause many direct issues, variable vessel behaviour during a campaign does. An installation campaign has a high focus on cycle times, and creating an extra variable for each installation asks for extensive planning and can lead to more installation time. The difference in the MP capacity of a vessel is included in this analysis. Still, it is believed that stern installation and thus longitudinal storage is superior to stern installation when looking at vessel behaviour.

Second, the stresses in the MP were evaluated for a range of MP types, directions and sea-states. It is seen that both globally and locally, stresses are higher during transverse storage. However, the stress levels are unlikely to be governing, and therefore it is concluded that the storage loads in MPs are indecisive. Further research is recommended into the MPs' support frames and sea fastening. Specifically, saddles for stacked storage are not considered in this thesis.

Finally, the wave's impact on MPs should be investigated more thoroughly. When MPs are stored transversely on a vessel, the bottom and top of the MP stick out. Vessel rotation decreases the air gap, which can cause waves to hit the ends of an MP. A quick calculation has been done into the effects of this. It appears that a roll angle of $1°$ causes the bottom tip of the MP to translate $1.2m$. This decrease in air gap causes, for the survival state, an increase of wave impact probability from 21.1% to 78.7% for 1 hour in such a sea state. This probability is considered significant and should be further investigated in future research. However, the probability of impact during operational and transit conditions for a week is only 3.2%, so this additional investigation has not been included in this thesis. The calculation for this probability can be found in Appendix C.

<div align="right">

4

</div>
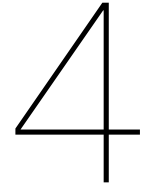
Upending Model Development

In subsection 1.3.3, the current market methods with high potential for both side and stern installation are shown. This chapter aims to provide an objective model which can determine the difference between side and stern upending. The earlier mentioned concepts are combined into a hypothetical concept, which can be placed in both locations. The model development is described step by step.

4.1. Limitations

Several assumptions are taken into account to make a model that would be feasible in a future installation.

- The MP L ($L_{mp} = 110m$, $D_{mp} = 11m$, $W_{mp} = 2600mT$) is used in the model, this MP is already longer than currently installed, and it is believed that this will present flaws in methods.

- During the installation, at least three other MPs will have to be stored on deck. Using this constraint, the deck will be optimally used.

- Horizontal transfer of the MP will not be presented but is considered for all methods. It was found that this step is highly dependent on choices made by a contractor, such as the presence of a secondary crane with a reasonable capacity or a skidding system.

- The crane, presented in section 2.5 is used as a constraint. At every step, the overturning moment and hoisting capacity is checked and considered. Only if these were both within the crane's capabilities the method was found to be valid. The used calculations for this can be found in Equation 4.1 to Equation 4.6 with the dimensions visualised in Figure 4.1.

$$F_{hoist} = \left(1 + \frac{a_z}{g}\right) W_{mp} + W_{mh} \tag{4.1}$$

$$F_{offlead} = W_{mp} \frac{a_x}{g} cos(\beta_{slew}) + F_{hoist} sin(\beta_{off}) \tag{4.2}$$

$$F_{sidelead} = W_{mp} \frac{a_y}{g} cos(\beta_{slew}) + F_{hoist} sin(\beta_{side}) \tag{4.3}$$

$$M_x = DAF * R_{hoist} F_{sidelead} \tag{4.4}$$

$$M_y = DAF \left(H_{hoist} F_{offlead} + R_{hoist} F_{hoist}\right) + R_{boom} W_{boom} \tag{4.5}$$

$$M_{tot} = \sqrt{M_x^2 + M_y^2} \tag{4.6}$$

with:

$$
\begin{aligned}
a &= \text{Acceleration of MP in x, y and z direction due to vessel motions} \\
\beta_{slew} &= \text{Angle of Crane w.r.t. Vessel} \\
\beta_{off} &= \text{Offlead angle from hoist downwards} \\
\beta_{side} &= \text{sidelead angle from hoist downwards} \\
DAF &= \text{1.1 (Dynamical Amplification Factor)} \\
g &= 9.81 m/s^2 \\
R_{mh} &= \text{Radius of Main Hoist} \\
R_{boom} &= \text{Radius of CoG of Boom} \\
W_{mp} &= \text{Weight of Monopile} \\
W_{mh} &= \text{Weight of Main Hoist Block} \\
W_{boom} &= \text{Weight of Crane Boom}
\end{aligned}
$$
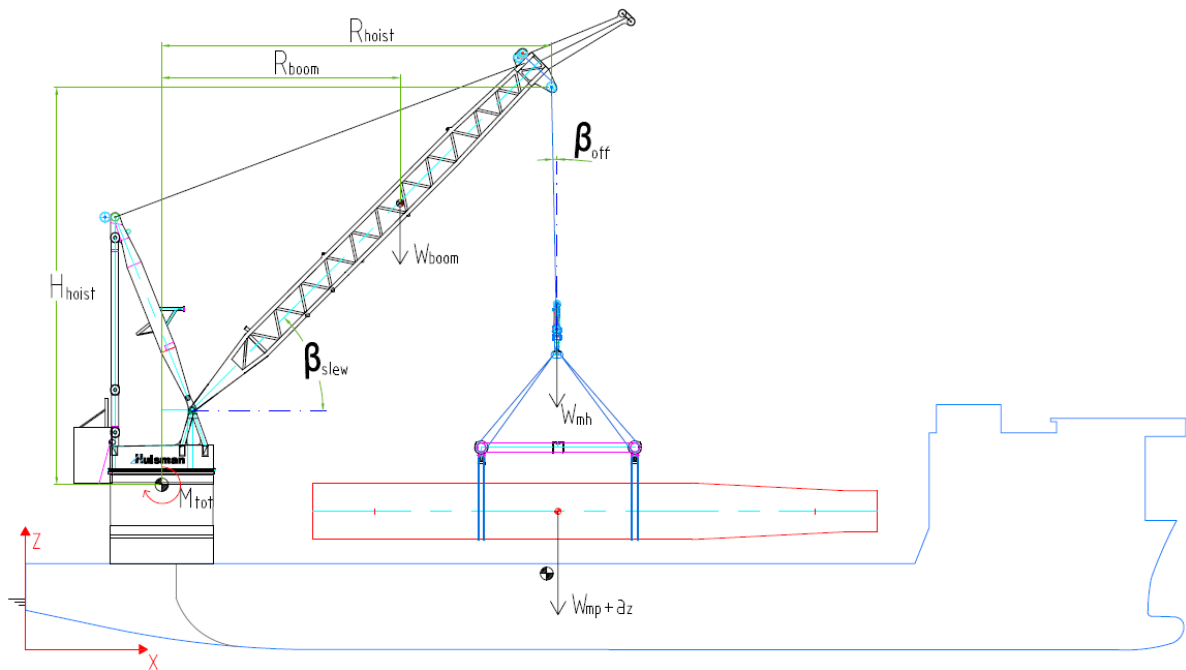
Figure 4.1: Sketch of Crane in arbitrary configuration, with key dimensions indicated. Out of plane dimensions are similar to the presented dimensions and will not be further explained.

4.2. General overview of model

As discussed in subsection 1.3.3, an upending bucket is a method which could be placed both on the side and on the stern of a vessel. This method has been seen on multiple vessels and is thoroughly thought out by designers. It is acknowledged that the general idea of a bucket is a future-proof method of upending Monopiles. However, this thesis aims to create a framework to compare directions which is not bound by a pre-defined method. Therefore, a model is created which is guided by the following characteristics.

- The MP rotates around a hinge which is positioned slightly above the CoG. By choosing this position, the gravitational acceleration of the MP will contribute to the upending.

- The hinge, in which the MP is positioned, can only exert a force on the MP in the Z direction (for the initial position $\theta_{mp} = 0°$ the global Z-axis corresponds to the MPs Z-axis). The hinge cannot induce a moment in the MP.

- To keep the MP in position, forces can be exerted at the top and bottom by tugger winches, which are secured on the vessel's deck.

- The top of the MP is connected to the main hoist and to the deck with a back-tension tugger.

The above-stated characteristics are visually presented in Figure 4.2. This method is used to keep as many degrees of freedom unrestrained, to objectively find the moments and forces in the MP and the upending equipment.

(a) XZ plane   (b) XY plane
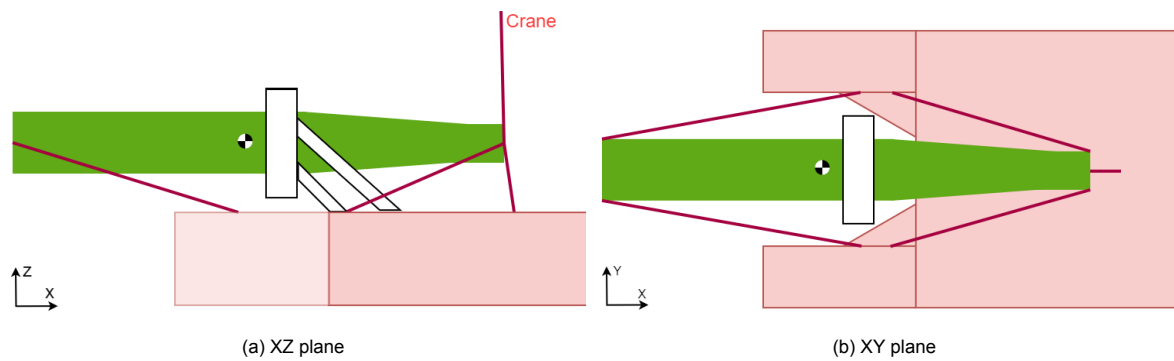
Figure 4.2: Schematic diagram of new concept with only MP, tuggerlines and vessel sketched.

4.2.1. Model input: Accelerations

During the upending procedure, the MP experiences a variety of accelerations due to the vessel's motions. Two reasons can be found for the difference between side and stern upending. First, the position of the MP on the vessels changes; thus, the actual acceleration in a particular direction varies. Second, due to the orientation of the MP, the out-of-plane acceleration in the side installation equals a_x, while it equals a_y for stern installation. This difference can be seen in Figure 4.3. The direction of this out-of-plane acceleration (a_{oop}) is considered challenging from a control perspective. The in-plane acceleration combined with the vertical acceleration of the MP is translated into angular acceleration (α_{ip}) of the MP's CoG as seen from the hinge of the upend bucket. This direction of acceleration is considered to be easier to control.

(a) YZ plane of side upending	(b) XZ plane of stern upending
(c) XY plane of side upending	(d) XY plane of stern upending
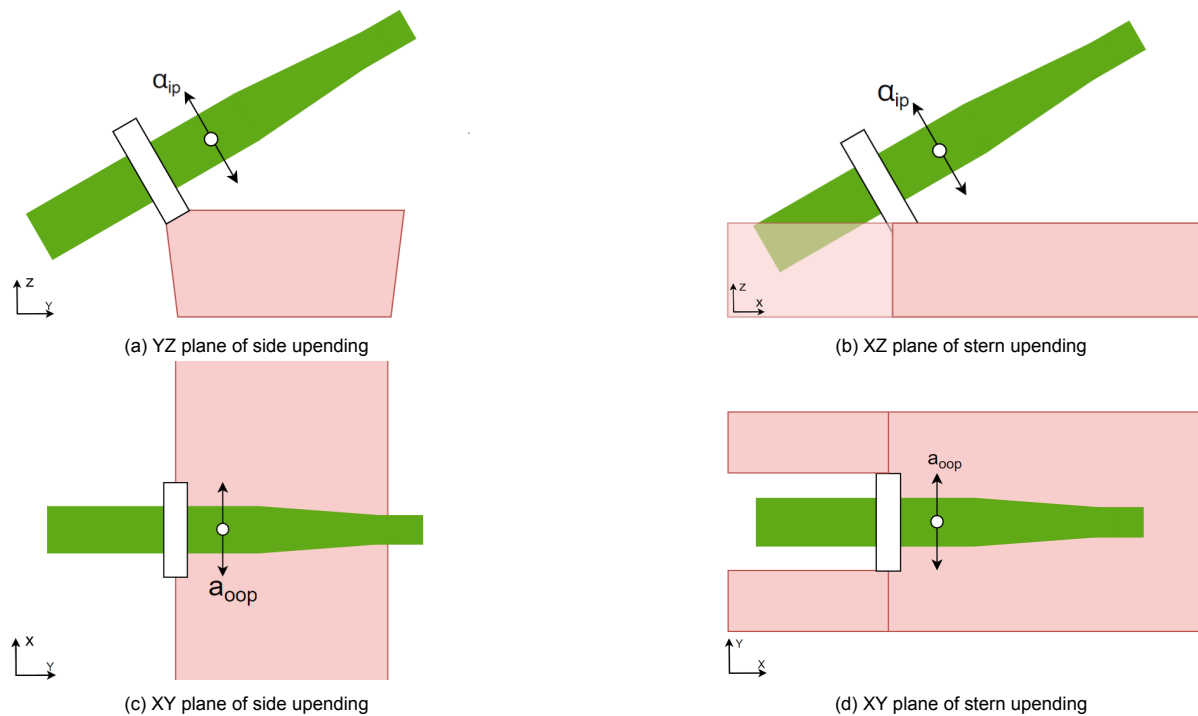
Figure 4.3: Sketches of Upending directions with acceleration direction indicated with arrow.

It should be noted that to compare these methods fairly, an optimal location for the side installation has to be found. Accelerations vary over the longitudinal axis of the vessel. An analysis has been executed in which the bucket's position was varied from stern to bow. During this analysis the operational environmental conditions were used ($H_s = 2.25m$ & $T_p = 6 - 10s$). The results can be found in Figure 4.4. The chosen position, $x = 80m$, is indicated with a vertical line. This position has been chosen such that the vertical acceleration is the lowest, as the range of this acceleration is two times higher than horizontal acceleration.
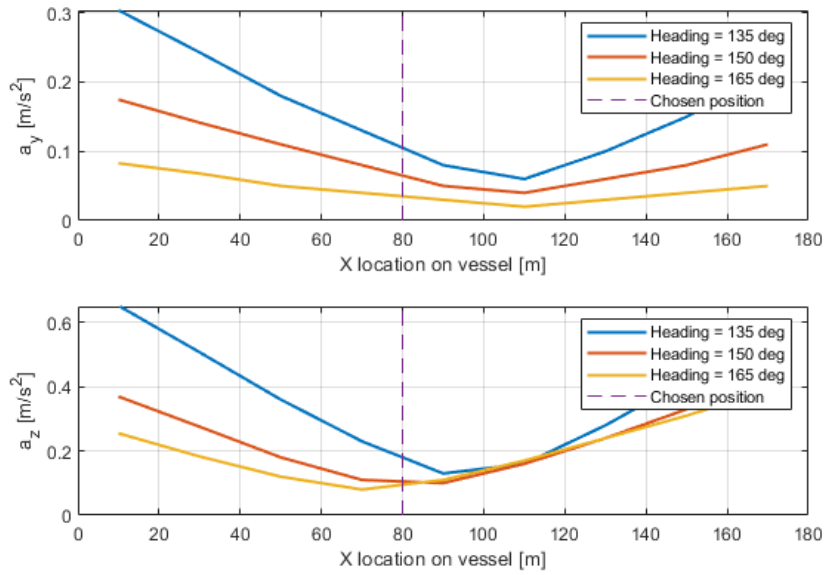
Figure 4.4: Accelerations in Y and Z direction for a bucket positioned at the side of a vessel at $y = 40m$ and $z = 22.6m$ for operational environmental conditions.

When looking at the results of this acceleration analysis, the first objective distinction between side and stern upending can be made. Acceleration in the out-of-plane direction, as indicated by Figure 4.5a is significantly higher during the complete upending procedure. This is the result of both the pitch and yaw motions of the vessel. First, within this range of periods, the vessel has quite some response in the pitch direction. As pitch motions of the vessel translate to accelerations in the x-direction, this is experienced as out-of-plane acceleration during side upending. Secondly, the vessel experiences more yaw motion in a $150°$ heading compared to the $165°$ heading. This motion is also translated into out-of-plane acceleration. The final reason for this difference is that, for these periods, the vessel's roll motion is remarkably low for stern installation heading.

However, in Figure 4.5b, it appears that stern installation experiences higher accelerations. This is again the result of the pitch motions, which now translate to in-plane accelerations. Although these accelerations are higher, it should be noted that gravity is not included in this figure. The angular acceleration of gravity , when the MP is horizontal ($\theta = 0°$), is $25 deg/s^2$.

(a) Out-of-plane Acceleration of CoG of MP

(b) In-plane Angular Acceleration of CoG of MP
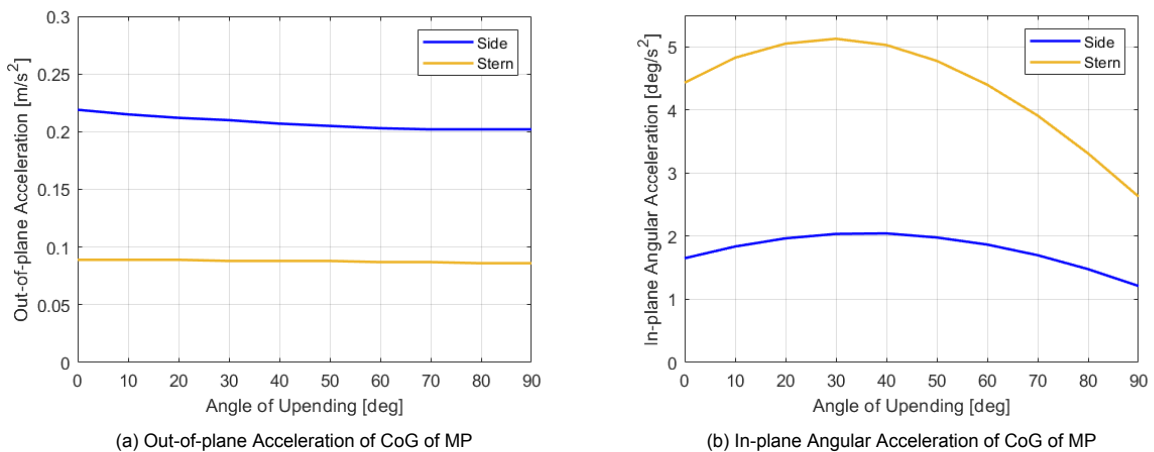
Figure 4.5: Acceleration of MP during upending procedure in out-of-plane and in-plane angular direction, for operational environmental conditions ($H_s = 2.25m$ & $T_p = 6 - 10s$)

4.3. Model setup

This model has been generated using the coordinate system as given in Figure 2.10. From this origin, all points of interest have been identified and vector calculations have been used to find forces and moments on elements of the structure.

In the validation process of this model, the following input loads have been used:

- Maximal acceleration of MP as found in subsection 4.2.1 for each specific upending angle θ_{mp}
- Maximal wave load (given by waves with period $T_p = 6s$) as described in subsection 2.3.1.
- 85th percentile wind load, using maximal average wind load, as described in subsection 2.3.2

According to the definitions on Figure 4.6 two transformation matrices have been created to induce rotations of the vessel and the MP. With a set of vectors containing information about the location of tugger winches and the hinge in which the MP rotates, a complete set of locations could be determined. Aspects of this model are shortly discussed.
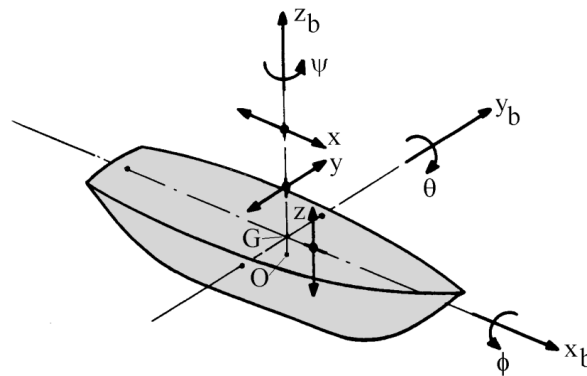
Figure 4.6: Definition of vessel motions in six degrees of freedom according to [31]

4.3.1. Out-of-plane Tugger cables

Connected to the bottom and top of the MP are four tugger cables originating from winches at deck level. The exact location of the winches is chosen such that these do not interfere with the crane or MP storage on deck. The indicated crane on Figure 4.7 will be disregarded in sketches in the remainder of this thesis but has been considered. These tugger cables will control the MP against out-of-plane moments induced by vessel acceleration, waves and wind. To verify the used model, a 2D balance of forces and moments is worked out analytically and with the model. It can be noted that the hinge exerts no horizontal force. This force has been added in a later stage of the model development.
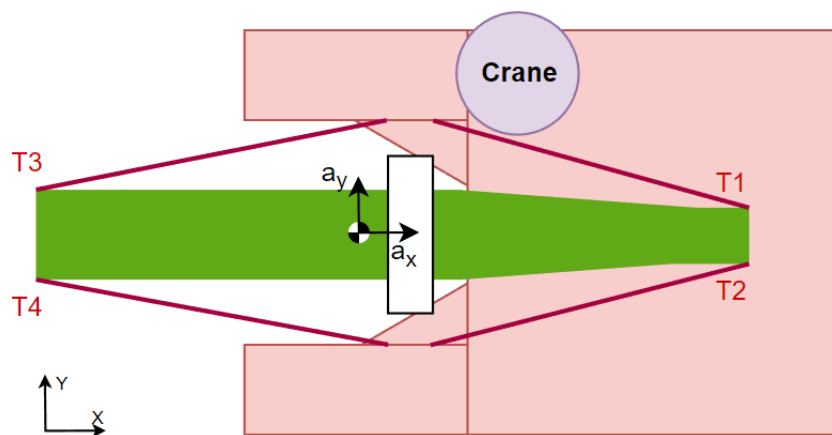
Figure 4.7: Indication of four tugger cables connected to MP at $\theta_{mp} = 0°$

The tuggers have a to-be-determined tension with a specified direction based on geometry. Therefore their force vector (in a $\theta_{mp} = 0°$ configuration for example) is defined as seen in Equation 4.7. For simplicity, these tugger forces have been collected in a matrix together with the back-tension tugger (explained in the next section).

$$\mathbf{f}_{t1} = \hat{f}_{t1} \cdot F_{t1} = \begin{bmatrix} -0.9695 \\ 0.1909 \\ -0.1540 \end{bmatrix} F_{t1} \tag{4.7}$$

$$\mathbf{F}_{tug} = \begin{bmatrix} \mathbf{f}_{t1} & \mathbf{f}_{t2} & \mathbf{f}_{t3} & \mathbf{f}_{t4} & \mathbf{f}_{t5} \end{bmatrix} \tag{4.8}$$

To find an equilibrium with the four tugger forces and accelerations in the X and Y direction, three equations of motions (EoMs) were defined. From the general sum of forces, the X and Y summations and from the sum of moments, the Z moment is taken. The sum of moments has been taken around the hinge, which is indicated as a white block in Figure 4.7.

$$\sum \mathbf{F} = W_{mp}\mathbf{a}_{mp} + \sum \mathbf{F}_{tug} \tag{4.9}$$

$$\sum \mathbf{M} = \mathbf{r}_{h2cog} \times \left(W_{mp}\mathbf{a}_{mp}\right) + \sum \mathbf{r}_{h2t} \times \mathbf{F}_{tug} \tag{4.10}$$

From this two summations of forces and moments, the following EoMs can be generated (looking solely at the XY plane). For this MP angle ($\theta_{mp} = 0°$) the forces due to accelerations of the MP are $W_{mp}\mathbf{a}_{mp} = \begin{bmatrix} 432 & -169 & -25756 \end{bmatrix}^\top kN$

$$-0.9690F_{t1} - 0.9690F_{t2} + 0.9630F_{t3} + 0.9630F_{t4} + 432 = 0 \tag{4.11}$$

$$0.1910F_{t1} - 0.1910F_{t2} + 0.1970F_{t3} - 0.1970F_{t4} - 169 = 0 \tag{4.12}$$

$$15.107F_{t1} - 15.107F_{t2} - 15.383F_{t3} + 15.383F_{t4} + 574.6 = 0 \tag{4.13}$$

From here, it can be seen that these three equations contain four unknowns and are therefore not solvable. Therefore, one of the tuggers has been set to zero to overcome this problem. This method is shortly described. First of all, the EoMs were re-written to a linear system.

$$\mathbf{A}\mathbf{x} = \mathbf{B} \tag{4.14}$$

$$\begin{bmatrix} -0.9690 & -0.9690 & 0.9630 & 0.9630 \\ 0.1910 & -0.1910 & 0.1970 & -0.1970 \\ 15.107 & -15.107 & -15.383 & 15.383 \end{bmatrix} \begin{bmatrix} F_{t1} \\ F_{t2} \\ F_{t3} \\ F_{t4} \end{bmatrix} = \begin{bmatrix} -432 \\ 169 \\ 574.6 \end{bmatrix} \tag{4.15}$$

The following conditional statement is implemented, using vector $\mathbf{B}$ to find the direction of forces. An additional vector $\mathbf{B}_{check} = \mathbf{T}^{-1}\mathbf{B}$ where $\mathbf{T}$ is the transformation matrix for MP rotations, is used to find the resulting load in the X direction.

$$\begin{cases} F_{t1} = 0, & \text{if } \mathbf{B}(2) < 0 \quad \& \quad \mathbf{B}_{check}(1) > 0 \\ F_{t2} = 0, & \text{if } \mathbf{B}(2) > 0 \quad \& \quad \mathbf{B}_{check}(1) > 0 \\ F_{t3} = 0, & \text{if } \mathbf{B}(2) < 0 \quad \& \quad \mathbf{B}_{check}(1) < 0 \\ F_{t4} = 0, & \text{if } \mathbf{B}(2) > 0 \quad \& \quad \mathbf{B}_{check}(1) < 0 \end{cases} \tag{4.16}$$

With this reduction of unknowns, the linear system could be solved. This equilibrium in three degrees of freedom is checked by hand and is correct.
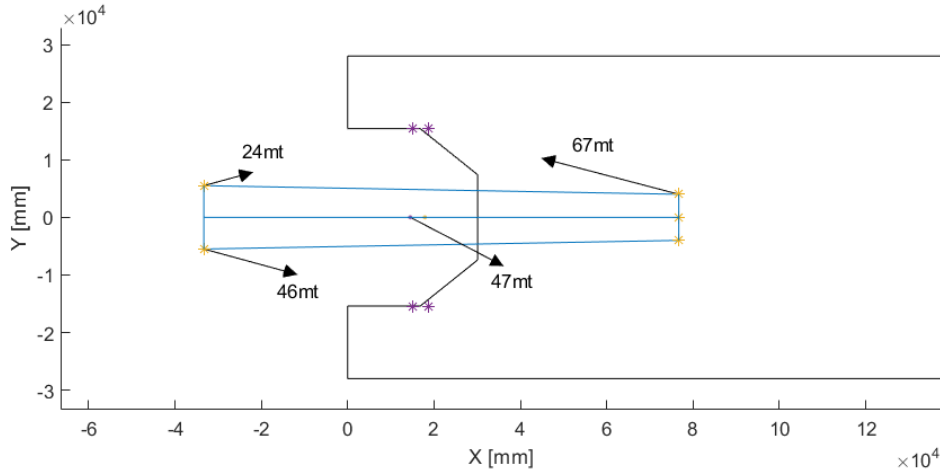
Figure 4.8: Result of 2D load analysis for MP angle $\theta_{mp} = 0°$

4.3.2. In-plane Tugger Cables

Besides the out-of-plane loads, the MP can be upended in a controlled way with a range of forces as explained in Figure 4.9. Each load is defined as follows:

$$W_{mp} = \text{Gravitational acceleration of MP}$$
$$\mathbf{T}_{1-4} = \text{Tugger cables as described in Figure 4.7}$$
$$\mathbf{T}_5 = \text{Back Tension Tugger cable connected to the deck}$$
$$\mathbf{F}_c = \text{Crane tension under a small angle}$$
$$\mathbf{F}_h = \text{Perpendicular load on hinge without friction}$$
$$\mathbf{F}_{wa} = \text{Loads induced on MP by waves, as described in subsection 2.3.1}$$
$$\mathbf{F}_{wi} = \text{Loads induced on MP by wind, as described in subsection 2.3.2}$$

Given that now two more unknowns are introduced in the system, the tension in T5 and the vertical force in the hinge, more equations of motions are to be defined. The earlier given sums of forces and moments are now extended to the following system. The moments are taken around the hinge.

$$\sum \mathbf{F} = W_{mp}\mathbf{a}_{mp} + \sum \mathbf{F}_{tug} + \mathbf{F}_{wi} + \mathbf{F}_{wa} + \mathbf{F}_c + \mathbf{F}_h \tag{4.17}$$

$$\sum \mathbf{M} = \mathbf{r}_{h2cog} \times \left(W_{mp}\mathbf{a}_{mp}\right) + \sum \mathbf{r}_{h2t} \times \mathbf{F}_{tug} + \mathbf{r}_{h2c} \times \mathbf{F}_c + \mathbf{r}_{h2wi} \times \mathbf{F}_{wi} + \mathbf{r}_{h2wa} \times \mathbf{F}_{wa} \tag{4.18}$$

with:

$$\mathbf{r}_{h2cog} = \text{Arm from Hinge to MP CoG}$$
$$\mathbf{r}_{h2t} = \begin{bmatrix} \mathbf{r}_{t1} & \mathbf{r}_{t2} & \mathbf{r}_{t3} & \mathbf{r}_{t4} & \mathbf{r}_{t5} \end{bmatrix}$$
$$\mathbf{r}_{h2c} = \text{Arm from Hinge to Internal Lifting Tool at top}$$
$$\mathbf{r}_{h2wi} = \text{Arm from Hinge to summarised wind load}$$
$$\mathbf{r}_{h2wa} = \text{Arm from Hinge to summarised wave load}$$
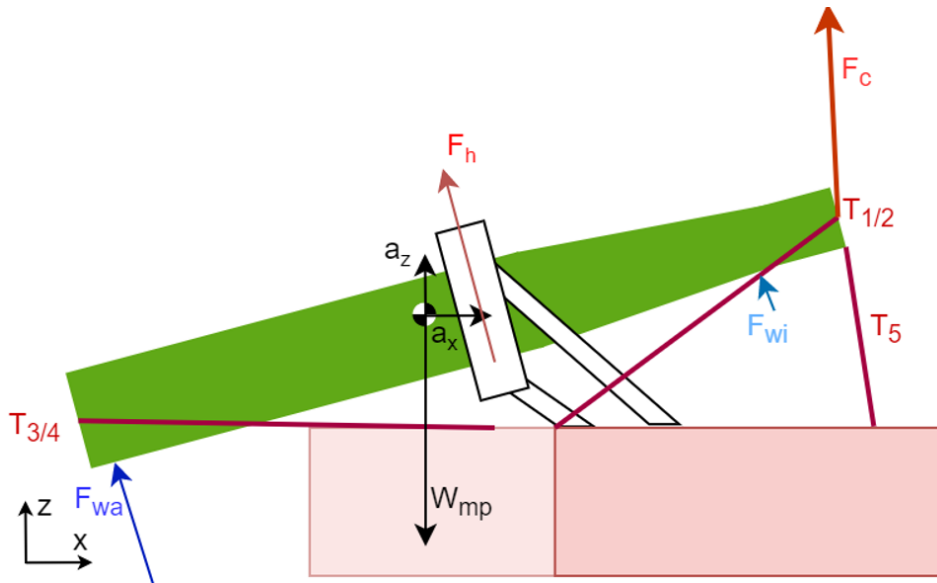
Figure 4.9: Overview of loads on MP in a arbitrary position

From this system, the sum of forces on X, Y and Z and the sum of moments around the Y and Z axis are taken and evaluated in a matrix equation as seen before. For example, the linear system for a specific MP angle ($\theta_{mp} = 20°$) is given below. The crane tension is pre-defined and is varied in a later stage of this report.

$$\begin{bmatrix} -0.781 & -0.781 & 0.907 & 0.907 & 0.151 & -0.500 \\ 0.176 & -0.176 & 0.219 & -0.219 & 0 & 0 \\ -0.599 & -0.599 & 0.360 & 0.360 & -0.989 & 0.866 \\ 8.517 & 8.517 & -8.222 & -8.222 & 56.620 & 0 \\ 12.174 & -12.174 & -14.590 & 14.590 & 0 & 0 \end{bmatrix} \begin{bmatrix} F_{t1} \\ F_{t2} \\ F_{t3} \\ F_{t4} \\ F_{t5} \\ F_h \end{bmatrix} = \begin{bmatrix} 1944 \\ -1048 \\ 23533 \\ -49916 \\ 26014 \end{bmatrix} \tag{4.19}$$

As this system still contains six unknowns and only five equations of motions, Equation 4.16 is used to disregard one of the tugger cables. This unused tugger is set to a constant tension (CT) of $F_t = 10mt$ to reduce the chance of snapping loads. Now, this system is solvable for a range of crane tensions. During the upending of this system, two things can be found.

It is realised that the sixth equation of motion (Φ moment) would be an alternative for Equation 4.16. However, due to the symmetry of the MP in this axis and the problems this presents, this thesis did not take into account the torsion control of the MP. The residual torsion has been checked in the model development phase and was found to be in the order of several kNm. These numbers were discussed with experts and found manageable in real-life situations.

4.3.3. Load evaluation

As discussed earlier, this model has been evaluated for both installation directions to get insight into the differences between side and stern. In Figure 4.10, a sketch of the side upending is added, in which it can be seen that the winch locations are such that the comparison will be fair. Note that Equation 4.16 is slightly adjusted for side installation. For both methods, a quasi-static approach is taken, where at every $10°$, the maximal loads are evaluated. The environmental states used for this analysis are presented in Table 4.1.

(a) YZ plane of side upending   (b) XY plane of side upending
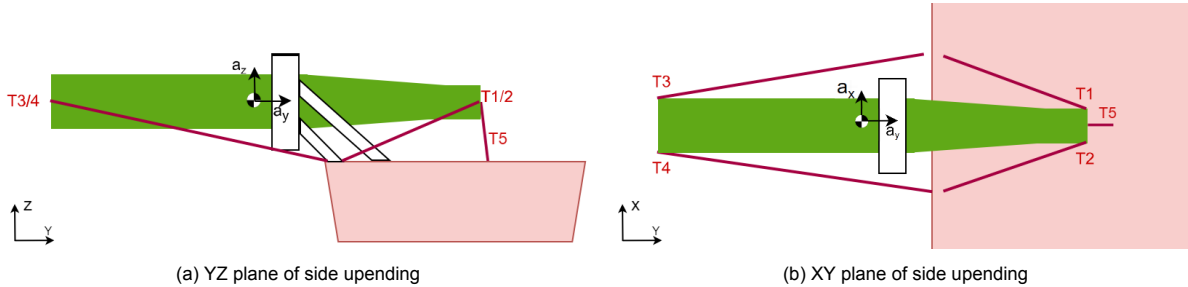
Figure 4.10: Sketches of Tugger Concept for side installation for a upending angle of $\theta_{mp} = 0°$

Table 4.1: Definition of environmental states used for load cases for upending

	Hs [m]	Tp [s]	Heading [°]
Stern	2.25	6-10	165
Side	2.25	6-10	150

First, the tugger on the top of the MP (T_1 or T_2) is evaluated. The results of evaluating this tugger load during the upending procedure can be found in Figure 4.11. A few things can be found by looking at the results.

- The tension in the crane does not influence the load in tugger 1, which indicates that this load is only influenced by the moment in the Z-axis of the MP, as the crane tension does not affect that moment.

- The change in load in this tugger is mainly due to changing wave loads. The effect of wave loading, which starts to act at an angle of $30°$, can be seen in an increase in both lines. Later in the upending process, side installation becomes less favourable due to the main direction of the wave loading.

- An unexpected drop in load between 80 and 90 degrees led to a more thorough investigation in this regime of the upending. This can be found in the figure, where it appears that there is some control issue on this point. It is believed that the geometry of the tugger lines caused such strange behaviour, and in a later stage, this is addressed.
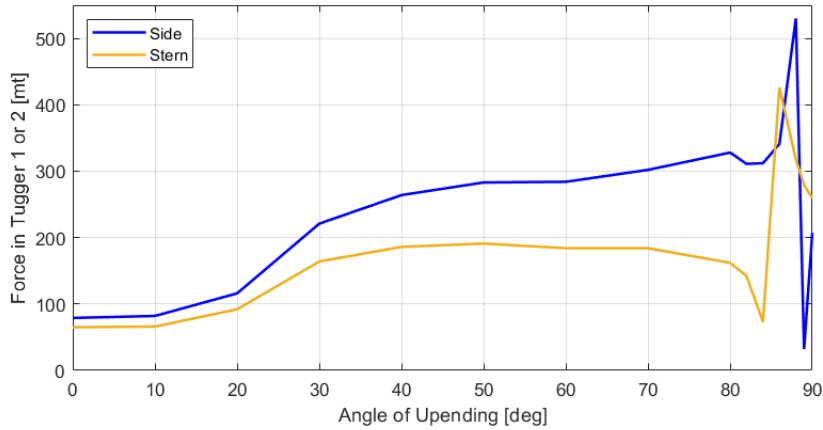
Figure 4.11: Forces in tuggers connected to the top of the MP (1 or 2), as seen during the upending procedure

Secondly, loads of the bottom two tuggers (T_3 and T_4) are evaluated and discussed. The evaluation results can be found in Figure 4.12, where a distinction is made in applied crane force. In Figure 4.12a, the crane tension is kept at a minimum, whereas in Figure 4.12c a constant tension of the MP's weight ($W_{mp} = 2600mt$) is set. In the central figure, a medium crane tension was used to show the evaluation of loads. A few things can be noted.

- Since the hinge can only exert a perpendicular force on the MP, a very significant force in the negative X direction is generated during the upending. In the current model, only tugger lines 3, 4 and 5 can act in the positive X direction. From these three, tugger 5 has a small angle with the vertical, and thus its X-direction load is limited. This results in a high load in the bottom tugger cables 3 and 4.

- In all load cases, a clear difference between side and stern can be seen. This is an indication that stern installation is a better choice when it comes to equipment capacity.

- The loads as seen in the current concept are incredibly high and are not considered achievable for an actual tool. Therefore an iteration of the model is required to make it more realistic.

(a) No Crane Tension

(b) Medium Crane Tension

(c) High Crane Tension
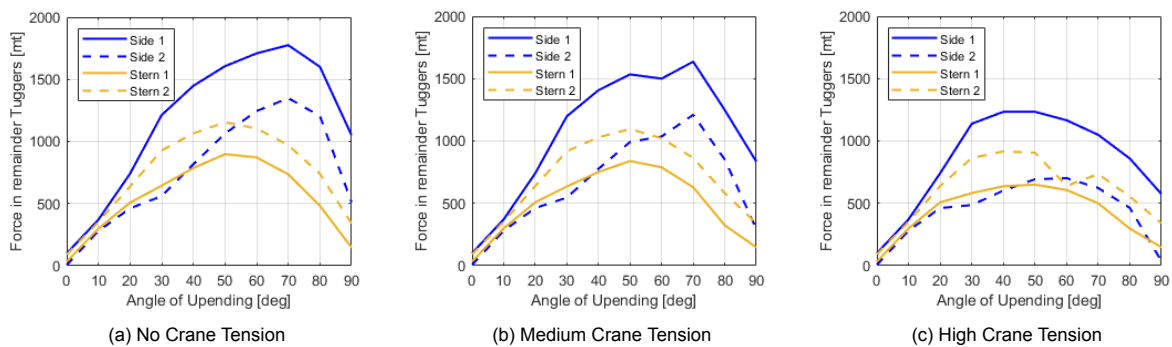
Figure 4.12: Forces in lower tuggers during the upending procedure for both side and stern installation

4.4. First iteration of model

Due to the unachievable high loads in the lower tugger lines, as seen in Figure 4.12, the model has been slightly adapted. This adaption is necessary to evaluate the difference between the side and stern installation in the most realistic way. A bucket has been added to the single ring gripper, which solely exerts an axial force in the MP. By reducing the impact of this bucket to axial forces, the out-of-plane forces and moments will still be counteracted by the tugger lines, and the bucket design might be lightweight. The updated concept is shown in Figure 4.13.
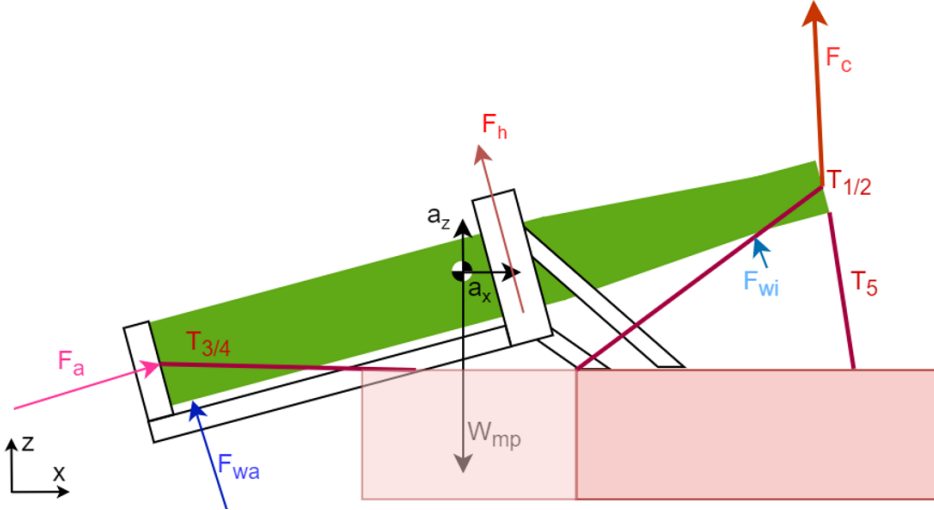
Figure 4.13: Overview of loads on MP in a arbitrary position for the adapted concept

The modification of the model for this iteration is done by updating Equation 4.17 into the following summations of forces. Equation 4.18 does not need updating as the axial force does not create a moment in the hinge. For clarity, the summation of moments is presented here too.

$$\sum \mathbf{F} = W_{mp}\mathbf{a}_{mp} + \sum \mathbf{F}_{tug} + \mathbf{F}_{wi} + \mathbf{F}_{wa} + \mathbf{F}_c + \mathbf{F}_h + \mathbf{F}_a \tag{4.20}$$

$$\sum \mathbf{M} = \mathbf{r}_{h2cog} \times (W_{mp}\mathbf{a}_{mp}) + \sum \mathbf{r}_{h2t} \times \mathbf{F}_{tug} + \mathbf{r}_{h2c} \times \mathbf{F}_c + \mathbf{r}_{h2wi} \times \mathbf{F}_{wi} + \mathbf{r}_{h2wa} \times \mathbf{F}_{wa} \tag{4.21}$$

As a new unknown is presented, in the form of the axial force exerted by the bucket, the EoM has six unknowns for five equations again. Therefore also Equation 4.16 is updated. For every case, only two tuggers are in active mode, whilst the others are in CT to prevent snap loads.

$$\begin{cases} F_{t1} = 10mt & \& \quad F_{t3} = 10mt, & \text{if } \mathbf{B}(2) < 0 \\ F_{t2} = 10mt & \& \quad F_{t4} = 10mt, & \text{if } \mathbf{B}(2) < 0 \end{cases} \tag{4.22}$$

4.4.1. Load evaluation

As seen earlier, the forces in the tugger lines are evaluated for the full range of MP angles. In Figure 4.14 the updated analysis results can be found. A few things can be seen from this figure. First, the loads are significantly lower. This results from the before-mentioned high X-directed loads, which are now accounted for by the axial bucket. Secondly, the difference between the side and stern is still seen, as expected. Thirdly, the angles $\theta_{mp} = 30°$ and $\theta_{mp} = 40°$ seem to be a governing load case for this system. The reason for this is the large arm at which the waves induce loads on the MP compared to the hinge.
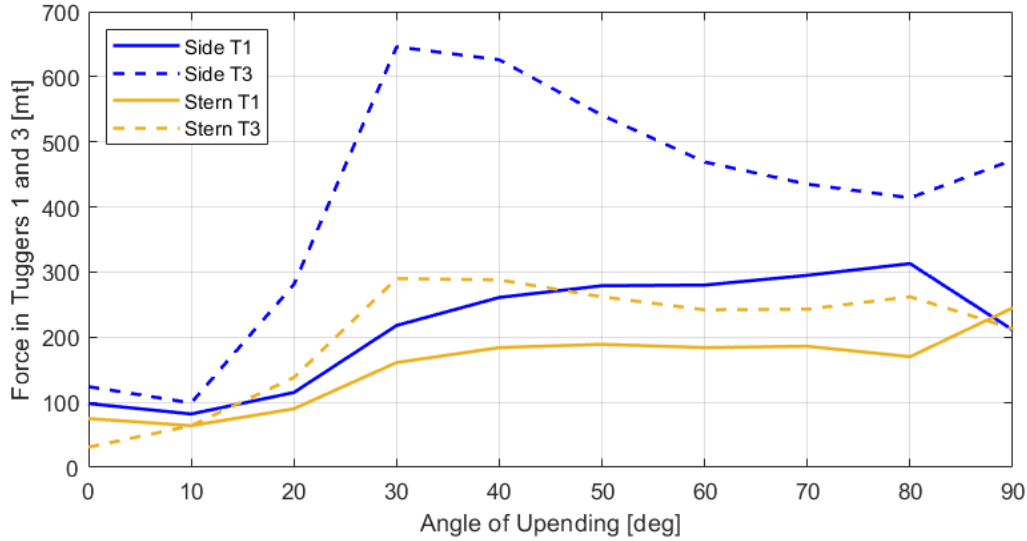
Figure 4.14: Forces in Tugger 1 and 3 (or 2 and 4) for the first iteration updated model for both side and stern installation.

4.5. Second iteration of model

After evaluation of the loads and discussions with experts of Huisman, two more updates have been incorporated into the model to make a clean comparison between stern and side. First, the earlier neglected reaction force in the hinge in the horizontal direction has now been included. The addition of this force leads to a tugger load which is now purely caused by the moment in the MP. Secondly, after evaluating all equations of motions and the sources for these, it appeared that the upper tugger lines (T_1 and T_2) were causing more loads in the lower tuggers whilst not contributing to the out-of-plane moment reduction. Therefore it has been decided to remove these lines. As the first decision would add an unknown to the system, whereas the latter decision removes two unknowns, the system is still solvable. The updated system which sets a specific tugger to CT is presented in Equation 4.23 and is notably reduced in complexity. The final schematic diagram of the model can be found in Figure 4.15. Note that, for clarity, the bottom tuggers keep their original numbers 3 and 4.

$$\begin{cases} F_{t3} = 10mt, & \text{if } \mathbf{B}(5) < 0 \\ F_{t4} = 10mt, & \text{if } \mathbf{B}(5) > 0 \end{cases} \qquad (4.23)$$

4.5.1. Load evaluation

When the final model is evaluated for a range of upending angles (θ_{mp}) for the operational environmental conditions, it can be seen that the model is now compromised to an objective, clean model which generates the loads in out-of-plane moment counteracting tuggers. The results are no longer dependent on a pre-defined crane load, and thus the system can be optimised. While looking at Figure 4.16 it can be seen that stern installation outperforms side installation throughout the complete upending procedure in the out-of-plane moment.

(a) XZ plane of stern upending for second iteration

(b) XY plane of stern upending for second iteration
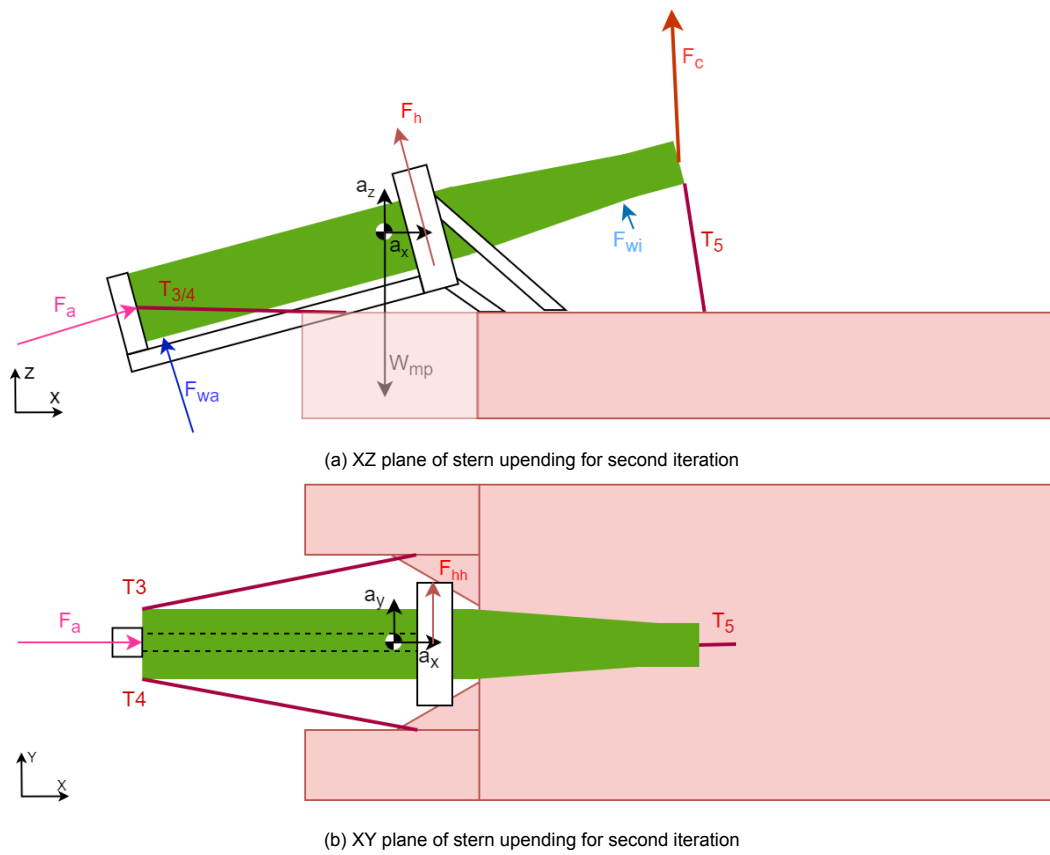
Figure 4.15: Schematic diagram of second iteration of concept. With two tugger lines removed and a horizontal reaction force in the hinge.
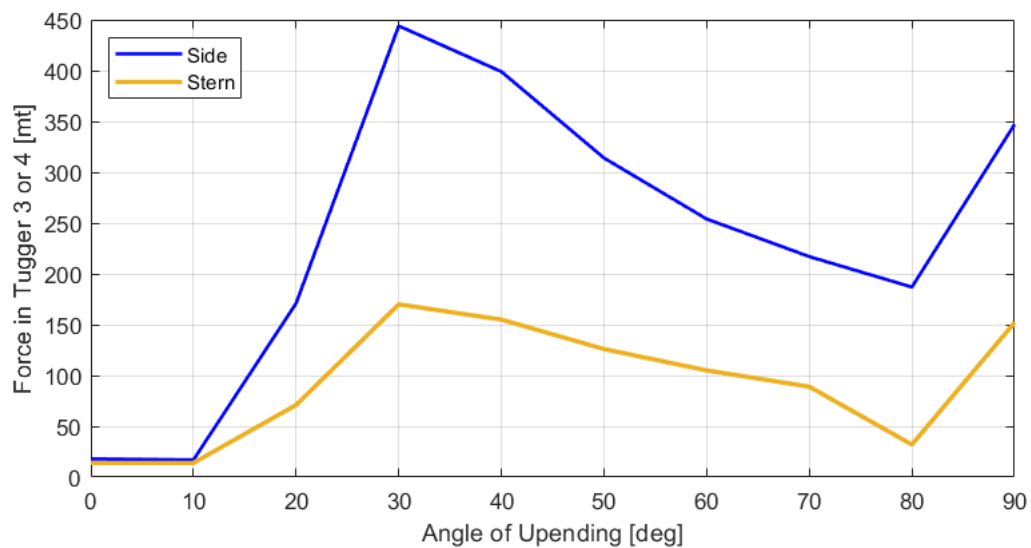
Figure 4.16: Forces in Tugger 3 (or 4) for the second iteration updated model for both side and stern installation.

4.6. Control Strategy

The last adaption to the model is the optimisation process, during which it finds the lowest achievable forces in the back tension tugger and main hoist.

The main hoist tension has, up till this point, been pre-defined in a constant tension (CT) controlled manner. In reality, this tension will slowly increase during the upending, such that the entire MP is hanging in the hook in the completely upended position.

The back tension tugger is an effective method of keeping the MP from suddenly rotating too much. This winch is controlled with position-keeping, and the load in this tugger can be controlled by adjusting the crane tension. Discussions with experts at Huisman led to defining a 'desired tension' in this line of $100mt$. The optimisation script has been written such that the crane tension is slowly increased until the tension in tugger T_5 is $100mt$. An example (for $H_s = 2.5m$ and $T_z = 6.5s$) of this crane load for the entire upending procedure, and the difference between doing this on the side vs stern, can be seen in Figure 4.17. It can be seen that for $\theta_{mp} = 90°$, the situation changes significantly, and it is expected that a change of control strategy is required for this step. When the MP is vertical, the lowering process starts, which is out of scope for this thesis.
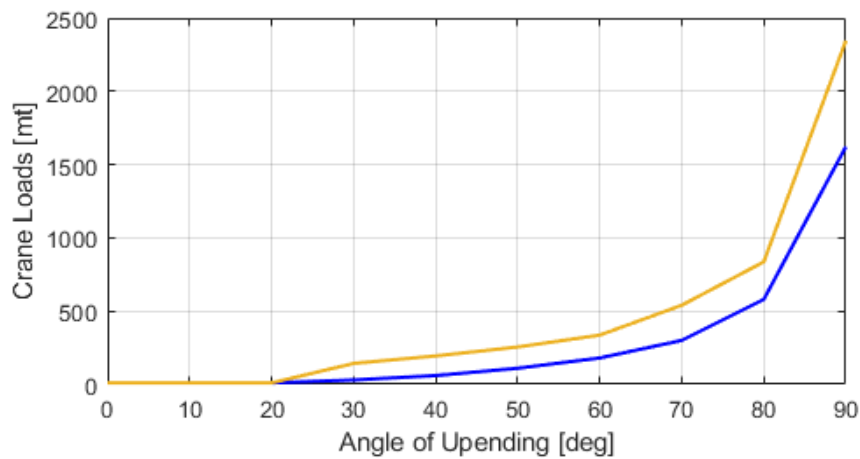
Figure 4.17: Required crane tension for the upending procedure when $T_5 = 100mt$ is desired. Sea state used in this graph is $H_s = 2.5m$ and $T_z = 6.5s$.

The bottom tuggers are to be controlled in a pre-tensioned position-keeping manner, compensating for the vessel's roll and pitch. The loads as found in the previous sections are maximal loads in this tugger, which indicates that the actual load in each of these tuggers will be varying between the pre-tension of $10mt$ and the maximal values as described earlier ($170mt$ for stern installation in a $30°$ angle).

4.7. Dynamic Extension of Model

By definition, the installation of an MP is a dynamic process. Wave loads and vessel motions are sinusoidal quantities, wind load is random to a certain extent, and position control winches have a frequency with which it operates. Therefore, a dynamic extension of the model is required to actually plan operations with this model. This thesis has placed these time simulations out of scope due to the focus on comparison rather than a planning tool. However, the feasibility of this model can be estimated by doing a frequency analysis. The natural frequency has been calculated for three systems; The tugger cable itself, the free pendulum created by hanging the MP in a hinge, and the complete system where tugger cables act as springs on the system.

4.7.1. Natural frequency of tugger cables

The frequency analysis of a cable in the axial direction is based on the stiffness and mass of this cable. Stiffness can be calculated using the equations below. The cable used for this is a $109mm$ wire rope, with a Minimal Breaking Load (MBL) of $1030mt$. The results show a very high frequency of this cable, which poses no issue for the considered operation.

$$K_{cable} = \frac{EA}{L} = 28\ 000 kN/m \tag{4.24}$$

$$W_{cable} = m_{109}L = 2\ 300 kg \tag{4.25}$$

$$f_{cable} = \sqrt{\frac{K_{cable}}{W_{cable}}} = 110 Hz \tag{4.26}$$

with:

$$E = 1E5 \text{ (Standard by Huisman)}$$
$$A = 0.25\pi D_{cable}^2$$
$$D_{cable} = 109mm$$
$$L = 33.2m$$
$$m_{109} = 69.4kg/m$$

4.7.2. Natural frequency of pendulum

When the MP is hanging in the bucket without tugger lines to control it, which could happen due to incidents with the winches, for instance, it is interesting to know whether the system would be excited by the waves or vessel motions. Therefore this analysis is added. The pendulum's frequency solely depends on the length between the CoG and the hinge, which makes this calculation relatively easy. To get insight into the sensitivity of this frequency, the pendulum's length is halved and doubled, which results can be seen in Table 4.2. With this analysis, it can be seen that, by increasing the distance between hinge and CoG, the natural frequency enters a regime sensitive to excitation by waves and motions of the vessel. Therefore, the length should be limited, or the tugger lines should be equipped with a fail-safe method which prevents them from becoming slack.

$$f_{pendulum} = \frac{\sqrt{g/L}}{2\pi} = 0.265 Hz \tag{4.27}$$

Table 4.2: Natural frequencies of simple pendulum

$L_{pendulum}$ $[m]$	$f_{pendulum}$ $[Hz]$	$T_{pendulum}$ $[s]$
1.6	0.375	2.7
3.4	0.265	3.8
6.8	0.187	5.3
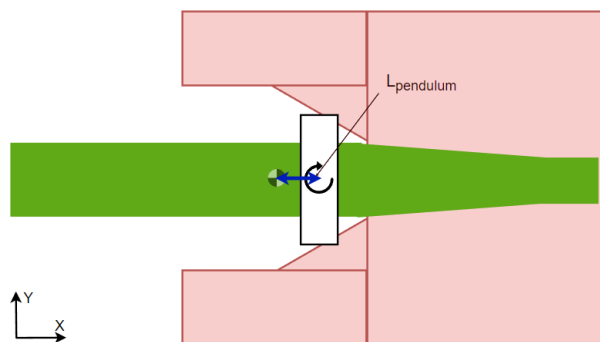
Figure 4.18: Sketch MP when seen as a pure pendulum

4.7.3. Natural frequency of mass-spring model

The last step in this analysis is slightly more challenging. The model uses the hinge as a point of rotation, so a rotational stiffness of the tugger lines is required. This is achieved by slightly rotating the MP around its Y-axis and determining the new lengths of the tugger cables. Then, after repeating this for a range of small angles, a linearised stiffness around its original position is calculated. The following steps have been executed for every upending angle θ_{mp}, as the system's geometry changes, which influences the natural frequencies.

$$\Delta L = L_0 - (r_{0-h} + r_{h-mpb} - r_{0-w}) \tag{4.28}$$

$$RF = \Delta L / \psi_{mp} \tag{4.29}$$

$$K_{rot,cable} = RF\ K_{cable} r_{h-mpb} \tag{4.30}$$

$$I_{33} = I_{33,mp} + W_{mp} r_{h-mpcog} \tag{4.31}$$

$$f_{model} = \sqrt{K_{rot,cable}/I_{33}} \tag{4.32}$$

with:

$$L_0 = \text{Original Length of Tugger Lines}$$
$$r_{0-h} = \text{Arm from coordinate system to hinge}$$
$$r_{0-w} = \text{Arm from coordinate system to winch locations}$$
$$r_{h-mpb} = \text{Arm from hinge to MP bottom connections}$$
$$r_{h-mpcog} = \text{Arm from hinge to MP CoG}$$
$$RF = \text{Rotational Factor, to incorporate for angles of tuggers}$$
$$\psi_{mp} = \text{Out-of-plane rotation of MP}$$
$$I_{33} = \text{Moment of Inertia in local z-axis}$$

The results of this analysis have been presented in a figure together with the natural period of the control system (assumption made by experts of Huisman) and the wave periods, which were earlier used as the operational state ($T_p = 6-10s$). The blue line indicates the natural periods for the model, as presented in this chapter. It can be seen that, for the lower angles, the system is both well controllable and not very sensitive to wave loading. At an upending angle of roughly $\theta_{mp} = 70°$, the natural control period is crossed, which does not pose an immediate issue but is good to realise. Finally, in an almost vertical position, the natural period does interfere with the wave frequencies, which indicates that in this phase, the gripper might have to be switched to active damping mode. To get an idea of the sensibility of the winch locations, two more locations have been investigated, where the geometry of the system slightly changed. These are indicated in yellow and red and are sketched in Figure 4.21. It can be seen that the hypothetical concept can be altered in such a way that undesired natural periods are prevented. It is concluded that the concept presented here has potential in future installation methods, although there remains a need for detailed design and thorough time-simulated analysis.
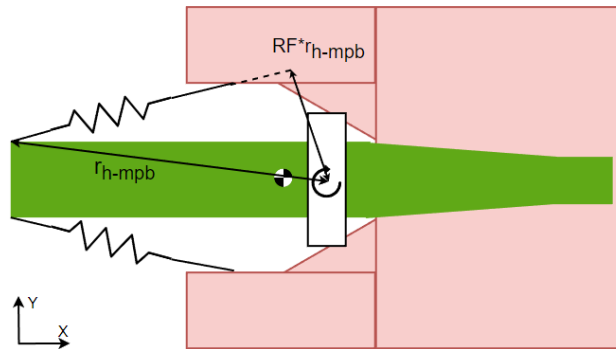
Figure 4.19: Overview of springs and the arm with the hinge for rotational stiffness
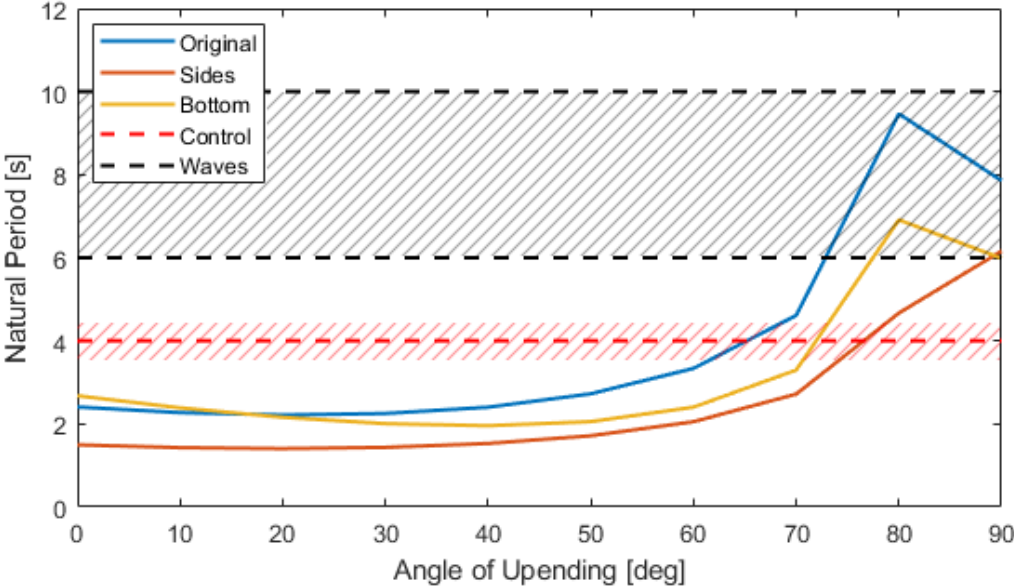
Figure 4.20: Natural period development during upending procedure, with in red and black the periods of control and waves indicated, respectively. Three lines are presented for three optional locations of winches.
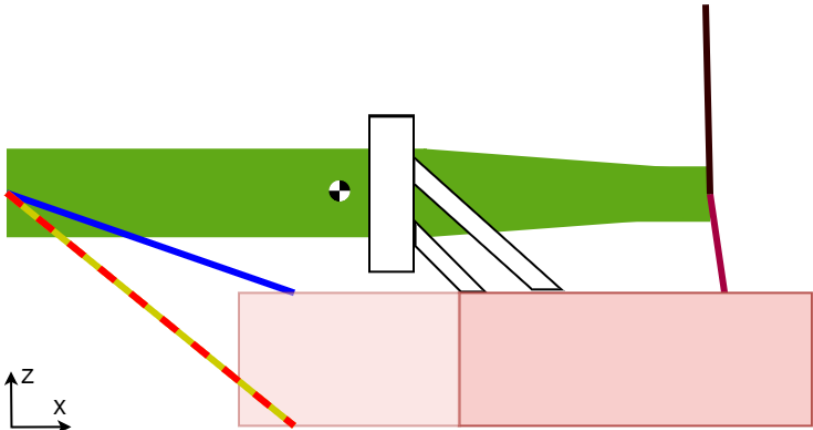
(a) XZ plane presenting extra considered winch locations
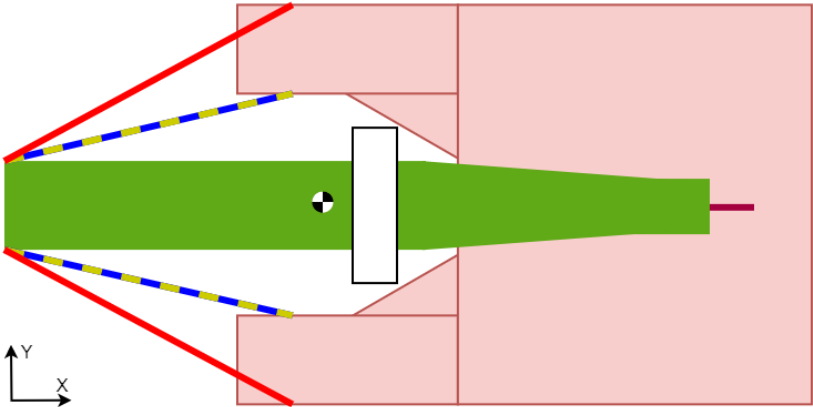
(b) XY plane presenting extra considered winch locations

Figure 4.21: Schematic diagram of alternative tugger winch locations, as used in the analysis of Figure 4.20

4.8. Sensitivity Analysis

In this thesis, various assumptions are made on which the model and calculations are based. To get insight into the sensitivity of the developed model, these assumed values have been altered one by one, while the model generates the required tugger load in tugger 3 and 4 for the updated system. For a fair comparison, the effect on the tuggers is normalised by dividing the updated value by the original value, after which a linear trend line is created through the data points.

As seen earlier, an upending angle of $\theta_{mp} = 30°$ is the governing load case, which has been used for this analysis. Furthermore, as this analysis is used to get insight into the behaviour rather than to find the system's limits, an operational sea state ($H_s = 2.25m/s$ & $T_p = 6 - 10s$) has been used.

The results have been split into environmental assumptions, being the wind speed, current speed and wave direction, and the model choices, being the weight of the selected MP, the distance from the hinge to the CoG of the MP and the pre-tension in the tugger lines. Finally, the whole MP (both weight and size) is scaled to get insight into the workings of this model for bigger and smaller MPs.

4.8.1. Environmental Assumptions

First, the environmental loads are evaluated. In Figure 4.22 the results are presented, where the wind speed and current speed are varied by multiplying the original value by a factor (ranging between 0.25 and 1.75), and the wave direction is varied by a $\Delta\psi$ from $-10°$ to $+10°$.

When looking at the results, it can be seen that an increase in wind speed leads to a reduction in loads. This was expected when looking at Figure 4.15, where it is seen that the wind load opposes the direction of the wave loads and thus relaxes the required tension. The second thing to be noted is the slight difference between side and stern, which results from the side loads being generally higher. The limited impact that the wind has is relatively smaller in this case. Finally, it can be said that the absolute impact of a variety in wind has minor effects, in the range of only 2%. The direction of the wind has also been compared, but this influence was negligible.

Secondly, the current speed is investigated. Here it can be seen that side and stern behaviour are similar and that an increase in current leads to increased loads. As the current is assumed to be in the same direction as the waves, this effect was expected. The impact of changing current speeds does not lead to a drastic increase in tugger loads. When the current direction was varied, while the wave direction was kept constant, negligible changes were seen, similar to the wind speeds.

Thirdly, the vessel heading (thus wave direction) is varied. In the stern direction, this variation is around the original $\psi = 165°$, while for side installation this variation is around $\psi = 150°$. It can be seen that the inclination of the line is significantly different. For stern installation, an increase in direction (more head seas) decreases the loading in the tuggers, whereas the loads will slightly increase for side installation. This result can be explained as the angle with the MP of wave impact leads to high out-of-plane loads for side installation. Increasing this even further leads to wave impacts perpendicular to the upending plane. For stern installation, however, an increase in vessel angle leads to more in-plane loads, as seen from the MP. As the angle between MP and waves is quite low ($15°$), the effect of this change is steep. It should be noted that this linear regression is only valid for this range of $\Delta\psi$. A higher difference in direction would lead to increasing loads again, as the symmetry axis of the vessel is then surpassed.
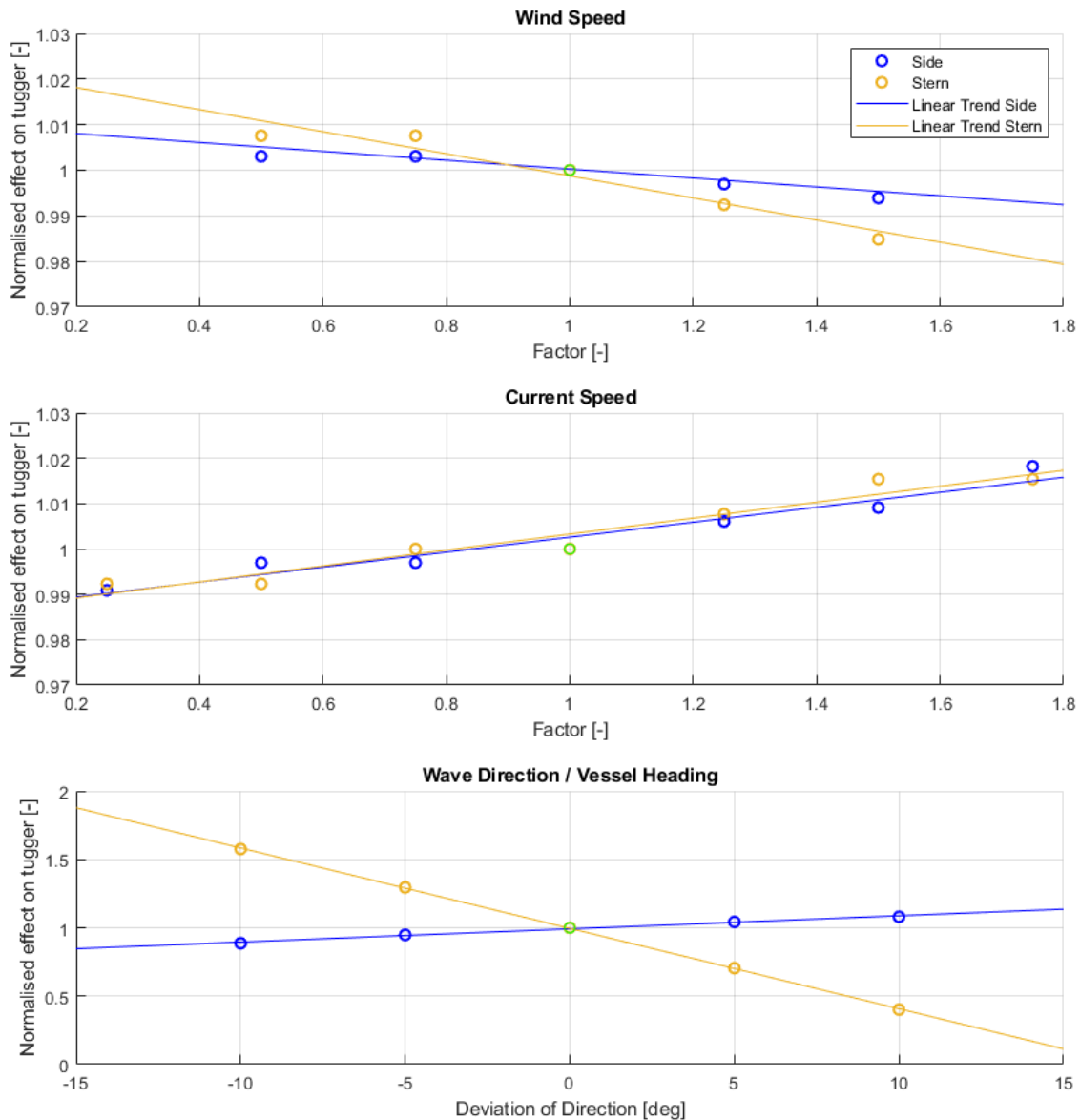
Figure 4.22: Sensitivity analysis for environmental assumptions, normalised on the tugger loads of the assumed value.

4.8.2. Model Assumptions

The second variations of assumptions have been executed on model choices and are presented in Figure 4.23. First, the weight of the MP is altered. As the MP is a project-specific design, there might be a site on which MPs of the same length are present, which weigh more due to a higher wall thickness. This effect of this is seen in the loads which are generated by accelerations. The graph shows that both for side and stern installation, the loads increase for higher weights. Compared to the other model choices, however, the effects of this weight increase are minor. The minor effect confirms that the linear D/t ratio was an acceptable assumption in this thesis.

When looking at the distance from the hinge to the MP CoG, significant changes in loads can be seen. Especially in the side installation method, increasing the submerged length of the MP leads to higher loads in the tugger system. As the impact of wave loading is more unfavourable for side installation compared to stern installation, the difference in steepness of the trend line makes sense. It should be noted that the impact of this distance is highest for all assumptions discussed here. For example, an increase of 50% in length can lead to loads being 8% higher. Therefore, this distance is to be chosen carefully in a potential concept.

Finally, the impact of the pre-tension in the tugger lines is presented. In the model, the loads in the tugger lines vary over time between the most unfavourable load of, for instance, $160mt$ for stern installation and the lowest load being the pre-tension in the cable. This pre-tension is required to prevent snap-loads from occurring. However, this pre-tension does result in a slightly higher load in the "load-bearing tugger". Therefore it is interesting to see the effect of this pre-tension on the required tension. The slope of this line is positive. Due to lower loads in general, this increase results in a higher normalised increase in stern installation compared to side installation. However, the absolute values of this increase are reasonable.
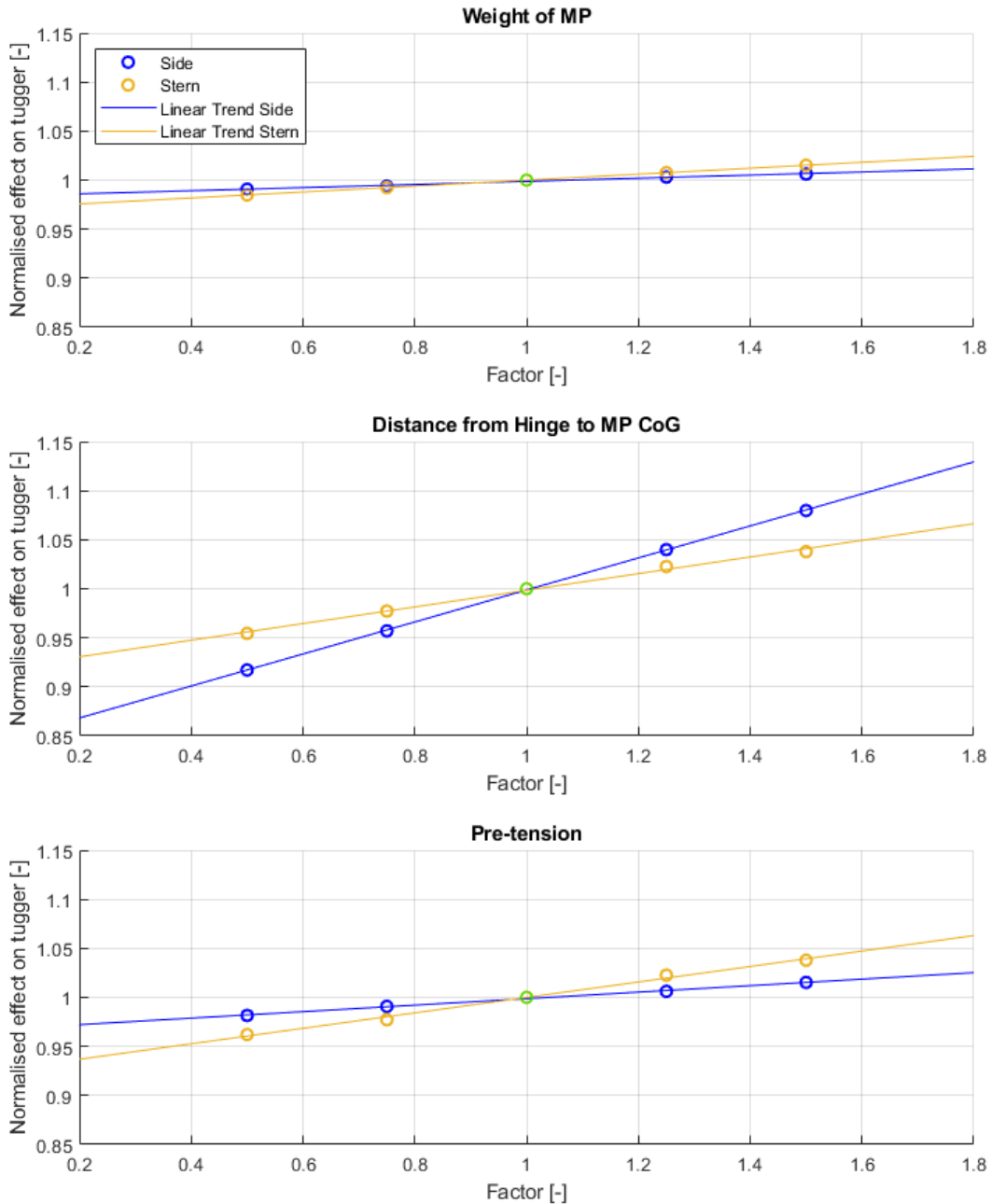
Figure 4.23: Sensitivity analysis for model choice assumptions, normalised on the tugger loads of the assumed value

4.8.3. Monopile selection

In this thesis, the MP "L" ($L_{mp} = 110m$ & $D_{mp} = 11m$) has been used for the model development. However, as seen in section 2.1, a variety of monopiles is seen in the current market. The impact of the monopile selection on loads of the model is presented in Figure 4.24. In this graph, the continuous lines represent the trend line found for the upending angle of $\theta_{mp} = 30°$. A quadratic trend line was found to have an R^2 value of 0.999 and, thus, pretty accurate. In Figure 4.25a and 4.25b, the trend lines for an upending angle of $\theta_{mp} = 50°$ and $\theta_{mp} = 70°$ are presented, which show that the quadratic behaviour is expected throughout the complete upending procedure.

It should be noted that the required tensions in the tugger lines increase significantly for increasing MPs. The vertical lines indicate the range of MPs as discussed in section 2.1. These give a good indication of the loads which can be expected in the coming years. These regression lines confirm the earlier mentioned issues of the future, in which MPs not only grow in size and weight, but the loads to control the MPs grow even harder.
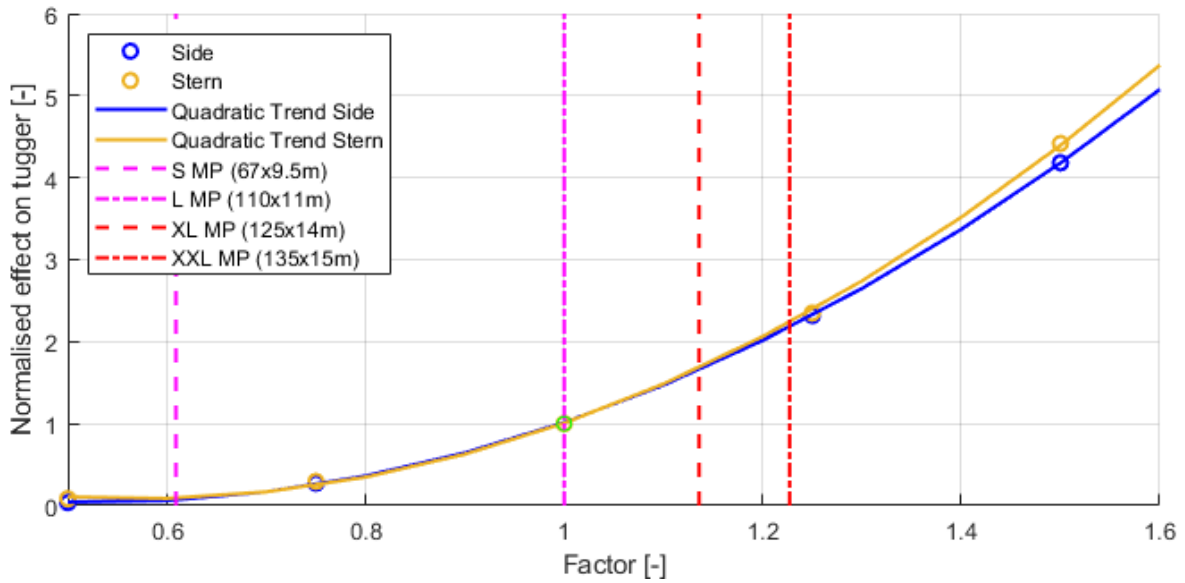
Figure 4.24: Sensitivity analysis for the scale of the MP, normalised on the tugger loads as seen on the assumed MP size, for $\theta_{mp} = 30°$

(a) $\theta_{mp} = 50°$

(b) $\theta_{mp} = 70°$
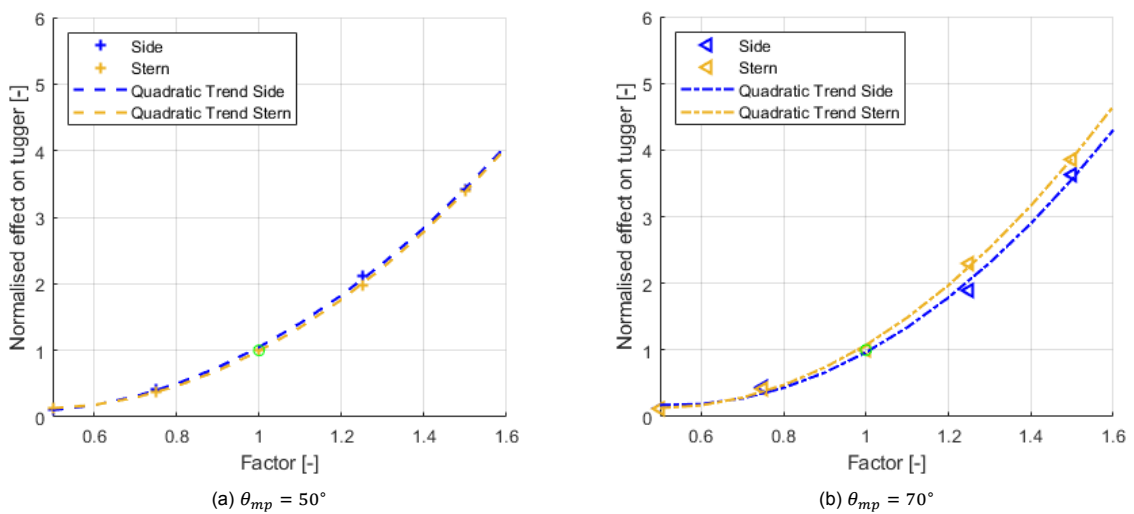
Figure 4.25: Additional analysis on normalised effect on tuggers for full scale of MP, where additional upending angles have been used.

4.9. Conclusions

In this chapter, an upending model has been developed with which the loads on equipment can be objectively defined. Two iterations led to a final model, which is then checked on the feasibility and sensitivity.

The current model uses two tugger lines at the bottom of the MP, and one back-tension tugger line at the top. Tugger lines 3 and 4 (bottom) are a proxy for the out-of-plane load control equipment, which is needed as the crane can not be used to control the load in this direction. The back-tension tugger line (5) is currently used as position control for the upending angle. It is believed that this method of restraining the MP from rotating has high potential, as it has been seen in the current market, is an elegant method, and does not require extremely heavy cables or winches.

The steel part of the model consists of a single ring gripper (with multiple roller boxes to spread the load) and a bucket-like extension to the bottom of the MP. The gripper acts solely as a hinge, which indicates that no control is required in this element. The extension of the bucket is used only for an axial force at the bottom of the MP and does not take any moment or Y- or Z-directed forces. It is believed that this is the minimum required construction for this installation method. As the gripper is already present at an installation vessel for the lowering and hammering phase of the installation, the extension could be a relatively quick and easy solution for the upending of the MP.

The model is checked on its feasibility using frequency analysis. The tugger line will most likely not encounter issues in control. The MP without tugger lines will have a natural period of around $4s$, which is not ideal but can be worked with. Finally, the complete system has a varying natural period, which stays below $4s$ for upending angles up till $\theta_{mp} = 70°$ and will encounter wave periods in a later stage. This issue can be solved by changing the geometry of the system.

The assumptions made to develop this model have been checked on their sensitivity. Especially the impact of the waves and the distance between CoG and hinge are elements that require further investigation. Finally, the entire MP is scaled up and down to get insight into future requirements of the equipment. A quadratic trend is seen, which indicates that for a growing MP, even quicker growing equipment is needed.

5

Workability difference

An interesting method to compare two installation methods is by comparing their workability, which is defined as the percentage of time that such a method could work in a particular period. The workability in this report is purely theoretical, and it is acknowledged that the reached values are incredibly high compared to real-life installations. However, comparing the workability of the two discussed methods creates insight into a method's actual advantages.

5.1. Input for evaluation

As discussed in subsection 2.2.1, the probabilities of certain sea states are known for the selected site. This probability is one of the inputs for this analysis. The second input is the model, which is run for the full sweep of sea states and a complete range of upending angles. From this information, the maximal equipment loads are compared to a set limit. Sea states which induce loads higher than the limit are considered not workable, and the percentage of remaining states in the table, multiplied by their respective possibility of occurrence, is defined as the workability for the season.

As this analysis has been executed per season, the wind input in the model also have been changed for each season. For this, the maximal wind speed per season was taken as the average in the Weibull curve, after which the 85th percentile was used as reference wind speed at the height of $h = 60m$.

5.2. Limit definition

As the model currently consists of a hypothetical concept, no actual equipment is used for comparison. Instead, a maximal tugger load is defined, on which the workability will be calculated. The used maximal tugger load is based on a wire rope with $D_{cable} = 109mm$ & $MBL = 10300kN$. Experts at Huisman advised on this type of wire and found this a suitable example for this analysis. This MBL is translated into a Safe Working Load (SWL) of $300mt$ by dividing the MBL with a Safety factor of 3 and subsequently with a Dynamic Amplification Factor for offshore lifting operations of 1.1 [10]. This SWL is the maximum load a tugger can handle and functions as an upper limit.

5.3. Results of analysis

The model has been used to sweep all sea states and upending angles, generating the quasi-static loads needed to upend the MP in a controlled manner. Subsequently, these loads have been compared to the limits defined in section 5.2, and the maximum sea states for each angle have been determined. As a system is as strong as its weakest link, all angles have been considered while creating the final workability limits. In Figure 5.1, the spring installation analysis results can be found. The occurrences between the two lines indicate the additional installation opportunities stern installation could utilise. Finally, the complete workability analysis results are summarised in Table 5.1, where a 32 percentage points workability increase is seen as a tremendous result.

Hs, bin		Hs,Mean	34	196	338	264	122	41	10	0	0	0	1005
> 14		14.5											0
13	14	13.5											0
12	13	12.5											0
11	12	11.5											0
10	11	10.5											0
9	10	9.5											0
8	9	8.5				1	1	1					3
7	8	7.5			1	2	1	1					5
6	7	6.5			2	3	3	1	1				10
5	6	5.5		1	4	7	5	3	1				21
4	5	4.5		2	10	12	11	5	1				41
3	4	3.5		6	25	32	20	8	2				93
2	3	2.5	1	20	62	65	33	11	3				195
1	2	1.5	5	60	128	97	37	9	2				338
0	1	0.5	28	107	106	45	11	2					299
Tz, Mean			3.5	4.5	5.5	6.5	7.5	8.5	9.5	10.5	11.5	12.5	
Tz, Bin			4	5	6	7	8	9	10	11	12	> 12	
			0	4	5	6	7	8	9	10	11		
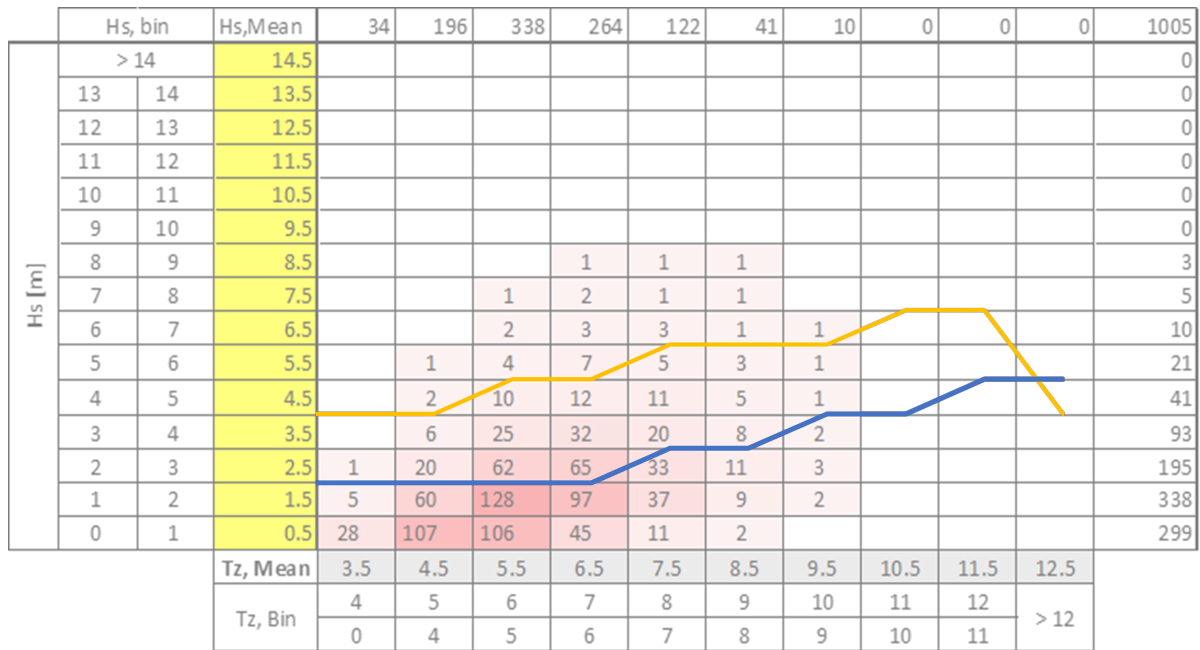
Figure 5.1: Scatter plot of operational limits for bottom tugger lines, with yellow indicating the maximum for Stern installation, and blue the maximum for side. The probability of sea states is presented for spring.

Table 5.1: Seasonal workability when tugger loads limits are set on $300mt$.

Season	Stern	Side
Spring	96.8%	68.3%
Summer	98.8%	72.4%
Autumn	95.3%	58.9%
Winter	93.7%	56.6%
All-Year	96%	64%

As the currently given workability numbers are extremely high (especially the stern numbers), some remarks on the given results need to be stated:

- In this thesis, the focus lies on creating an objective distinction between side and stern installation. Therefore the actual numbers are less interesting than the difference between these numbers.

- The currently given workability is a theoretical optimum. However, during actual operation, the conditions need to be favourable for a longer time, as installation takes at least a couple of hours. Therefore the probability is reduced.

- These workability numbers are solely for the operations of the control equipment used for the upending. Although this step in the installation is considered the most direction-dependent, other steps might pose more weather-dependent and could therefore govern the workability of the actual installation.

- This analysis considers optimal circumstances within each sea state. However, there is a considerable probability that these circumstances will not be met at certain times. Examples of this are; DP is considered able to position the vessel at roughly the correct heading, whereas this might be problematic with local currents or other external influences; A weather window might open up while the vessel is not ready yet for upending and installation due to logistics; Equipment damage can lead to unexpected downtime; A wave spectrum other than JONSWAP can be developed locally due to, e.g. bathymetry, which can cause the vessel to respond differently than in the current calculations.

<div style="text-align: right; font-size: 4em;">6</div>

Practical Implications

Before concluding this research, a look back on what has been achieved would be useful. This thesis looked into a practical problem experienced during the current installation of MPs and will become more severe in the near future. However, it is realised that the solution as proposed by this research does come with a few downsides, which not all have been discussed. Therefore, this chapter aims to create insight into the possibilities and challenges that this research has discovered.

6.1. Logistics

The installation of an OWF is a highly complex logistical procedure. The industry of offshore contractors sees a shift from one-off installation sequences, as seen in oil and gas, into the continuous installation sequences necessary to install a wind farm. A delay of a few hours due to weather, equipment downtime or unexpected logistical delays was never seen as a big issue, but can now delay the complete campaign severely due to its repeating characteristic. A few aspects of this are discussed.

First, in the sequence, the installation process begins with fabricating an MP. This will be done in various locations, but the final assembly will most likely be done in a port with large storage facilities, such as SIF. From this port, either an installation vessel or a feeder vessel will transfer the MPs to the field. However, this procedure can already become more challenging for increasing MP sizes. Besides the discussed effects of storage, such as an affected vessel behaviour, somewhat more practical boundaries will have to be met. For instance, when a set of 6 XXL MPs are stored transversely on a vessel, the dimensions of the load are now $135m$ wide and $90m$ long. This means that the vessel is more than twice as wide as the largest container vessel in the world and $10m$ wider than the Pioneering Spirit. This width causes challenging port logistics, which could lead to delays in the sequence. Longitudinal storage, with fewer MPs being transported, might pose as an easier and more robust alternative.

Second, when the MPs are in the field, the onboard logistics on the vessel are also challenging. Transferring a $4500mt$ object from the vessel's side towards its centerline (as will have to be done for stern installation) requires more than a simple lift or drive. Keeping the operation safe and controlled while keeping the vessel stable costs time and planning. On the other hand, working at a significant distance from the vessel's hull, as will be necessary for side installation, also comes with high risks and possible delays.

Third, the reversibility of the procedure becomes more complex in the future. When the installation sequence has to be stopped halfway due to, e.g. bad weather or equipment failure, the vessel should be able to return the MP to the deck or eject it if needed. New methods, such as the proposed method of this thesis, make this reversing more complex and sometimes even impossible. Growing MPs are tougher to handle and, therefore, tougher to control when things go wrong.

6.2. Equipment

The equipment used to install an MP from an installation vessel is also discussed shortly. Assumptions and choices were made in this thesis, which should be reflected upon.

The upending process, followed by the lowering and hammering, is a complex procedure with lots of equipment and control systems. Only a part of this process has been researched in this thesis, but the whole scope will have to be analysed to determine the installation method. It is believed that combining an upending tool with a lowering and positioning tool could be beneficial concerning safety and time. The upending sequence in this thesis is analysed using a single ring gripper with a bucket-like extension to exert a force in the axial direction on the MP. The characteristics of the gripper are not taken into account, as it is not used in damping or position control mode in this process; thus, it acts solely as a hinge. The tugger lines in this thesis are used as a proxy for out-of-plane load comparison but are a potential solution in the upending process.

The method does pose as an option to install both over the side and stern of the vessel, albeit that side installation requires stronger tugger lines. Interviews with specialists of Van Oord, Heerema and Seaway7 provided insight into the possibility of using a method for a specific period of the year. For example, a contractor might choose side installation in the summer, during which a high vessel capacity can be beneficial as the weather is usually calm this season. Then, when the sea states are getting rougher, the vessel could be re-outfitted for stern installation in roughly 1-2 weeks, after which it could sail into the field with fewer MPs to make use of every small weather window to install a monopile.

It should be noted that the presence of a stern recess is necessary for this quick transformation of the installation method. This recess is not yet seen in current installation vessels and requires quite some engineering to implement in a design. Therefore, it would be best to consider the presence of such a recess from the very start of the design of a vessel. First, the fact that less upward water pressure is present at the stern requires a stronger mid-ship design to account for more bending stress. Besides that, more ballast will be needed at the vessel's bow to keep it level. Secondly, the location of the vessel propellers will need to be adjusted. Instead of three propellers, the design should incorporate two or four propellers on the sides to prevent high loads on the MP due to this centre propeller. There might be alternatives for the recess, such as placing large slabs of steel on the sides of the stern and reinforcing these with braces. However, this method has not been investigated thoroughly yet and might bring more issues.

As mentioned before, the gripper's characteristics have not been considered. However, in addition to this comparison between side and stern, the required velocity and stroke of the gripper for lowering are presented in Table 6.1 for operational sea state ($H_s = 2.25m$ & $T_p = 6 - 10s$). In Appendix D a set of design requirements for an upending bucket is presented. Although this detailed design is left out of scope for this thesis, the requirements give some insight into the differences between the side and stern for the steel bucket design.

Table 6.1: Velocity and Stroke comparison for side ($x = 80m$, $y = 40m$, $z = 22.6m$) vs stern ($x = 22m$, $y = 0m$, $z = 22.6m$) location of gripper.

Parameter	Symbol	Stern	Side	Unit
	v_x	0.091	0.148	m/s
Velocity	v_y	0.136	0.121	m/s
	v_z	0.380	0.156	m/s
	s_x	0.146	0.247	m
Stroke	s_y	0.227	0.199	m
	s_z	0.658	0.268	m

7

Conclusion & Recommendation

7.1. Conclusions

In a world where increasingly growing energy consumption and increasing environmental awareness are challenging each other every day, installing renewable energy sources seems to be the only solution. Combined with a reduction in costs of these sources, renewable energy has been the fastest-growing source in the last decade. A significant share of this growth is taken by offshore wind energy. High wind speeds, lower visual, noise and areal constraints and the availability of more complex foundation structures make offshore wind increasingly interesting. The monopile foundation dominates the current bottom-fixed foundation market and is expected to do so in the coming years while growing in size and weight. The installation of such monopiles experiences a shift from traditional jack-ups toward floating installation vessels due to their flexibility and speed.

This thesis has focused on a possible improvement on the current installation methods used by floating vessels, namely by switching the installation position from the side hull to the vessel's stern. This new location could lower the equipment requirements and increase the year-round installation capacity of a vessel. However, after research into the possible installation methods and their (dis)advantages, a knowledge gap in the installation direction appeared. Therefore, the question arises, can stern installation of monopiles improve all-year installation performance for floating vessels? This question has been answered using several smaller questions, which are responded to in the following paragraphs.

The knowledge gap consists of two main subjects. The first is the MPs' storage on an installation vessel's deck. Here both the stresses in the MP and the effect of MPs on vessel behaviour are investigated. There is a difference between the side and stern installation when looking at stresses in MPs, but both global en local stresses are well below the yield stress. Therefore, this effect of storage is considered to be non-decisive. However, transverse MP storage significantly affects the vessel's behaviour more than longitudinal storage. Although fewer MPs can be stored when installing over the stern, the vessel's behaviour stays more constant, so planning an installation can be done more accurately.

The second governing step in the installation procedure is the upending of the MP. This step is the most constraining from the MP handling perspective and introduces the most significant moments on the vessel side or stern. An objective model that compares equipment loads for a hypothetical concept in both installation directions is generated. Tugger lines used to control the out-of-plane MP swinging (the hardest to control) experience significantly lower loads when the MP is installed over the stern of the vessel compared to the side. Due to this finding, it can be said that upending the MP over the vessel's stern causes relaxed tool requirements, which can either save money or improve workability windows.

To clearly define performance, a set of KPIs has been formulated. The KPIs concerning storage are shortly reflected upon here. The indicator for upending, workability, is extensively discussed in a later paragraph.

Stresses in MP

The bending stress experienced by the MP due to storage on the vessel's deck is found to be non-decisive for the method selection. A difference between the side and stern stresses was found, especially for XXL MPs. However, the absolute value of the stress was both globally and locally significantly lower than the yield stress.

Moment of Inertia of Vessel

The effect of transverse storage (for side installation) on the roll MoI is significantly higher than that of stern installation storage. When looking at the pitch, the stern installation affects the MoI more. Finally, in the yaw direction, side and stern affect the MoI equally. The effect on the roll is highest and therefore found to be least favourable. Thus, stern installation is favoured when looking at the Moment of Inertia.

Installation with a floating vessel will lead to motions of the vessel and, therefore, accelerations at every position on the vessel. However, the nature of motions (heave, pitch or roll) combined with a specific position on the vessel will lead to different dynamics for stern compared to side installation. This research compares MP accelerations between side and stern for out-of-plane and in-plane (angular) accelerations. The mentioned plane is the XZ plane of the vessel for the stern installation and the YZ plane for side installation. The in-plane acceleration is combined with gravitational acceleration and is considered relatively easy to control with a crane and back tension tugger line. On the other hand, the out-of-plane acceleration creates a moment in the equipment which is harder to control. A model has been developed that allows for accurate assessment of all accelerations by introducing tugger lines. Not only are tugger lines common practice in the offshore industry to limit accelerations in chosen directions, but in this research, they also allow for quantitative comparison of forces and, therefore, to compare the dynamic performance of installation setups. Calculating the sum of forces and moments in the MP for a range of upending angles and positions, the forces in tugger lines could be determined. Using the developed models, it is found that stern installation has a significantly better dynamic performance for this reference vessel. Reasons for this are the out-of-plane accelerations, which for side installation are higher than those for stern installation. Additionally, the wave loading on the MP is less favourable for side installation, which causes more loads in the motion-restricting tuggers.

Workability

Based on the above, it is concluded that the main factor defining installation performance is, in fact, workability. This is defined as the percentage during which installation is possible, given the environmental probability of a timeframe. Workability in this thesis is divided into four seasons, in which the possibility of installation is investigated. When limiting the strength of the tugger lines to a reasonable number, the installation boundaries are determined. The developed model predicts a year-round workability difference of 32 percentage points, with side vs stern being 64% vs 96%. The most notable difference is found in winter, with a 56.6% vs 93.7% difference. This creates a tremendous benefit for stern installation over stern installation. It is noted that, although statistically correct, the actual workability for side vs stern will be significantly lower as minimum period lengths (e.g. hours in succession) and some other factors, discussed more thoroughly in this thesis, are not considered. Still, the results confirm that, for a given vessel, stern installation is superior to side installation.

Equipment requirements must be determined if the hypothetical concept on which the model is based would be materialised and translated into an actual upending concept. In the current workability analysis, a maximal tugger load of $300mt$ is used, which translates to an MBL of $1030mt$. This type of SWL can be found in wire rope with a diameter of $109mm$ or bigger. Besides these tugger lines, a gripper with a bucket-like extension for axial loads will need to be designed. The design of such a tool is out of scope for this thesis, but the loads induced by the MP for various sea-states are presented in Appendix D for future design steps.

7.2. Recommendations

As the installation of an OWF is a highly complex process, further research is required before stern installation becomes the new standard. Therefore, the following aspects of MP installation are not considered but might pose perfectly for follow-up research. This section is split into academic recommendations for further research and recommendations for Huisman to continue on the executed work.

7.2.1. Recommendations for scientific research

Transport to the field

In this thesis, the impact of transport of MPs on the deck of the installation vessel is investigated, where it was discovered that the vessel's behaviour is quite significantly affected by this transport. However, two remaining transport methods, a wet tow and feeder vessel transport, are not discussed while these can provide a solution for this issue. A system such as Barge-Master, upgraded to take cargo as large as an MP, might be a solid option for the future, as the transfer between feeders and installation vessel is no longer as weather dependent as it is nowadays.

Besides these additional methods, the currently used method also has its flaws which should be looked into. The reference vessel's behaviour (RAOs) was determined for an empty vessel with a certain draught. The increase in MoI has indicated that the vessel's behaviour would change when multiple piles are stored on the deck. Therefore, an analysis of updated RAOs is highly recommended, as the vessel needs to be able to operate in all loading conditions.

Wave impact analysis

Within the transport to the field, the survival state should be more thoroughly investigated. In such a state, the probability of wave impact on transversely stored XXL MPs is higher than 75%, which indicates that the system should be designed for this (Appendix C). Both the saddle and MP design might be dependent on this.

Onboard Logistics

When a specific type of upending is chosen, multiple methods are known for transferring the MP from the stored position into the upending tool, depending on the vessel's layout and characteristics. The methods described in Appendix B are mature techniques which can all be selected for both side and stern installation. Therefore this research did not extend to new or updated methods for this step. However, the onboard logistics do pose for interesting future research. For example, lifting the MPs from a stacked frame is weather-sensitive, and options for a cargo-house type of robot which could safely pick MPs from the top shelf would be interesting. Besides that, an analysis of HSE should be executed, as some steps in the sequence might differ in that perspective. Finally, every step of the sequence should be tested on workability to provide a complete overview of this.

Dynamic completion of the model

It is realised that the dynamic analysis of this thesis is limited to a natural frequency assessment. Although this gives a good first insight into the workings of a tool, a complete dynamic analysis would be an appropriate next step for this research. The following aspects should be looked into:

- Include damping (hydrodynamic and control)
- Include inertia of bucket
- Include 6th degree of freedom (torsion)
- Time simulations with varying phases
- Test model on other vessels
- Define error margins

7.2.2. Recommendations for Huisman

Currently, Huisman is investigating methods to install wind turbines, varying from a relatively simple split block upending to the design of a complete wind turbine installation vessel. Following this thesis, a few remarks are made on future developments.

Wave Loading

The main difference in loading between side and stern, and the reason that $\theta_{mp} = 30°$ governs the upending, is the wave loading on the MP. The direction of impact is assumed such that shielding would be present, and shielding is taken into account by capping the waves at a minimum of $T_p = 6s$. Interesting follow-up research would be an analysis on the heading of the vessel. In this analysis, the impact of heading for both motions of the vessel, as well as loads on the MP should be found. Secondly, the wave interaction between vessel and MP should be looked into more thoroughly. Between the MP and vessel, a standing wave could be generated, which can lead to higher loads on the MP than expected.

Constraining the MP

When looking at the concepts as developed at the moment, it was noted that all concepts included the MP swinging freely in the crane. Either two cranes, a split block, or an A-frame plus the main crane lift the MP. In all concepts, the MP is constrained by tuggers rather than a connection to the deck. The concept, described in this thesis, limits the lifting of the MP to a minimum, by rolling it towards the stern until the CoG of the MP is located behind the hinge point. This way, gravity helps in the upending, while the MP is still constrained to the deck at the hinge point, which is believed to be a promising concept. It is recommended to Huisman to include such a method in its evaluation of concepts.

A
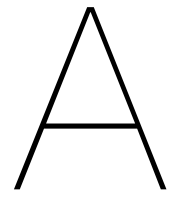
Flowchart of Upending Methods
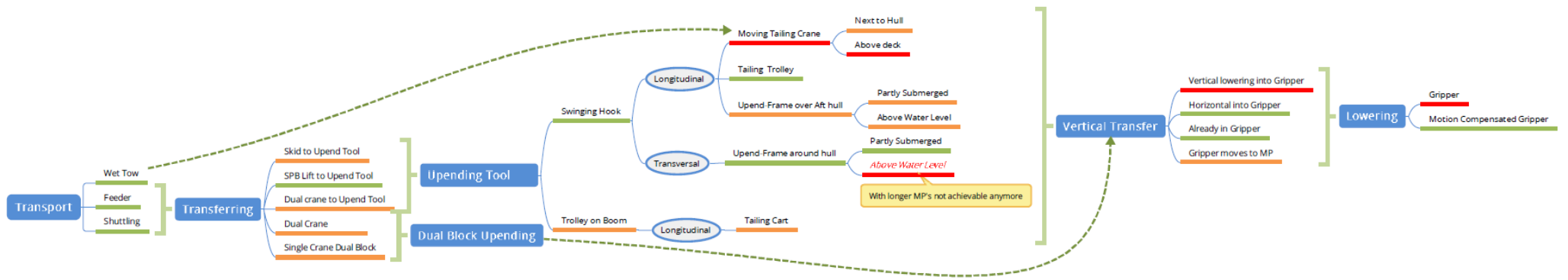
Figure A.1: Installation Methods of a Monopile
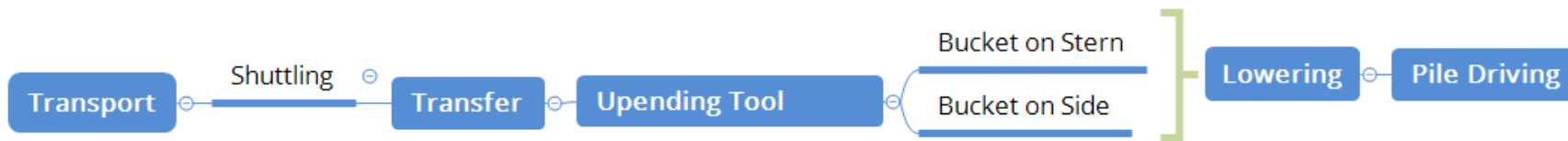
Figure A.2: Installation Methods of a Monopile which are discussed in this thesis after demarcation

B

Installation Methods for Monopile

The installation of the foundation of a wind turbine is becoming more complex in the coming years. Due to the scarcity of shallow waters, OWFs are moving into deeper waters, which makes the foundations larger and heavier. This thesis focuses on the MP foundation type, which consists of a single tubular partly driven into the seabed as seen in subsection 1.1.3. The installation steps of such an MP are shortly explained, after which the governing steps are investigated more thoroughly.

In Appendix A the installation sequence is presented in a flowchart. It can be seen that some methods are skipping certain steps, which can be seen as an advantage in saving time. The steps are shortly discussed, with the different methods explained.

Some of the discussed methods have, up till now, only been seen on jack-up barges or platforms. Therefore it is unknown whether these methods are suitable for floating installation vessels. Motions of crane booms can cause dynamic instability during procedures. This consideration is considered when comparing methods and will be addressed in further research.

Transport from port to the field
After manufacturing the MPs, they are transported to the field to be installed. Three methods are shortly discussed.

Wet Tow: Two watertight plugs are inserted in the ends of the MP such that it can float due to buoyancy. With the help of one or two tugs, the MP is towed to the field, where it is lifted out of the water by the installation vessel. Although tugs are highly available and the procedure is relatively simple, the workability of this method is relatively low. Moreover, a continuous installation calls for highly advanced planning, consisting of enormous steel plugs, which are difficult to handle. This method is considered not to be future-proof.

Feeder: A specialised vessel delivers the MPs to the installation vessel, which stays in the field. Using this method, continuous installation is made possible. However, getting the MP on board the installation vessel is weather-sensitive and might cause delays. Motion-compensated feeders are currently being developed, but the capacity of such systems is not sufficient yet. The loads on the MP during transport can be minimised with this method. However, extra handling is undesirable.

Shuttling: In this procedure, the installation vessel sails from the field to the base port to load MPs on its deck. As the motions of the vessel in port are significantly lower than at sea, the handling is relatively easy. However, the deck layout of the vessel might cause higher loads on the MP, which is discussed in Chapter 3. In addition, shuttling is expensive, as the vessel with the highest day rate is not always busy installing. Finally, shuttling is not always possible due to, e.g. the Jones Act in the USA.
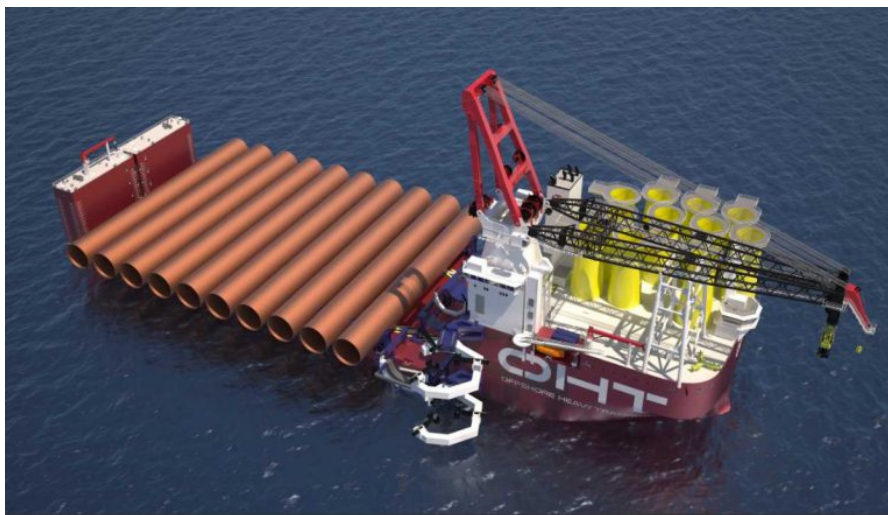
Figure B.1: Semi-Submersible Heavy Transport Vessel OHT Alfa Lift shuttling MPs and TPs [12]

Horizontal Transfer of MP

When arriving in the field, the MP needs to be transferred into an upending tool. Whether the MP has been transported by a wet tow, feeder or shuttle indicates the types of transfers that would be possible. As the installation procedure is complex and irregular, it might be so that multiple transfer methods are combined in actual operation. Three ways can be found in the current market, described shortly.

Skidding or Driving: The MP is supported by saddles, which can be transported over the deck by a skidding system or a Self-Propelled Modular Transporter (SPMT). The first can follow a track, and the second can drive in all directions. This is a mature method, which is considered a safe option due to the lack of lifting. However, a disadvantage is the lack of stroke such a system has. In addition, it cannot easily pick up stacked MPs.

Spreader Bar Lift: The standard lifting method for MPs is using a spreader bar with a single crane. The spreader bar creates two lift points in which slings can be connected to lift the MP. A tugger system is needed to control the load, which limits the workability of such a system. A significant advantage is an option to stack MPs. Figure B.3a shows such a system.

Dual Crane Lift: When a vessel is equipped with two high-capacity cranes, a dual crane lift can be executed. Here the two cranes work together, increasing the lift's complexity but also the controllability. However, two cranes take significantly more deck space than a single crane.

Upending of the MP

After horizontally transferring the MP into an upending tool, the MP is rotated such that it can be installed. This rotating over the short axis of the pile is called upending. Various methods are seen in the current markets, which will be discussed here. In Appendix A an overview can be seen of all methods. Here the distinction between methods is also somewhat clearer than when explained in the text.
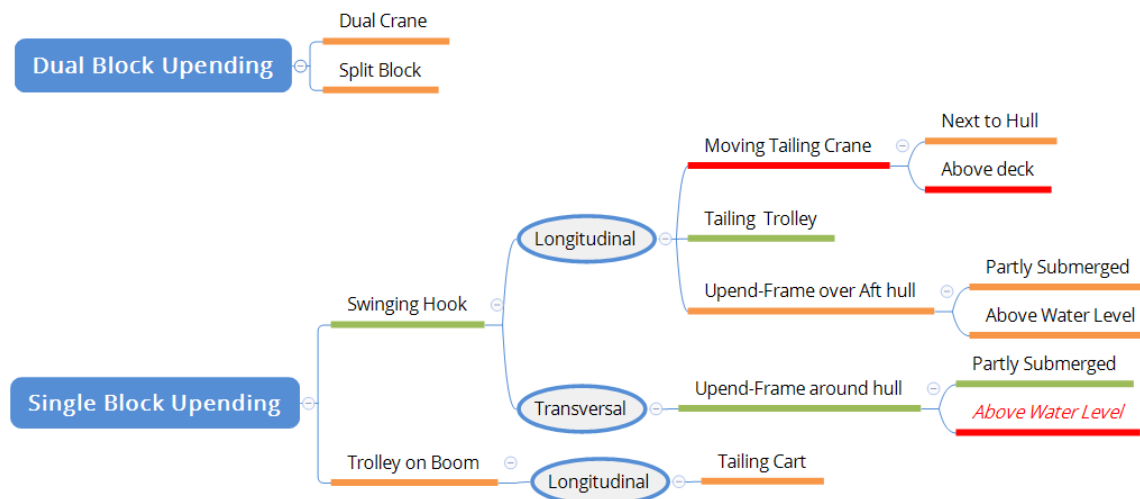
Figure B.2: Methods for Upending an MP with three main categories being Dual block, Swinging hook and Trolley on boom methods. Colour coding indicates technology readiness level, with green as "in use", orange as "potential" and red as "not futureproof or proven"

Dual Crane Upending: A straightforward way to upend MPs is by lifting it with two cranes and lowering one of the blocks while slewing the cranes towards each other. When the MP is hanging vertical, the lower connection is removed. Again, the two cranes must work together closely, which is complex. In addition, wave forces can cause swinging of the MP, as it is freely hanging in the cranes. This method is not further considered in this thesis due to the need for two main cranes, which limits the concept's applicability.

Split block Upending: Just like the dual crane upending, this method consists of two blocks hooking on the MP with one block lowering its end of the MP until vertical. However, the two blocks are now connected to one crane, as seen in Figure B.3b. This system contains little rotational stiffness, creating the need for a tugger system for control. In addition, the hook-on of a split block is significantly more complicated than a dual crane hook-on. However, due to the lack of expensive tooling, this method might be applicable in the future. For now, this method is too control-sensitive and therefore disregarded in the remainder of this thesis.

Tailing crane/trolley: In this concept, the bottom of the MP is used as a hinge point. This can be done by lifting the bottom with a small crane or using a hinge on a trolley that can drive along the deck (Figure B.3c) while lifting the top of the MP with the main crane. This system has the advantage that the MP bottom is constrained for movement in the Y and Z directions. A tailing crane has been seen on earlier designs of vessels, which in a later stage has been replaced by a trolley. This indicates that the potential of a trolley is higher than that of a crane. A disadvantage of this system is the need for a free pathway on which the trolley can drive. Secondly, the system has not yet been used on a floating vessel; thus, its applicability is unknown.

Upend Bucket: A bucket consists of a (half) ring with bottom support in which the MP is positioned (as seen in Figure B.3d). The MP is rotated around a point positioned further up the MP compared to the tailing trolley, reducing the required crane height. This upending can be done either entirely above water, minimising the loads on the MP, or semi-submerged. In the latter method, wave loading on the MP is present. A bucket can be placed on the side or stern of a vessel. The side is a well-known practise which can be seen as a standard in the current market. The MP sticks out of the vessel's hull on both sides, one end in the bucket and one end in which an upending tool will be connected. An advantage of this is that the vessel's width does not limit the maximal length of the MP. However, inserting an upending tool far from the deck is complex. Secondly, the MPs laying in this transverse direction might influence the vessel's Moment of Inertia and thus its response to the waves. When the bucket is positioned on the stern of the vessel, the upending tool can be easily connected above the deck, but the vessel's length can limit the MP's length. The MoI of the vessel might be less affected by

(a) Transfer of an MP using a spreader bar for the Walney Extension wind farm (Dong Energy)[13]
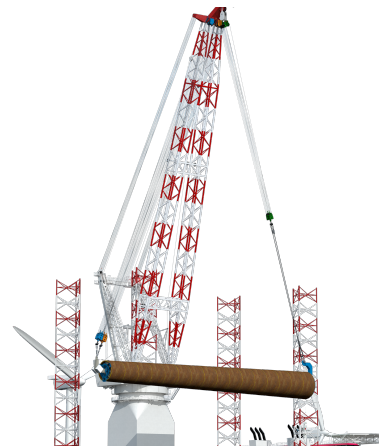
(b) Split block upending as presented by Huisman, here a triple main hoist is used, where 2/3rd of the capacity is used in the left hook [24]

(c) Upend trolley as used on Aeolus (van Oord) fabricated by TWD [49]

(d) Upend bucket as designed by IQIP [28]

Figure B.3: Visualisation of installation steps of offshore wind monopile foundations

longitudinal storage. The accelerations and wave loading on the stern method are believed to be lower than those on the side. This hypothesis is investigated in a later stage of this thesis.

Double Trolley System: A novel method of upending consists of two trolleys. One trolley drives over the deck with the bottom part of the MP connected to it, similar to the tailing trolley discussed above. The second trolley drives vertically over the crane boom, supported by the boom and its hoist cables. In this concept, the MP is fully constrained during the entire process of upending. For this, a specifically designed crane with a long boom and significant deck space is needed. But, the MP is fully constrained during the complete upending, which is a considerable advantage. Furthermore, as the procedure can be executed over the vessel's longitudinal axis, no ballasting will be needed. An example of this method is given in Figure B.4. However, for this thesis, this method is considered unproven and is thus not taken into account.

Vertical Transfer of MP
As seen in Appendix A, many configurations for MP installation can be found. For an installation in which upending and lowering are executed with a separate tool, a vertically hanging transfer is necessary to get the MP from upending tool to the lowering tool. Three methods are found for this step. These will be discussed shortly below.

Vertical Insertion in Gripper: When the gripper is made from a solid ring, i.e. without hydraulic arms that can open the ring, the MP needs to be lowered vertically from above. This method is considered unsafe due to the lack of an ejecting strategy when position control fails. Secondly, the free-hanging MP can swing and hit the gripper on the top, causing severe damage. Therefore this method is not further considered.

Figure B.4: A double trolley system for a fully constrained upending of the MP presented on the concept vessel Zephyr from Huisman

Slew into gripper: The standard in today's operation is slewing the MP in the gripper. This method opens the arms, creating a bigger area to catch the MP. This gripper is considered safer and is seen on various vessels. The slewing of the MP should be done slowly to avoid swinging. This method is more challenging on floating vessels due to the vessel's motions.

Gripper moves to MP: A very elegant method is when the gripper moves towards the upended MP and secures it from this position. Here the MP can be controlled at all times using a tailing trolley or bucket. This novel method is seen on concept vessels and has so far not been seen during an actual campaign. Therefore the concept is not considered but is believed to have a high potential for the future.

Lowering the MP to the seabed
When the gripper is safely secured in the gripper, the lowering process begins. During this phase, the gripper is usually passive as it acts as a guide for the MP. Novel grippers also have a damping control during the lowering to prevent the MP from swinging in its second eigenmode. As the MP is lowered, a range of swinging modes can occur. This is mainly due to the changing length of the hoist cable in combination with the hinging characteristics of a single gripper ring. The waves excite the MP below the gripper, and the CoG is shifted from above the gripper to below. All these effects are dynamically challenging, and extensive control is needed. Within this installation step, not much variety is seen in the market except for the variety in gripper characteristics. Grippers can come in single or double rings, with or without damping.

Pile Driving
To gain the strength to withstand various loads during its lifetime, the turbine must be safely connected to the seabed. For Monopiles, this connection is created by hammering the complete MP to a certain penetration depth [36].

Piles can be driven into the soil using various methods, from traditional hydraulic hammers to novel methods such as BLUE piling technology [29] or a Vibro hammer[43]. Much research is done to find methods which are environmentally friendly and still efficient [21]. As currently so much research is done in this field, it is placed out of scope for this thesis.

C
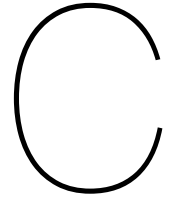
Probability of Wave Impact

A sea state consists of a spectrum of waves. When all these waves are collected into a probability, a significant wave height H_s is calculated. In this thesis, this significant wave height has been used to find vessel motions and wave loads on MPs. However, due to the fact that this is still a spectrum, higher waves can and will occur during the installation. This appendix provides a probability calculation for the chance of a wave hitting the MP during transport. In Figure C.1 the decrease in air gap can be seen for a Small and XXL MP laying transversely on the deck. This air gap reduction is significantly more present in XXL MPs, as can be seen in the sketch. Below, the probability calculation is presented [47], after which the conclusions are presented in Table C.1.

Figure C.1: Indication of reduction of air gap for a Roll angle of 1° for both MP XXL and MP Small

$$m_0 = (H_s/4)^2 \tag{C.1}$$

$$Q_{\eta_{crest}} = exp\left(-\frac{\eta^2}{2m_0}\right) \tag{C.2}$$

$$Pr\{all\ \eta_{crest} < \eta\} = \left(1 - Q_{\eta_{crest}}\right)^N \tag{C.3}$$

$$N_{1hour} = 3600/T_p = 3600/6 = 600 \tag{C.4}$$

$$N_{1day} = 3600 * 24/T_p = 3600 * 24/6 = 14400 \tag{C.5}$$

$$N_{1week} = 3600 * 24 * 7/T_p = 3600 * 24 * 7/6 = 100800 \tag{C.6}$$

with:

$$m_0 = \text{Spectral Moment}$$
$$Q_{\eta_{crest}} = \text{Probability of } \eta \text{ occuring for 1 wave}$$
$$\eta = \text{Height from sea level}$$
$$Pr = \text{Probability}$$
$$N = \text{Number of waves in certain period}$$

While looking at the results of this analysis, it can be seen that for operational and transit states the chances of impact are very low and therefore not considered in this thesis. For survival mode, however, the chances of impact are already significant for a 1-hour stay in these conditions. For a duration of a day or longer (highly unlikely) the chances are basically 100% that a wave will hit the MP in either position. Note that, during these situations, also green water will be created, causing significant loads on the vessel and its equipment. Further research is recommended into the loads on MPs when waves are hitting them, as loss of load is highly undesired and dangerous.

Duration	No Rotation			MP Small 1°			MP XXL 1°		
	Hour	Day	Week	Hour	Day	Week	Hour	Day	Week
Operational	0.00%	0.00%	0.00%	0.00%	0.00%	0.00%	0.00%	0.00%	0.00%
Transit	0.00%	0.00%	0.03%	0.00%	0.03%	0.23%	0.02%	0.47%	3.21%
Survival	21.18%	99.67%	100%	41.48%	100%	100%	78.76%	100%	100%

Table C.1: Probability of waves exceeding the air gap for multiple load cases and durations of operation.
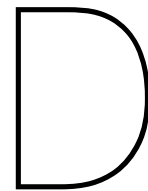
Basis of Design for Upending bucket

The upending tool used for this thesis has not been designed in detail. The purpose of this research has been the comparison between side and stern installation, with a focus on the upending procedure. However, as the model does incorporate the bucket and evaluates the loads hereof, the following information could be used to generate a detailed design. In Figure D.1 the dimensions of the tool (over stern) are presented.

In Figure D.2 the loads perpendicular to the hinge (vertical when $\theta_{mp} = 0°$), are presented. It can be seen that originally, the MP rests almost completely on the roller boxes, which is the reason for the three sets of rollers on which it is sketched. After a while in the upending process, the loads are reduced and finally even negative, which indicates that the gripper should be closed for the upending procedure. The hinge also exerts a horizontal force (Y-axis of the vessel) on the MP, which is shown in Figure D.3. Here the difference between side and stern is more distinct, which is the result of higher horizontal loads from the waves in the side setup. Furthermore it can be seen that the loads are generally not very high.
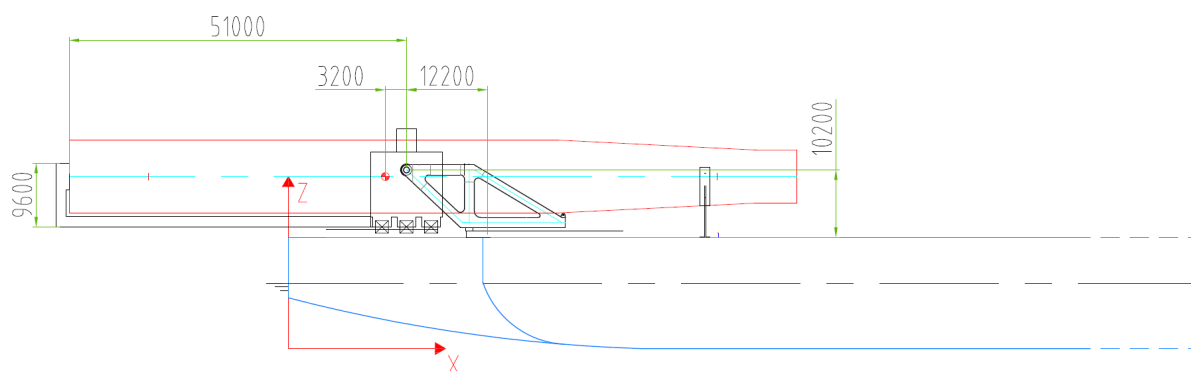
Figure D.1: Dimensions of bucket used for this research

The final design input is the axial loads, exerted by the bottom part of the bucket-like upending tool. These loads counteract the negative X-directed loads which are generated by the hinge and appear to be necessary for this concept to work (with reasonable tugger loads). The axial load increases up to an upending angle of $\theta_{mp} = 70°$, after which the load is mostly taken by the crane, as seen earlier in Figure 4.17.
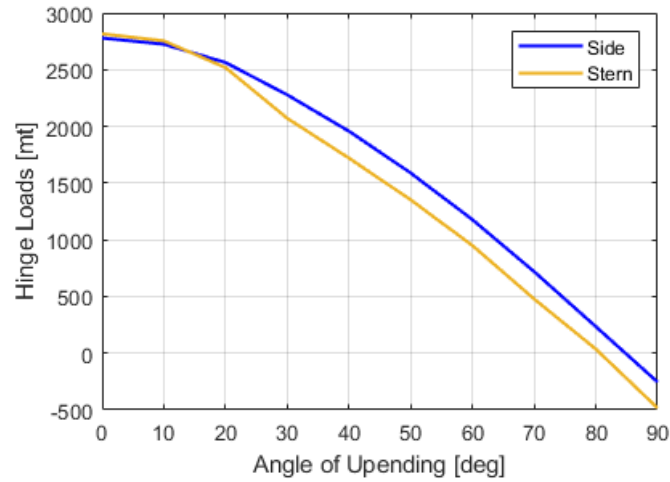
Figure D.2: Perpendicular loads in hinge for $H_s = 2.5m$ & $T_p = 6.5s$ with $\theta_{mp} = 30°$
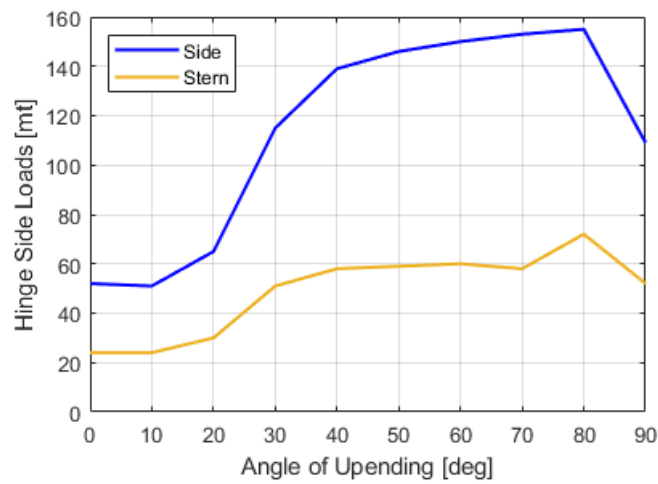
Figure D.3: Horizontal loads in hinge for $H_s = 2.5m$ & $T_p = 6.5s$ with $\theta_{mp} = 30°$
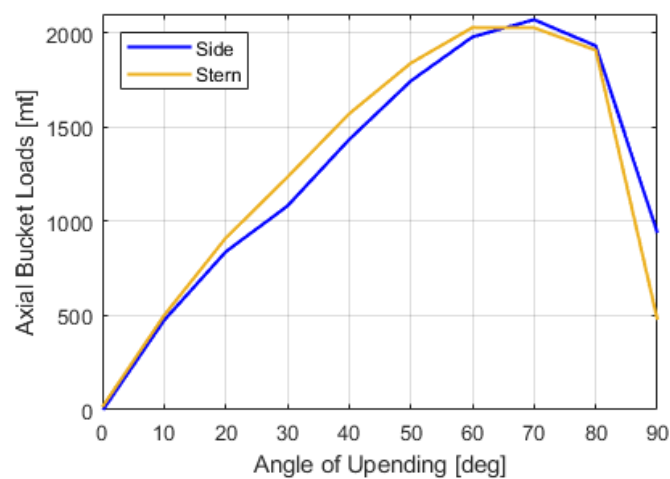
Figure D.4: Axial bucket loads in hinge for $H_s = 2.5m$ & $T_p = 6.5s$ with $\theta_{mp} = 30°$

Bibliography

[1]   Aliyu Abdullahi, Ying Wang and Subhamoy Bhattacharya. 'Comparative Modal Analysis of Mono-pile and Jacket Supported Offshore Wind Turbines including Soil-Structure Interaction'. In: *International Journal of Structural Stability and Dynamics* 20 (July 2020). DOI: `10.1142/S021945542042016X`.

[2]   International Renewable Energy Agency. *Global Atlas for Renewable Energy - Location [57.8; 5.71]*. URL: `https://globalatlas.irena.org/workspace` (visited on 20/12/2021).

[3]   Selma Atilhan et al. 'Green hydrogen as an alternative fuel for the shipping industry'. In: *Current Opinion in Chemical Engineering* 31 (2021), p. 100668. ISSN: 2211-3398. DOI: `https://doi.org/10.1016/j.coche.2020.100668`.

[4]   Jake Badger et al. *Global Wind Atlas*. URL: `https://globalwindatlas.info/` (visited on 20/12/2021).

[5]   S. Bilgen. 'Structure and environmental impact of global energy consumption'. In: *Renewable and Sustainable Energy Reviews* 38 (2014), pp. 890–902. ISSN: 1364-0321. DOI: `doi.org/10.1016/j.rser.2014.07.004`.

[6]   Charles L. Bretschneider. 'Generation of waves by wind, state of the art'. In: International Summer Course Lunteren, The Netherlands. National engineering Science Company, Washington D.C., Sept. 1964.

[7]   B. Bulder et al. 'Floating OffShore Wind Turbines for Shallow waters'. In: (Jan. 2002).

[8]   Our World in Data. *Global Primary energy consumption by source*. 2019. URL: `https://ourworldindata.org/grapher/global-energy-substitution?time=1880..latest&country=~OWID_WRL` (visited on 08/12/2021).

[9]   Our World in Data. *Modern renewable energy generation by source, World*. 2020. URL: `https://ourworldindata.org/grapher/modern-renewable-prod` (visited on 08/12/2021).

[10] DNV Noble Denton. 'Marine operations and marine warranty'. In: *DNV-ST-N001* (2021), p. 16.2.

[11] Adnan Durakovic. 'Heerema Tests Floating installation of XXL Turbines Method Offshore'. In: *OffshoreWind.biz* (2021). URL: `https://www.offshorewind.biz/2021/10/15/heerema-tests-floating-installation-of-xxl-turbines-method-offshore/` (visited on 26/11/2021).

[12] Adnan Durakovic. 'MAN Heart for OHT Alfa Lift'. In: *Offshore WIND* (Jan. 2019). URL: `https://www.offshorewind.biz/2019/01/31/man-heart-oht-alfa-lift/`.

[13] Dyneema. *Switching to lightweight lifting slings saves days on wind farm installation*. URL: `https://www.dsm.com/dyneema/en_GB/applications/ropes-lines-slings-chains/lifting-slings/case-study-dynamica-walney-offshore.html` (visited on 13/12/2021).

[14] General Electric Renewable Energy. *Haliade-X offshore wind turbine*. URL: `https://www.ge.com/renewableenergy/wind-energy/offshore-wind/haliade-x-offshore-turbine` (visited on 03/06/2022).

[15] MingYang Smart Energy. *Leading innovation: MingYang Smart Energy launches MySE 16.0-242, the world's largest offshore Hybrid Drive wind turbine*. URL: `http://www.myse.com.cn/en/jtxw/info.aspx?itemid=825` (visited on 03/06/2022).

[16] Offshore Engineer. 'IOG Spuds Blythe Development Well'. In: (Aug. 2021). URL: `https://www.oedigital.com/news/489630-iog-spuds-blythe-development-well` (visited on 26/11/2021).

[17] Mohamed El-Feky. 'Maximum allowable loads from a PU roller into monopiles'. MA thesis. Delft University of Technology, May 2022.

[18] Luiza Ferreira. *Fixed Wind Foundations: An Independent Concept Screening Approach*. URL: `https://2hoffshore.com/blog/concept-screening-fixed-wind-foundations/` (visited on 15/11/2021).

[19] 'Floating Foundations: A Game Changer for Offshore Wind Power'. In: *Innovation Outlook: Off-shore Wind (IRENA)* (2016). URL: `https://www.infrastructureusa.org/floating-foundations-a-game-changer-for-offshore-wind-power/` (visited on 15/11/2021).

[20] T. Gast. 'An alternative, workability oriented approach to monopile upending'. MA thesis. Delft University of Technology, Apr. 2021.

[21] GROW. *Gentle Driving of Piles (GDP)*. 2021. URL: `https://www.grow-offshorewind.nl/project/gentle-driving-of-piles` (visited on 25/11/2021).

[22] Klaus Hasselmann et al. 'Measurements of wind-wave growth and swell decay during the Joint North Sea Wave Project (JONSWAP)'. In: *Deut. Hydrogr. Z.* 8 (Jan. 1973), pp. 1–95.

[23] N Hogben, N.M.C Dacunha and G.F. Olliver. *Global Wave Statistics*. Britisch Maritime Technology Limited, 1986. ISBN: 0946653380.

[24] Huisman. *Offshore Wind Equipment - Product Brochure*. 2021.

[25] Huisman. *Technical Specification - Motion Compensated Monopile Gripper*. Tech. rep. A21-13120. Sept. 2021.

[26] Huisman. *Technical Specifications TMC 270000-5000. SWL 5000mT*. Apr. 2020.

[27] IEA. *Key World Energy Statistics 2020*. 2020. URL: `https://www.iea.org/reports/key-world-energy-statistics-2020`.

[28] IQIP. *Pile guiding & positioning frame*. URL: `https://www.ihciqip.com/en/products/handling-equipment/pile-guiding-and-positioning-frame` (visited on 13/12/2021).

[29] IHC IQIP. *IQIP and Delft University of Technology start joint work on the BLUE piling technology improvements*. 2020. URL: `https://www.ihciqip.com/en/news/iqip-and-delft-university-of-technology-start-joint-work-on-the-blue-piling-technology-improvements` (visited on 25/11/2021).

[30] Zhiyu Jiang. 'Installation of offshore wind turbines: A technical review'. In: *Renewable and Sustainable Energy Reviews* 139 (Apr. 2020). DOI: `10.1016/j.rser.2020.110576`.

[31] J.M.J. Journée and W.W. Massie. *Offshore Hydromechanics*. 1st ed. Delft University of Technology, Jan. 2001.

[32] Joyce Lee and Feng Zhao. *Global Wind Report 2021*. GWEC, Mar. 2021, p. 53.

[33] Lin Li et al. 'Analysis of lifting operation of a monopile for an offshore wind turbine considering vessel shielding effects'. In: *Marine Structures* 39 (2014), pp. 287–314. ISSN: 0951-8339. DOI: `https://doi.org/10.1016/j.marstruc.2014.07.009`.

[34] Yanfei Li, Xunpeng Shi and Han Phoumin. 'A strategic roadmap for large-scale green hydrogen demonstration and commercialisation in China: A review and survey analysis'. In: *International Journal of Hydrogen Energy* (2021). ISSN: 0360-3199. DOI: `https://doi.org/10.1016/j.ijhydene.2021.10.077`.

[35] Yuan Enzo Liu. 'Monopile Forever. Overcoming the technical boundaries of monopile foundations in deep waters'. 2021.

[36] Walter Musial et al. *Offshore Wind Market Report: 2021 Edition*. 2021. URL: `https://www.energy.gov/sites/default/files/2021-08/Offshore%5C%20Wind%5C%20Market%5C%20Report%5C%202021%5C%20Edition_Final.pdf`.

[37] MPI Offshore. *Aeolus*. URL: `https://www.mpi-offshore.com/equipment/aeolus` (visited on 26/11/2021).

[38] Rajendra K. Pachauri et al. *Climate Change 2014 Synthesis Report*. 2015.

[39] Adrian Ramirez, S. Mani Sarathy and Jorge Gascon. 'CO2 Derived E-Fuels: Research Trends, Misconceptions, and Future Directions'. In: *Trends in Chemistry* 2.9 (2020), pp. 785–795. ISSN: 2589-5974. DOI: `https://doi.org/10.1016/j.trechm.2020.07.005`.

[40] Daniel Rippel et al. 'A Review on the Planning Problems for the Installation of Offshore Wind Farms'. In: *IFAC PapersOnLine 52-13* (2019), pp. 1337–1342. DOI: `10.1016/j.ifacol.2019.11.384`.

[41] Raymond J. (Raymond Jefferson) Roark. *Roark's formulas for stress and strain.* eng. Eighth edition / Warren C. Young, Richard G. Budynas, Ali M. Sadegh. New York: McGraw-Hill, 2012. ISBN: 9780071742474.

[42] ALAN R. ROGERS and LYNN B. JORDE. 'Genetic Evidence on Modern Human Origins'. In: *Human Biology* 67.1 (1995), pp. 1–36. ISSN: 00187143, 15346617. URL: `http://www.jstor.org/stable/41465052`.

[43] Zohaib Saleem. *Alternatives and modifications of Monopile foundation or its installation technique for noise mitigation.* Tech. rep. Delft University of Technology: North Sea Foundation, Apr. 2011.

[44] Arunjyoti Sarkar and Ove Gudmestad. 'Study on a new method for installing a monopile and a fully integrated offshore wind turbine structure'. In: *Marine Structures* 33 (Oct. 2013), pp. 160–187. DOI: `10.1016/j.marstruc.2013.06.001`.

[45] Hyunkyoung Shin et al. 'Model test of new floating offshore wind turbine platforms'. In: *International Journal of Naval Architecture and Ocean Engineering* 5.2 (June 2013), pp. 199–209.

[46] Bakker Sliedrecht. *Seaway Heavy Lifing - Oleg Strashnov - Heavy Lifting Vessel DP 3.* URL: `https://www.bakkersliedrecht.com/nl/referenties/seaway-heavy-lifting-oleg-strashnov-heavy-lifting-vessel-dp-3/` (visited on 26/11/2021).

[47] M.F.S Tissier, A.J.H.M Reniers and D.P. Rijnsdorp. *Ocean Waves - Lecture - Short-term wave statistics - Part 2/2.* Oct. 2021.

[48] TWD. *Innovation - Hammock Seafastening.* URL: `https://twd.nl/innovation/innovation-hammock-seafastening/` (visited on 20/06/2022).

[49] TWD. *Our Solutions.* URL: `https://twd.nl/markets/offshore-wind/` (visited on 13/12/2021).

[50] 'Vindeby Offshore Wind Farm: For Demonstrating the Viability of Offshore Wind as a Clean Energy Powerhouse (Most Influential Projects: #32)'. In: *PM Network* 33 (2019), pp. 66–67.

[51] I.L. Wijnant, H.W. van den Brink and A. Stepek. *North Sea Wind Climatology Part 2: ERA-Interim and Harmonie model data.* Royal Netherlands Meteorological Institute, 2014.

[52] Xiaoni Wu et al. 'Foundations of offshore wind turbines: A Review'. In: *Renewable and Sustainable Energy Reviews* 104 (Apr. 2019), pp. 379–393. DOI: `10.1016/j.rser.2019.01.012`.

[53] Michiel Zaaijer and Axelle Viré. *Reader - Introduction to Wind Turbines: Physics and Technology.* Oct. 2020.